DNA Repair Mechanisms in the Radioresistant Bacterium *Deinococcus radiodurans* and in Human

Dissertation
zur
Erlangung der naturwissenschaftlichen Doktorwürde
(Dr. Sc. Nat.)
vorgelegt der
Mathematisch-naturwissenschaftlichen Fakultät
der
Universität Zürich
von
Rebecca Buob
von
Zürich

Promotionskomitee

Prof. Dr. Ulrich Hübscher
Prof. Dr. Josef Jiricny
Prof. Dr. Suzanne Sommer

Zürich, 2009

CONTENT

1. Summary

1.1. English

Cells encounter a plethora of DNA insults every day. To counteract these detrimental effects on the genome, they have evolved sophisticated mechanisms; on the one hand the cells detect the damage by specific DNA damage sensor proteins, which activate checkpoint proteins to either halt the cell cycle to allow repair, or, in cases of too massive DNA damage, guide the cell into controlled cell death, called apoptosis. Various DNA repair pathways on the other hand attempt to repair the damage, in the best case restoring the unaltered DNA, therefore preventing genome instability. The aim of this thesis was to investigate different DNA repair mechanisms in two different organisms, first in the radioresistant bacterium *Deinococcus radiodurans* (*D. radiodurans*) and second in human cells. In the first part, two putative DNA ligases of *D. radiodurans* were investigated, leading to the biochemical characterization of the NAD^+-dependent DNA ligase of *D. radiodurans*. The DNA ligase activity was most efficient in the presence of 1mM $MnCl_2$ whereas the substitution of $MnCl_2$ by $MgCl_2$ or $CaCl_2$ reduced the activity about ten fold. A second, putative ATP-dependent DNA ligase showed no apparent ligase activity, although an adenylyltransferase intermediate could be identified. Furthermore, the characterization of the putative O6-methylguanine-DNA methyltransferase (MGMT) of *D. radiodurans* was performed. Although cloning and purification were successful, the enzymatic characterization was not possible because no methyltransferase activity was observed, although folding of the protein was correct as it bound to DNA.

In the second part, the in our laboratory discovered interaction of the human Rad9/Rad1/Hus1-complex (9-1-1 complex) with the apurinic/apyriminidinic endonuclease 1 (Ape1) was further characterized. With the use of protein fragments it was found that the endonuclease activity of Ape1 is located in its N-terminus. Furthermore the results indicated that the interaction of the 9-1-1 complex with Ape1 involves the entire Ape1 protein. In addition, observation was made indicating a previously unknown interaction of the 9-1-1 complex with human DNA polymerase λ.

1.2. German

Zellen erfahren jeden Tag viele DNA Schäden. Um diesen nachteiligen Effekten auf das Genom entgegenzuwirken, haben die Zellen hochstehende Mechanismen entwickelt; auf der einen Seite detektieren sie die Schäden durch spezifische DNA Schadenssensor-Proteine, welche ihrerseits Checkpoint-Proteine aktivieren, die entweder den Zellzyklus anhalten, um die DNA Reparatur zu ermöglichen, oder, falls die Schäden zu massiv sind, die Zelle in den kontrollierten Zelltod, die Apopotose, führen. Die verschiedenen DNA Reparaturmechansimen auf der anderen Seite, versuchen den Schaden zu reparieren und im besten Fall die unveränderte DNA wieder herzustellen und dadurch genomische Instabilität zu verhindern.

Das Ziel dieser Studie war es, verschiedene DNA Reparaturmechanismen in zwei verschiedenen Organismen, nämlich in *Deinococcus radiodurans* (*D. radiodurans*) und in menschlichen Zellen, zu untersuchen. Im ersten Teil dieser Dissertation wurden zwei vermeintliche DNA Ligasen von *D. radiodurans* bearbeitet, was zur biochemischen Charakterisierung einer NAD^+-abhängigen DNA Ligase geführt hat. Es konnte gezeigt werden, dass die DNA Ligaseaktivität in der Gegenwart von 1mM $MnCl_2$ am effizientisten war, wobei die Substitution von $MnCl_2$ durch $MgCl_2$ oder $CaCl_2$ die Ligaseaktivität etwa um das zehnfache reduziert hat. Bei der zweiten, vermeintlich ATP-abhängigen DNA Ligase konnte keine Ligaseaktivität festgestellt werden, obwohl ein Adenylyltransferase Intermediat gebildet wurde. Im weiteren wurde die O6-methylguanin-DNA methyltransferase (MGMT) von *D. radiodurans* untersucht. Obwohl die Klonierung und die Reinigung erfolgreich waren, war die biochemische Charakterisierung nur bedingt möglich, da keine Methyltransferaseaktivität festgestellt werden konnte. Die Faltung des Proteins schien korrekt, da die MGMT an DNA binden konnte.

Im zweiten Teil dieser Dissertation wurde die in unserem Labor beschriebene Interaktion zwischen dem Rad9/Rad1/Hus1-Komplex (9-1-1 Komplex) mit der apurinischen/apyrimidinischen Endonuklease 1 (Ape1) weiter untersucht. Durch den Gebrauch von Protein-Fragmenten konnte gezeigt werden, dass sich die Endonuklease Aktivität im N-terminalen Teil des Proteins befindet.

Weiter deuten die Erkenntnisse darauf hin, dass in der Interaktion zwischen dem 9-1-1 Komplex und Ape1 das komplette Ape1-Protein involviert ist. Schliesslich zeigen initiale Beobachtungen, dass der 9-1-1 Komplex auch mit der DNA-Polymerase λ interagiert, was bis dato nicht bekannt war.

2. Introduction

2.1. *Deinococcus radiodurans*

2.1.1. Characteristics of the radioresistant bacterium *Deinococcus radiodurans*

Deinococcus radiodurans (*D. radiodurans*) is a non-motile, non spore-forming bacteria belonging to the genus of the *Deinococcae*. Due to its pigments it has a pink to almost orange color. It is considered as a gram-positive bacteria although it differs in the composition of its cell envelope, which is similar to gram-negative bacteria. *D. radiodurans* contains a thick peptidoglycan layer and an outer membrane, some strains also having paracrystalline S-layers/lipid-composition of their cell wall and also have a different type of cell layers. The bacteria grow as chemoorganotrophic obligate aerob in rich media, whereby they reach their maximal generation time of 80 minutes when kept at 30°C. Growth only ceases with temperatures below 4°C and above 45°C (reviewed in [1, 2]).

D. radiodurans was discovered in 1956 in canned beef that was treated with what was supposed to be a sterilizing dose of ionizing radiation at that time [3]. Its genome however was only fully sequenced in 1999 [4]. It consists of 2 chromosomes, 1 megaplasmid and a smaller plasmid, which all together encode for around 3200 proteins. The genome is present as multiple copies per cell, ranging from 4 to 10, which depends on the phase of the cell cycle [5, 6]. Additionally, there were reports stating that the DNA forms a doughnut-shaped, ring-like structure, but this observation is still under debate [7]. But what makes *D. radiodurans* such an extraordinary organism is that it is one of the most radioresistant bacteria known to date, exponentially growing cultures withstanding up to 15,000 Grays (Gy) of irradiation with a shoulder of resistance at around 5,000 Gy without loss of viability [8]. The average lethal dose of 50% for mammals is about 5 Gy. Even more astonishing are those numbers in the view that an ionizing radiation (IR) dose of 6,000 Gy leads to about 200 double-strand breaks, over 3000 single-strand breaks and over 1,000 base damages [9-11]. This makes clear that there must be very sophisticated DNA repair pathways to deal with such high amounts of DNA

damages. Different models suggesting pathways that might explain the radioresistance have been proposed (reviewed in [7]):

First, scientists considered mechanisms that would protect the *D. radiodurans* genome from the huge damage. Under discussion were the pigments, which also give the bacterium its color. But this theory was discarded soon thereafter, since no links were found between pigmentation and radioresistance. Then, another idea was put forward, based on the fact that *D. radiodurans* has high internal levels of Mn^{2+} and only low amounts of Fe^{2+}. Also here, a connection to radioresistance was anticipated, assuming that the Mn^{2+} ions could somehow protect the DNA from heavy damages. But this approach had to be dismissed too, since there was experimental proof that the DNA of *D. radiodurans* was shattered into pieces as it is the case for the DNA of any other organism. However upon irradiation the DNA repair process seems to be very quick, reconstituting the whole genome within 3 hours of recovery. This moved the focus of curiosity away from passive protection mechanisms and towards very active DNA repair processes.

Here too, rather passive aspects were considered first. It was proposed that the number of genome copies per cell was important. This is based on the assumption that having more than just one copy of the genome per cell facilitates the process of finding another stretch of homologous DNA. Thus, the repair enzymes can use this as a DNA matrix for the re-synthesis of the damaged or lost DNA parts. But, although this might indeed help to rebuild parts of the genome, it cannot be the only reason for this stunning radioresistance observed, as also *Escherichia coli* (*E. coli*), which is not considered to be specially resistant to IR nor to UV or other damaging agents, can also have multiple copies of its genome at some points of its growth.

Next, an unusual form of *D. radiodurans* DNA was proposed for its ability to repair its genome fast and accurate. Based on the tight compaction of the DNA into ring-like structures, it would hamper broken DNA strands to fall apart and diffuse to distant sites of the cell. This could be beneficial for repair processes like homologous recombination. As mentioned before, this theory is now under debate, as the putative doughnut-shaped structure could not be confirmed when using another means of microscopy. However, latest findings suggest that the compaction of the genome is of importance as knock-out

strains for the histone-like, nucleoid-associated protein HU are lethal due to decompaction of the *D. radiodurans* genome (H. H. Nguyen, paper in press).
Finally, another appealing possibility could be that *D. radiodurans* evolved new, additional repair enzymes, which are unique to this bacterium. After the full sequencing of the genome, researchers were disappointed to mainly find the common set of bacterial repair proteins with only a few so far unknown proteins. But up to now none of the new proteins has proven to be the one and only responsible for the extraordinary capabilities of *D. radiodurans*. Another approach which is most favored and sustained, suggests that *D. radiodurans* has a similar set of repair enzymes as do other bacteria, but that it evolved sophisticated ways to use these enzymes in a more efficient way.
In favor for this thesis are recent findings highlighting a new mechanism, called "extended synthesis-dependent strand annealing" (ESDSA; Figure 1 and [12, 13]). In these two articles the authors found that the previously described *D. radiodurans* DNA polymerase (pol) III and DNA pol I are involved in ESDSA, together with the recombinase A (RecA) and RadA proteins. In general, DNA pol III seems to be the main polymerase, which is essential for global DNA synthesis, at least under normal growth conditions, whereas DNA pol I seems to contribute to the survival potential, probably due to is potential involvement in base excision repair (BER) pathways. RecA seems to play an essential role in promoting degradation of DNA ends as well as DNA synthesis priming after recession. RadA is believed to play an additional role in priming, but only when RecA is present; in the absence of RecA, RadA seems to work in another pathway. It is proposed that in ESDSA, the shattered chromosomal fragments are first extensively degraded by exonucleases such as RecA and RadA. This leads to single-stranded overhangs, which can work as templates as well as primers for the subsequent massive DNA synthesis, which is observed after a 1.5 hr period of degradation. In this synthesis, "patchworks" of DNA fragments are built up, consisting of "old" DNA stretches (which existed before irradiation and act as primers), as well as newly synthesized DNA parts. This synthesis is primed by the recessed, single-stranded overhangs, which invade overlapping single- or double-stranded (via D-loop formation) templates. This normally involves RecA-like activities, which is confirmed by the fact that RecA deficiency

impedes DNA synthesis. DNA pol III is essential for the initiation of this repair synthesis, whereas both DNA pols I and III are required for subsequent efficient elongation. The third Deinococcal DNA pol, DNA pol X_{Dr} seems not to be involved in this process. This is corroborated by the fact that deletion of DNA pol X_{Dr} does not lead to increased radiation sensitivity although showing a reduced rate of repair of double-strand breaks [14]. After this DNA synthesis step, ESDSA is accomplished by the RecA-dependent inter- and intramolecular crossovers to process these longer or shorter DNA stretches into single-unit sized, circular chromosomes.

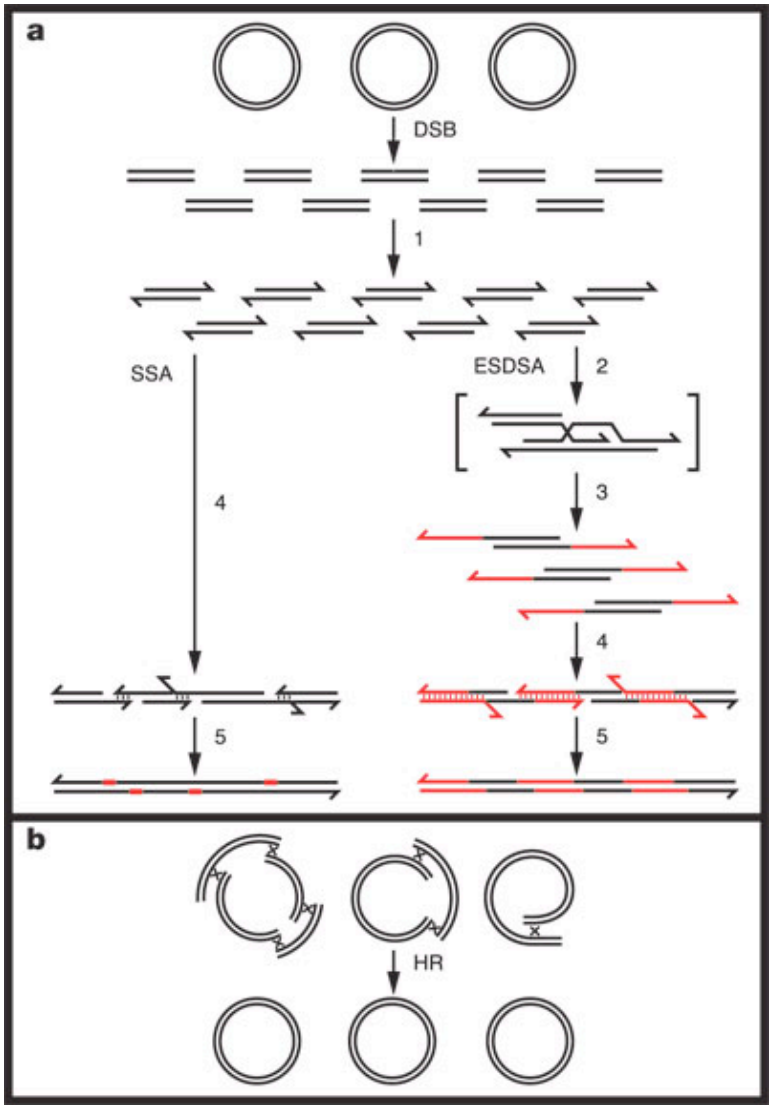

Figure 1. Two alternative two-step processes of reassembling shattered chromosomes. A) The multiple copies of the genome of *D. radiodurans* are randomly shattered into pieces of double-stranded DNA. The ends are then recessed, most probably by exonucleases (1). Then, one of two possible events can occur: either the recessed ends work as primers and templates in ESDSA (2), giving rise to newly synthesized single-stranded DNA, probably through a moving D-loop.

These newly synthesized single-stranded overhangs can engage in several rounds of extension until they find a complementary partner strand (3). The base pairing of complementary strands occurs (4), which is further processed into linear double-stranded DNA. A similar outcome is achieved by SSA, wherein the recessed DNA ends can rejoin directly through the annealing of complementary single-stranded overhangs of overlapping fragments from different chromosomal copies, thereby generating short gaps, which are filled in by the action of a DNA polymerase. **B)** The linear stretches of double-stranded DNA are then processed into circular plasmids via homologous recombination. DSB: double-strand breaks; SSA: single-strand annealing; ESDSA: extended synthesis-dependent strand annealing; HR: homologous recombination. Reproduced from Zahradka et al., Nature (2006) **443**, 569-73.

Recently, another new opinion was put forward. Daly suggested that the high Mn^{2+} and low Fe^{2+} could have a beneficial effect towards the protection of proteins rather than the DNA itself. He argues that a cell needs functional enzymes first, before it can start repairing the shattered genome and that also proteins are targets of free radicals that are produced upon radiation [15].
In summary, the current opinion is that it is most probably not one trait that accounts for *D. radiodurans*' amazing radioresistance but that it is a combination of several pathways and peculiar properties that render *D. radiodurans* so radioresistant.

2.1.2. DNA Ligases

DNA ligases are a very important class of enzymes, not only involved in DNA replication but also in DNA recombination and DNA repair. Their importance is further underscored by the fact that they are essential [16]. Additionally, they exist in all three kingdoms of life, bacteria, archaea and eukaryotes [17]. Bacterial ligases mainly use NAD^+ as a cofactor, whereas eukaryotic, viral and archaeal enzymes use ATP as nucleoside monophosphate donor [18], thus being termed NAD^+-dependent and ATP-dependent DNA ligase, respectively [19]. Recent data, however, state additional ATP-dependent ligases in bacteria, pointing into the direction that also prokaryotes have evolved different ligases for different tasks, as it is the case for eukaryotes. *D. radiodurans* is one of the examples where, in addition to a common bacterial NAD^+-dependent DNA ligase, also an ATP-dependent DNA ligase has been predicted from the DNA sequence [20].

Despite their different requirements concerning the co-factors used, the catalytic mechanism is conserved amongst the different classes of DNA ligases. Also the 4 distinct domains with several protein folds like a zinc (Zn)-finger, an oligomer-binding (OB) β-barrel, a helix-hairpin-helix (HhH) motif and the BRCA1 C-terminus (BRCT) domain are conserved to different degrees amongst the species but also in between the kingdoms [17, 19, 21].

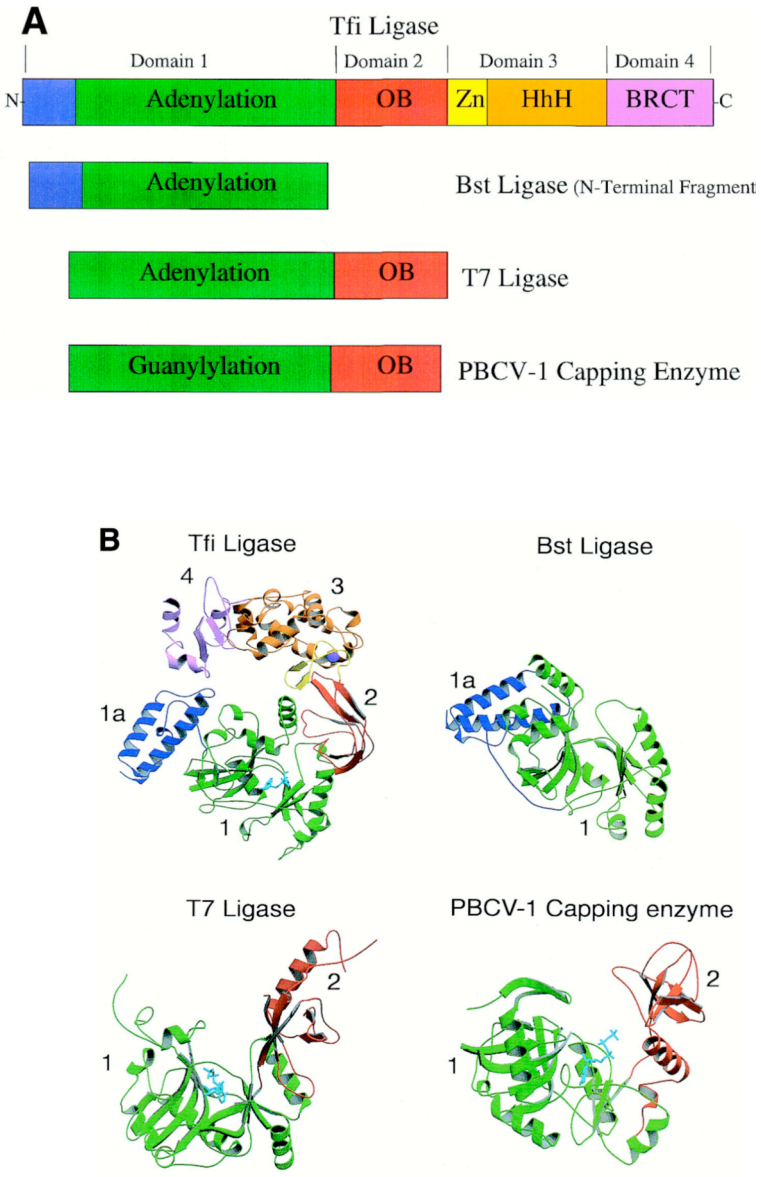

Figure 2. Domain structure of DNA ligases. A) Schematic representation of four different DNA ligases from *Thermus filiformis* (Tfi), *Bacillus stearothermophilus* (Bst), Bacteriophage T7 (T7) and Chlorella virus PBCV-1. Blue: subdomain 1a, green: adenylation domain, red: oligomer-binding (OB) fold, yellow: subdomain 3a (Zn-Finger), orange: subdomain 3b, Helix-hairpin-Helix (HhH) motif, pink: BRCA1 C-terminus (BRCT) domain. **B)** Ribbon diagrams for the four DNA ligases from A).

Colors are as in A). Reproduced from Doherty et al., Nucl. Acids Res. (2000) **28**, 4051-8.

The involvement of all the DNA ligases in the processes mentioned above consist in their ability to covalently rejoin DNA ends by forming a phosphodiesterbond between a 3`-hydroxyl and a 5`-phosphate of the DNA-backbone. This is achieved by three successive, but distinctive catalytic steps, involving two covalent intermediates (Figure 3). In step one, the enzyme itself is adenylated via a ε-aminolysyl phosphoramidate bond, using either ATP or NAD^+ as donor. In step two, the nucleotidyl moiety is transferred from the enzyme onto the 5`-phosphate end of the nick, thereby activating the 5`terminus for the attack of the 3`-hydroxyl in the third step, which restores the phosphodiester bond between the two separated strands of DNA, thereby sealing the nick [19, 22].

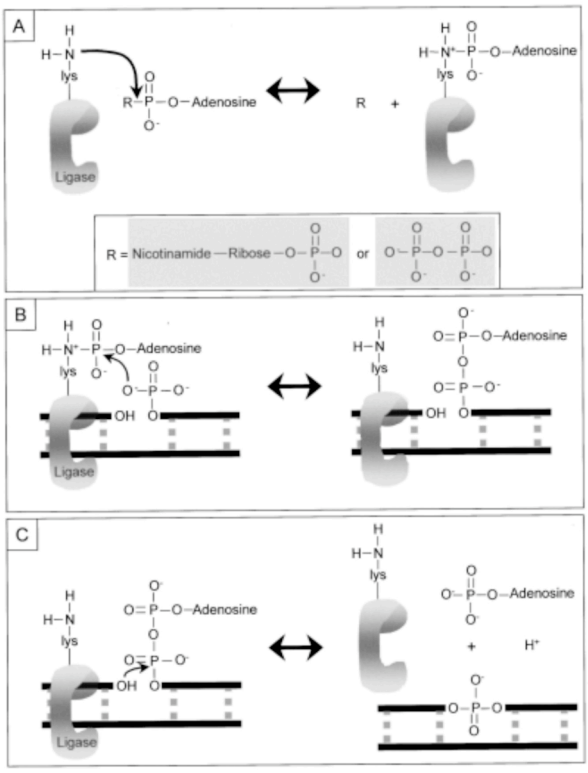

Figure 3. Ligation mechanism of bacterial DNA ligases. A) The amino-group of the catalytic lysine reacts with NAD^+ or ATP, thereby leading to a phosphoamide-linked AMP. **B)** In a next step, the 5'-phosphate at the nick attacks the activated phosphoryl group of the AMP, leading to an adenylated DNA. **C)** In the last step, the 3'-OH-group of the DNA at the nick attacks the activated phosphate at the 5', thereby

forming a phospodiester bond, thus sealing the nick and liberating the DNA ligase and the AMP. Reproduced from Wilkinson et al., Mol Microbiol (2001) **40**, 1241-8.

2.1.3. O6-methylguanine-DNA methyltransferase (MGMT)

Besides damages that target the DNA backbone and thereby lead to DNA strand breaks, there are also endogenous as well as exogenous factors that alter the structure of DNA bases. One example for this are alkylating agents which are also used as anti-cancer drugs [23-26]. One lesion that is produced is O6-methylguanine. This base-substitution has a high mutagenic and cytotoxic potential, as the O6-methylguanine will frequently mispair with a thymine instead of a cytosine in the next replication round, thus leading to a G-C → A-T transition mutation. Even if the mispairing is recognized by the mismatch repair machinery, the wrongly base paired thymine will be excised, leaving behind the altered O6-methylguanine, which might again recruit a thymine instead of the correct cytosine, which then again attracts the mismatch repair proteins. As a consequence, the futile mismatch repair might lead into apoptosis ([27, 28]; reviewed in [29]).

Besides the mismatch repair system that is making an attempt to repair those lesions, the cell evolved specialized proteins that are responsible for removing the different alkyl-adducts. The one dedicated to O6-methylguanine is called O6-methylguanine-DNA methyltransferase (MGMT). It exists in all three kingdoms of life and despite the low primary sequence similarity found amongst the members of this protein family, the overall domain structure is nearly the same, with structural motifs involved in DNA recognition, substrate binding and selectivity of the alkyltransfer mechanisms (reviewed in [30]).

The human MGMT is 22 kDa in size and ubiquitously expressed in normal tissues. It can be phosphorylated and ubiquitinated and may function in transcription regulation, cell cycle control and apoptotic signaling (reviewed in [31] and [32]). MGMT-mediated repair is unique compared to other repair pathways in four different aspects [32, 33]:

- MGMT acts alone, without another protein or a co-factor.
- it binds the alkyl group covalently to an internal cystein and therefore acts as a transferase enzyme as well as an acceptor protein.
- it is inactivated through this action.

- repair occurs in a stoichiometric fashion, which can easily lead to saturation if the DNA-adducts are occuring in excess.

The last three points highlight the unique feature of this protein, which cannot turn over, because the bond between the transferred methyl group and the acceptor cysteine, which resides in a highly conserved motif, is extremely stable. It is therefore often referred to as “suicidal” or “kamikaze” protein. Said that, it is clear that any substrate for the protein acts also as an irreversible inhibitor. Bearing this in mind, it seems reasonable that mice lacking MGMT are viable and show no obvious phenotypes unless they are treated with alkylating agents [34, 35]. Also, cells that have lost the MGMT-activity due to promoter hypermethylation or mutations in the MGMT gene are sensitized to the killing effects of alkylating agents [36-38], but this in turn can be attenuated by the additional loss of the mismatch repair system (MMR), as then, no futile attempt to repair the O6-guanine-thymine mismatch is undertaken, thus preventing induction of apoptosis [39-42].

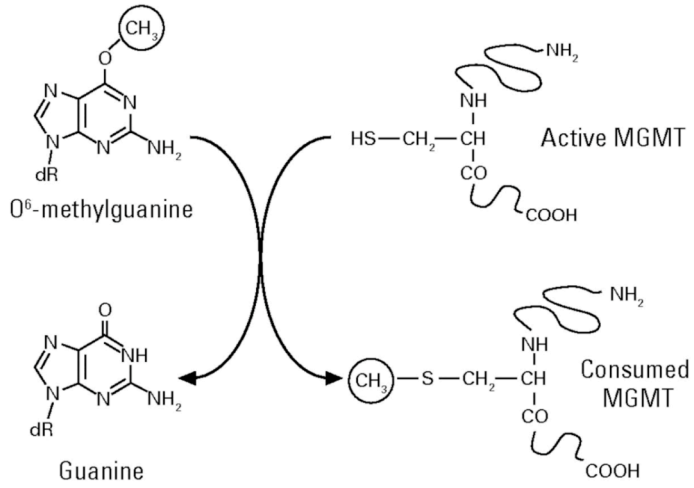

Figure 4. Mechanism of action of O6-methylguanine-DNA methyltransferase (MGMT). In the transferase proficient state, the cysteine in the active site is unmethylated. It then reacts with the methyl-group of the O6-methylguanine, whereby the methyl group is covalently attached to the MGMT. The MGMT cannot be recycled after this and is therefore degraded by the ubiquitin-dependent proteasomal pathway. Reproduced from Hegi et al., J. Clinic. Oncol. (2008) **26**, 4189-99.

2.2. DNA damage response

Cells suffer from a plethora of different assaults on its genome every day. DNA damaging agents are produced endogenously as products of normal

cellular metabolism, e.g. reactive oxygen species like superoxide anions, hydroxyl radicals or also hydrogen peroxide, which are products of oxidative respiration and lipid peroxidation occurring in the cell. Also do some chemical bonds in the DNA tend to spontaneously disintegrate under physiological conditions, leading to abasic sites or, in the case of spontaneous or induced deamination of bases, give rise to miscoding bases such as uracil (from cytosine), hypoxanthine (from adenine), xanthine (from guanine) and thymine (from 5'-methyl cytosine). There are also exogenous sources of DNA damages e.g. IR, UV radiation and environmental toxins (e.g. from tobacco smoke), as well as chemical agents used in chemotherapeutics (reviewed in [43]). The resulting DNA damages may be simple base alterations but they may also include DNA backbone damages such as single- and double-strand breaks or even DNA interstrand cross-links as well as DNA-protein cross-links.

The cell evolved different damage response reactions to counteract these lesions (reviewed in [44]):

- removal of the lesion and restoration of the continuity of the DNA duplex by different repair pathways,
- activation of DNA damage checkpoints, which leads to an arrest in the cell cycle, allowing the cell to repair damaged or incompletely replicated chromosomes,
- induction of transcriptional responses which cause changes in the transcription profile of the cell,
- and ultimately, in case of extensive DNA damage, induction of apoptosis.

For removal of the lesion, the cell has evolved highly sophisticated repair pathways, all specialized in one or a few kinds of damages.

Small chemical alterations are, if they are not repaired in a direct repair mechanism as it is the case for O6-methylguanine and MGMT, mostly targeted by base excision repair (BER). Mispaired nucleotides, as well as insertions and deletions are removed via the mismatch repair (MMR) pathway. Nucleotide excision repair (NER) concentrates on a wide class of helix-distorting lesions that interfere with base pairing as well as with transcription and replication. For DNA double-strand breaks bacteria

preferentially use homologous recombination (HR), whereas in mammalian cells more than 90% of double-strand breaks are repaired by non-homologous end-joining (NHEJ) (reviewed [43-47]).

2.2.1. Base Excision Repair (BER)

2.2.1.1. Overview

As depicted in Figure 4, BER is initiated by glycosylases that release the damaged base, thereby forming an abasic site (AP), although these sites can also be formed as a direct damage product, for example through spontaneous base loss. The glycosylases are lesion specific. Some are simple or monofunctional glycosylases and hydrolyse the N-glycosidic bond, leaving behind an abasic site with an intact phosphodiester bond. Bifunctional glycosylases not only excise the damaged base but also incise the backbone 3` to the AP-site in an β- or β, δ-elimination reaction, leading to a single-strand break in the DNA backbone and to a 3`-α, β unsaturated aldehyde or a 3`-phosphate, which is turned into a normal 3`OH-group by apurinic/apyrimidinic endonuclease 1 (Ape1) or polynucleotide kinase (PNKP), respectively. Ape1 then incises 5` to the AP-site. Finally, DNA pol β replaces the damaged nucleotide and DNA ligase IIIα (lig IIIα), in a complex with X-ray repair cross-complementing group 1 (XRCC1), can ligate the nick. This is the case for the so-called short-patch (SP-) BER, because DNA pol β only fills in one single nucleotide [48-51].

There is also a second, so-called long-patch (LP-) BER, which is particularly used when the 5`-moiety is refractory to the DNA pol β AP-lyase excision activity. In this case, strand displacement synthesis occurs using the proliferating cell nuclear antigen (PCNA)-dependent DNA pols ε or δ, together with the loading enzyme replication factor C (RF-C), replacing a 2-12 nucleotide long strand. The so created flap-structure is then cut by flap endonuclease 1 (Fen1) and the resulting nick is sealed by DNA ligase I ([52, 53], reviewed in [54, 55]).

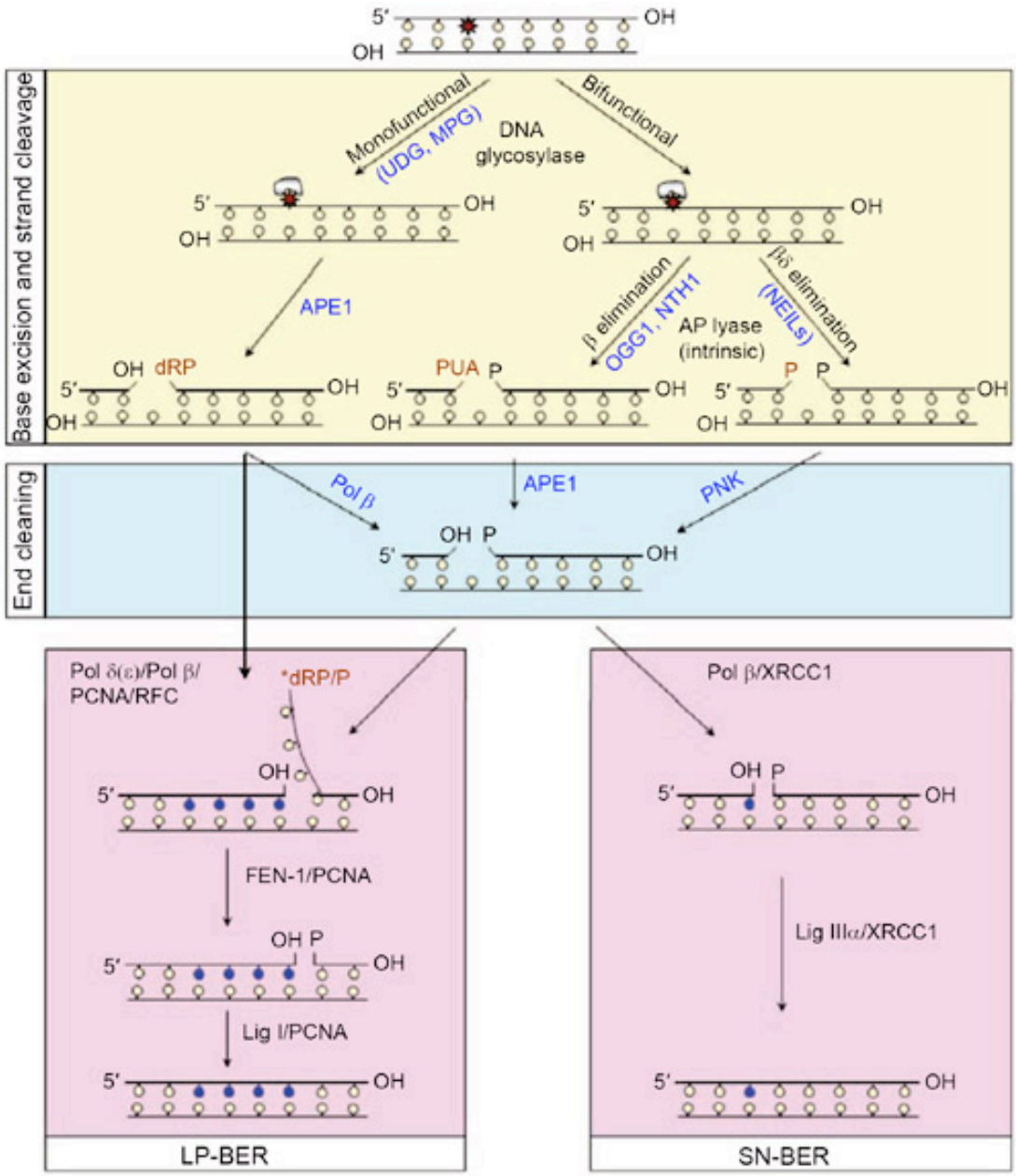

Figure 4. Schematic representation of the known base excision repair (BER) sub-pathways. BER is induced by a damaged base, which is recognized either by a mono- or a bifunctional glycosylase. After simple removal (monofunctional glycosylases) Ape1 processes the 5'-end making it available for DNA pol β. In case of bifunctional glycosylases Ape1 activity is not necessarily needed, as these glycosylases process the 5'-ends themselves. After processing of the 3'-end, one of two sub-pathways is chosen, depending on the biochemical structure of the 5'-end at the lesion. Either long-patch (LP-) BER is chosen, wherein DNA pols δ or β, together with proliferating cell nuclear antigen (PCNA) and replication factor C (RF-C) can perform strand displacement synthesis, generating a flap of two to ten nucleotides, which is subsequently removed by flap endonucease 1 (Fen1). The nick is finally sealed by DNA ligase I. In short-patch (SP-) BER, DNA pol β synthesizes only one nucleotide. The 5'-phosphate is available for sealing the nick by DNA ligase III, therefore the action of Fen1 is refractory. Reproduced from Hedge et al., Cell Res. (2008) **18**, 27-47.

2.2.1.2. Apurinic/apyriminidic endonulcease 1 (Ape1)

Apurinic/apyrimidinic endonuclease 1/redox effector factor-1 (Ape1/ref-1) is the major AP endonuclease in mammalian cells. Besides its function in BER, it also works as a redox factor, keeping transcription factors in a reduced, active state. It is also involved in the *in vivo* activation of bioreductive drugs through reduction. Furthermore, it stimulates DNA-binding of important transcription factors such as e.g. Fos, Jun, NFκB, HIF-1α or p53 [56-61]. Additionally, it acts as a negative regulator of the parathyroid hormone promoter and is part of the HREBP-transcription factor complex. In line with these important functions is the finding, that mice nullizygous are embryonic lethal [62-64].

AP endonucleases are classified into 2 families, according to their homology to the *E.coli* exonuclease III (*xth*) and endonuclease IV (*nfo*) [65]. Human Ape1 belongs to the Exo III-family, together with mouse APEX or Drosophila RrpI. This enzyme class is characterized by its strong AP hydrolytic activity and an additional 3`-diesterase activity.

Although there is only about 25-40% sequence identity between the human Ape1/Ref-1 and its prokaryotic homologs, there is a high degree of homology amongst the mammalian AP-endonucleases on the protein-level (reviewed in [65]). Human Ape1/Ref-1 is a 2.6kb gene, coding for 5 exons (whereof the first is non-coding) separated by 4 introns. These are translated into 318 amino acids, which gives rise to a 37kD protein, consisting of 2 domains, each of which is made up of a 6-stranded β-sheet, surrounded by α-helices, thereby forming a 4-layered α/β-sandwich [65-70].

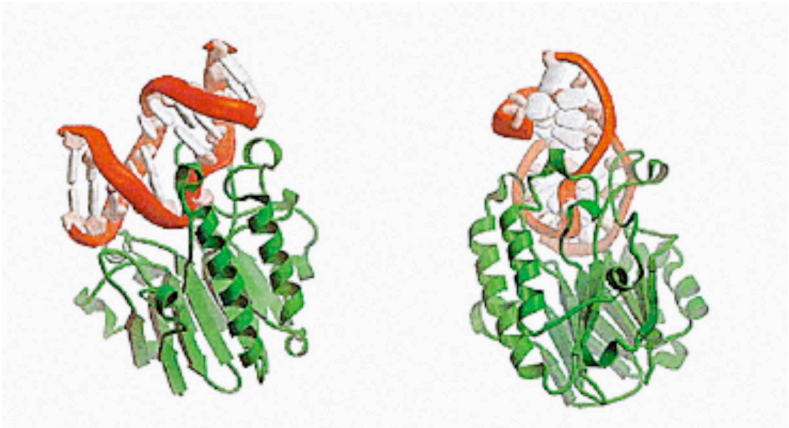

Figure 5. Christal structure of Ape1 bound to DNA. Reproduced from Wilson et al., Nat Struct Biol (2000) **7**,176-8.

Different residues responsible for substrate recognition, Mg^{2+} positioning and building up of the active site nucleophil have been identified [69, 71].

The expression profile of Ape1/Ref-1 is complex and heterogenous, differing among tissue types and even between neighboring cells, which may be explained by its multifunctional roles in the cell [66, 72-74]. In some cell types, it is solely found in the nucleus, sometimes in association with chromatin (e.g. in the cerebellum), sometimes not (e.g. in epidermal cells), whereas in other cells, it is cytoplasmatically localized (e.g. in macrophages or spermatozytes), but again other cells show nuclear as well as cytoplasmatic staining (e.g. in adrenal cortical cells) (reviewed in [65]).

Ape1/Ref-1 is regulated at the transcriptional as well as at the post-translational level. Translational regulation includes induction by oxidative agents, which transiently increase the mRNA and protein level due to *de novo* synthesis, thereby increasing the cells` resistance to killing by H_2O_2, MMS and other genotoxic agents.

Post-translational modifications are mainly manifested in phosphorylation of different residues, but the effects of these are not fully understood yet but seem to be dependent on the type and site (amino acid residue) of the modification. Furthermore, Ape1/Ref-1 is acetylated by p300, which has yet to be linked to a modulation of the repair capacity, but appears to be linked to its redox potential exclusively (reviewed in [48]).

Last but not least, Ape1/Ref-1 is reduced by thioredoxin (TRX), thereby enhancing the sequence specific binding of AP-1 and p53, which is mediated through Ape1/Ref-1.

This underscores the important involvement of Ape1/Ref-1 in processes like DNA repair, cell cycle control, apoptosis, angiogenesis, cellular growth and differentiation, neuronal excitation, hematopoiesis and development (reviewed in [65]).

2.2.2. Cell cycle checkpoint

2.2.2.1. Overview

Cells are challenged with a variety of DNA damages every day. To counteract the detrimental effects of these endogenous and exogenous insults, the cells have evolved elaborate mechanisms to ensure genomic stability. One damage response mechanism is the initiation of cell cycle checkpoints. DNA damage checkpoints were first defined as non-essential regulatory pathways that control the ability of cells to arrest the cell cycle in response to DNA damage, allowing time for DNA repair (reviewed in [75]). However, this definition is too simple. Emerging evidence suggests that these pathways are additionally involved in the control of DNA repair pathways, the composition of telomeric chromatin and the movement of repair proteins to sites of damage, activation of transcriptional programs, telomere length and, induction of apoptosis. Cell cycle checkpoints have been identified at the G1/S and G2/M boundaries, as well as during the S phase and potentially also in mitosis.

The signal transduction in checkpoint response is thought to be organized into sensors, which recognize the DNA damage, mediators and transducers, which mediate and transmit the signal to the effectors, which then in turn ultimately trigger the different responses to the damages [76].

In general, two main pathways can be distinguished, although they may interact at various stages:

(i) Replication stress and other single-strand generating DNA damages like UV irradiation induce the phosphorylation of checkpoint kinase 1 (Chk1) by Ataxia telangiectasia and Rad3 related kinase (ATR). Activated Chk1 stabilizes stalled replication forks, blocks the firing of late replication origins and arrests cells in the G2 to M phase.

(ii) Double-strand breaks, for example induced through IR, are believed to trigger Ataxia telangiectasia mutated kinase (ATM) activation, which in turn phosphorylates checkpoint kinase 2 (Chk2). This leads, amongst other outcomes, to phosphorylation of p53, which, via transcriptional activation of p21, prevents the entry from G1 into S phase of the cell cycle.

In spite of the simplified view presented above, G2/M arrest most likely functions via an interplay between the transducer kinases Chk1 and Chk2.

Furthermore, abolishment of G2/M arrest is mediated by another class of proteins, namely the Cell division cycle phosphatases (Cdc25), which are themselves phosphorylation targets of Chk1 and Chk2 and are required to remove the inhibitory Cyclin dependent kinase (Ckd) phosphorylation, thereby allowing progression from G2 into mitosis (reviewed in [76, 77]).

The Rad9/Rad1/Hus1 (9-1-1) complex was originally found in genetic screens for sensitivity to genotoxins. The complex was found to be targeted to the nucleus and to DNA damage sites after genotoxic stress, implicating a role in DNA damage recognition ([78] and reviewed in [77]). Further insights came then from molecular modeling, reveilling a structural resemblance to PCNA, a doughnut-shaped homotrimeric clamp, which is loaded around DNA at sites of replication, serving as a sliding platform to tether replication proteins to the DNA [79-87]. Additional studies found that ATM-mediated phosphorylation of Rad9 was necessary for IR-induced checkpoint activation and that loading of the 9-1-1 complex to the damaged sites affects the target specificity of ATR, thereby further highlighting a role in sensing DNA damage and also implicating a role in the activation of checkpoint signaling pathways [88]. Furthermore, the alternative clamp loader, Rad17-RFC_{2-5}, known to be important for efficient loading of the 9-1-1 complex to damaged sites, was shown to be critical, as disruption of phosphorylation of Rad17 by ATM and ATR relieved G2 arrest, thereby leading to an increased sensitivity upon genotoxic stress [89].

Growing evidence suggests that the 9-1-1 complex not only acts as a sensor of DNA damage, but is also involved in DNA damage repair. It was shown that the 9-1-1 complex interacts with and stimulates various BER components [90-98].

Taken together, the 9-1-1 complex appears to not only mediate proper checkpoint activation and signaling through ATM and ATR, but it can also stimulate conventional DNA repair pathways, thereby providing an unique link between cell cycle checkpoints on one hand and repair pathways on the other hand.

2.2.2.2. Structure of the 9-1-1 complex

The three human proteins Rad9, Rad1 and Hus1 form a heterotrimeric complex, the 9-1-1 complex. The single subunits interact in a head-to-tail fashion comparable to PCNA, giving rise to a ring-shaped, 110 kDa sized protein-complex, which is 10 +/- 2 nm in diameter and has a hole of 2-3 nm in its middle ([99] and Figure 6).

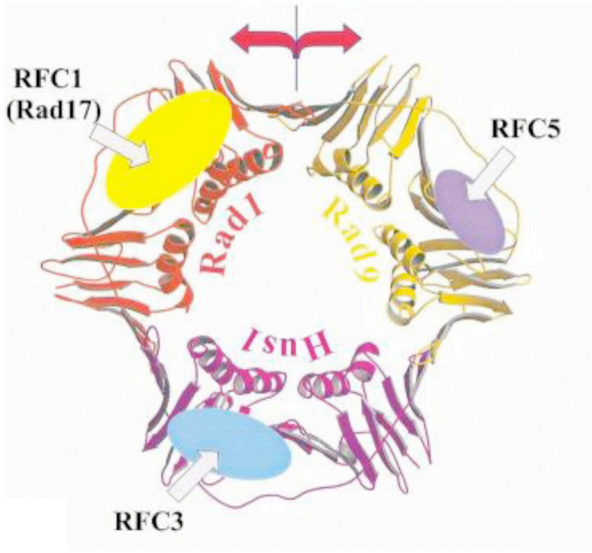

Figure 6. Structure of the Rad9/Rad1/Hus1 (9-1-1) clamp and topography of the interactions with the subunits of the checkpoint clamp loader, Rad17-RF-C_{2-5} complex. The white arrows indicate the interaction sites with Rad17-RF-C_{2-5} subunits. Reproduced form Venclovas et al., Protein Sci. (2002) **11**, 2403-16.

Rad1 and Hus1 together build a pre-complex in the cytoplasm before associating with Rad9 and being translocated to the nucleus through the NLS residing in the C-terminal end of Rad9 [79, 82, 85, 100]. Through this controlled transport from the cytoplasm to the nucleus a sort of quality control is achieved, as for the integrity and also functionality of the complex, all three subunits are needed [101]. Furthermore, it was found that in $Hus1^{-/-}$ mouse embryonic fibroblasts (MEFs) the levels of Rad9 decreased and that Rad9 localized exclusively in the cytoplasm, indicating that transport of Rad9 is also dependent on the presence of Hus1 [101]. The finding that the entire complex is likely necessary for translocation into the nucleus was further underscored

in fission yeast, where nuclear localization was also dependent on Rad9 as well as on Rad1 [80].

2.2.2.3. Rad9

The human Rad9 consists of 391 amino acids giving rise to a protein of 43 kDa. It shares 25% identity and 52% similarity with the *Schizosaccharomyces pombe* (*S. pombe*) Rad9 protein, which is consistend with the finding that the human protein can at least partially complement the radiosensitivity of a yeast Rad9 null mutant [102].

Rad9 is a nuclear protein that exerts a multitude of cellular processes as for example the mediation of G2/M and S-phase checkpoint activations through the regulation of phosphorylation of Rad17, Chk1, Chk2 and others upon replication block and DNA damage [78, 87, 103]. Additionally, it is thought to be a critical player in chromosomal stability and integrity as knock-out cells display an increased frequency of chromosomal abnormalities. Furthermore, $Rad9^{-/-}$ mice are embryonic lethal [103, 104].

Over ten phosphorylation sites have been mapped in the 110-amino acid C-terminal domain, some of which are required for phosphorylation of Chk1 and interaction with DNA topoisomerase II binding protein 1 (TopBP1). In contrary, the 110-amino acid domain is not required for the interaction with Rad1 or Hus1 [87, 88].

2.2.2.4. Rad1

Human Rad1 is a 283 amino acids protein. It is 32 kDa in size and predicted to be highly acidic. Like the human Rad9 protein, it is highly conserved, demonstrated by 31% identity and 42.6% similarity to the *S. pombe* Rad1 protein. It exists in three different variants, Rad1-a being the largest; Rad1-b contains an in-frame stop codon in the middle of the Rad1-a open reading frame, resulting in the deletion of nucleotides 199 through to 307. The third variant is missing residues -59 through to 21 of Rad1-a, which eliminates the putative translation start codon of Rad1-a [105]. Rad1-a shows 3` to 5`exonuclease activity, which is not seen with the two other Rad1 forms.

Loss of Rad1 *in vivo* leads to a destabilization of Rad9 and Hus1. Disruption of the 9-1-1 complex leads to major defects in S-phase control, as well as chromosomal abnormalities and radioresistant DNA synthesis. Furthermore, in cells depleted for Rad1 the ATR-dependent Chk1 activation is impaired, but not the one of Chk2, mediated by ATM [106].

2.2.2.5. Hus1

Mammalian Hus1 is 31 kDa in size, consisting of 280 amino acids, which confer a 30% identity to the *S. pombe*. It is expressed throughout embryonic development, which is also mirrored in the embryonic lethality of $Hus1^{-/-}$ mice [107, 108]. Hus1 is rapidly degraded in the cytoplasm via the ubiquitin-proteosomal pathway if it is not in a heterodimeric pre-complex with Rad1, thereby being stabilized. In *Xenopus leavis* egg extracts as well as in *S. pombe* ATR-dependent phosphorylation of Hus1 is observed [109]. Furthermore, in Hus1 knock-out MEFs, abrogated checkpoint response to UV irradiation was observed along with replication blocks, increased apoptosis, increased frequency of chromosomal abnormalities and S-phase specific accumulation of phosphorylated H2AX, which is a marker for double-strand breaks in DNA [107, 108].

2.2.3. DNA polymerase λ

DNA polymerases are template-directed machines for the phosphoryl transfer, which are needed to build up long polymers of nucleotide monophosphates in DNA replication and repair. Since the discovery of the first eukaryotic DNA pol α in 1957 the number of eukaryotic polymerases has grown to about 20 known DNA pols today, which were all classified according to their primary sequence, giving rise to the DNA pol families A, B, X, Y and RT. DNA pol λ belongs, together with DNA pol β, terminal deoxyribonucleotidyl transferase (TdT), DNA pol μ and the African swine fever virus DNA pol to the DNA pol X family [110].

DNA pol λ is a single-subunit enzyme, lacking a 3`→5` exonuclease activity (Figure 7). The human 575 amino acids enzyme consists of an N-terminal

BRCT domain, important for protein-protein interactions, a serine-proline rich region, which is involved in post-translational modifications of the enzyme [111], as well as a 39kDa catalytic core, which shares 33% amino acid similarity with the catalytic core of DNA pol β [112]. Furthermore, the catalytic core can be subdivided into an N-terminally located 8kDa domain, containing the dRP lyase activity and the polymerase domain, which itself again is further subdivided using the terminology of a human right hand [113]; the fingers domain includes important residues for interaction with the incoming deoxyribonucleoside triphosphates as well as for the template base to which it is paired. The thumb may play a role in positioning the duplex DNA and in processivity and translocation. The palm finally contains the catalytic carboxylates [112].

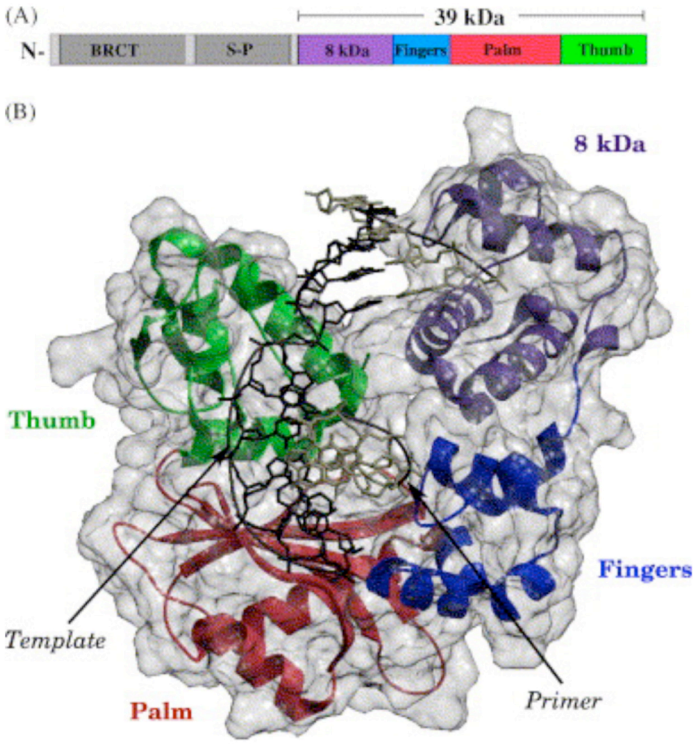

Figure 7. Structure of the human DNA polymerase λ. A) Schematic representation of the domain structure of DNA pol λ. Grey: BRCA1 C-terminus (BRCT) domain and serine-proline (SP) domain, violet: 8kDa domain, blue: fingers domain, red: palm domain, green: thumb domain. **B)** Ribbon diagram of DNA pol λ in contact with DNA, representing the spatial distribution. Color code is as in A). Reproduced from Garcia-Diaz et al., DNA Repair (2005) **4**, 1358-67.

Unlike for DNA pol β, the fingers and thumb domain of DNA pol λ do not switch from an open to a closed conformation upon dNTP binding; rather DNA pol λ is in a closed conformation (and therefore in an active state) also before dNTP binding [114]. This implicates that catalysis only depends on the correct positioning of the substrate. The discrimination between correct and incorrect insertion is likely related to subtle conformational changes in the active site. Additionally, interactions with the minor groove of DNA could contribute to nucleotide selectivity; base damage or also non-Watson Crick base pairs might result in a non-catalytical positioning of the 3`-O or the α-phosphate, thereby preventing catalysis.

Nonetheless, DNA pol λ has an unusually low fidelity and an unique error specificity; its average single base deletion error rate exceeds its average single base substitution error rate [112]. This might be in relation to its ability to use template-primer with limited base pair homology at the primer terminus, which is the case in NHEJ where DNA pol λ seems to play a crucial role. In favor for this would also be the fact that DNA pol λ has a dRP lyase activity, which can remove blocking 5`-terminal sugar phosphate (dRP) groups. Besides its supposed function in NHEJ, DNA pol λ is also involved in BER. Studies carried out in our laboratory suggested important roles of RP-A in helping DNA pol λ to faithfully act: RP-A, together with PCNA, can suppress completely the deoxyribonucleotidyltransferase activity of DNA pol λ, while stimulating its polymerase activity [115]. RP-A, but not PCNA, selectively prevents the misincorporation of an incorrect nucleotide by DNA pol λ, without affecting correct incorporation [116]. RP-A and PCNA thus allowed the correct incorporation of dCTP opposite a template 8-oxo-G by DNA pol λ 1200-fold more efficiently than incorrect dATP. Furthermore, RP-A and PCNA enhance the fidelity of translesion synthesis of 2-OH-A in a repeated sequence by DNA pol λ [117]. RP-A and PCNA can therefore act as molecular switches to activate the DNA pol λ-dependent highly efficient and faithful repair of A:8-oxo-G mismatches in human cells, while they inhibit the less faithful DNA pol β thus coordinating the DNA polymerase selection in 8-oxo-guanine repair [118]. Taken together, These findings suggested for the first time a novel accurate mechanism to reduce the deleterious consequences of oxidative

damage and, in addition, point to an important role for RP-A and PCNA in determining a functional hierarchy among different DNA pols in the lesion bypass of 8-oxo-G [119].

3. Aim

The aim of this thesis was to characterize four different DNA repair proteins.
In the first part, two DNA repair enzymes of the radiationresistant bacterium *D*. *radiodurans* should be studied and biochemically characterized, being first, two putative DNA-ligases and second a methyl guanine methyltransferase.
In the second part, two enzymes involved in human DNA repair were studied, being first the interaction between the 9-1-1 complex and Ape1 and its fragments, and second, an interaction between the 9-1-1 complex and DNA pol λ.

4. Materials and Methods

4.1. Chemicals

Protein G beads were from Amersham Biosciences. Anti-HA beads were from Sigma. All other reagents were of analytical grade and were purchased from Merck or Fluka. Primers were from Microsynth.

4.2. Proteins and Antibodies

Bovine serum albumin (BSA) was purchased from New England Biolabs. Human MGMT was from Sigma or Alexis (see Results). The human His-Rad9-1-1 complex was purified as described [96]. DNA pol λ was expressed and purified as described [120]. Anti-DNA polλ and anti-Ape1 antibodies were raised in rabbits against the recombinant wild-type proteins by standard methods. Anti-DNA pol β antibody was from Thermo. Anti-His antibody was from Qiagen. Anti-Rad9 antibody was a gift from R. Freire (Teneriffe, Spain), anti-Rad1 antibody, together with the anti-Hus1 antibody was from Santa Cruz Biotechnology. Secondary anti-mouse and anti-rabbit antibodies were from Amersham biotechnology. Anti-goat antibody was from Santa Cruz Biotechnology.

4.3. Buffers and Solutions

Coomassie stain	**Coomassie destain**
0.25% (w/v) Coomassie blue R250 40% (v/v) methanol 10% (v/v) acetic acid	10% (v/v) acetic acid 10% (v/v) isopropanol

EDTA (0.5M, pH 8.0)
Dissolve 186.1g EDTA (disodium salt) in 800ml H_2O
While stirring, gradually add 20g NaOH
Adjust with ddH_2O to 950ml
Adjust pH to 8.0 using 1.0 M NaOH
Adjust with ddH_2O to 1 l
(autoclave)

DNA loading buffer (10x, for agarose gels)
50% (v/v) glycerol
50mM Tris/HCl, pH 7.5

20mM EDTA
0.1-0.2% Bromophenol blue
0.1-0.2% Xylene cyanol
if needed add 5µl of 5mg/ml Ethidium bromide to the DNA loading buffer

Ethidium bromide
50mg Ethidium bromide
dissolve in 10ml H_2O
use 10µl per 100ml agarose solution

TAE (10x)
400mM Tris base
10mM EDTA
11.5ml glacial acetic acid
adjust to pH 8.0

Hybridization buffer (10x)
300mM Tris/HCl, pH 7.5
500mM NaCl
10mM EDTA

TBE (10x)
900mM Tris base
900mM Boric acid
20mM EDTA

DNA polymerase λ buffer (10x)
500mM Tris/HCl, pH 7.5
500mM NaCl
10mM β-mercaptoethanol

Stop buffer (PAA gels)
96% Formamide
20mM EDTA
0.02% Bromophenol blue
0.02% Xylene cyanol

Laemmli buffer (4x)
500mM Tris/HCl, pH 7.5
4% (w/v) SDS
20% (v/v) glycerol
40mM DTT
0.02% (w/v) Bromophenol blue

TBST (10x)
10mM Tris/HCl, pH 7.5
150mM NaCl
0.1% (v/v) Tween 20

Resolving gel buffer for SDS-PAGE
1.5M Tris base
0.4% (w/v) SDS
adjust to pH 8.8 with HCl

Stacking gel buffer for SDS-PAGE
0.5M Tris base
0.4% (w/v) SDS
adjust to pH 6.8 with HCl

Running buffer for SDS PAGE (5x)
125mM Tris/HCl, pH 7.5
1M glycine
0.5% (w/v) SDS

Transfer buffer for SDS PAGE
25mM Tris/HCl, pH 7.5
150mM glycine
20% (v/v) Methanol

Dilution Buffer Ape1
25mM Tris/HCl, pH 7.5
2.5mM ß-Mercaptoethanol
75mM NaCl
15% glycerol

dRP-Lyase Buffer (10x)
500mM Tris/HCl, pH 7.5
200mM KCl
20mM DTT
5mM $MgCl_2$

4.4. Western blot analysis

Proteins were separated on a 15% SDS-PAGE gel (40% stock solution Acrylamide/Bis, solution (37.5:1), (Serva)) and electroblotted for 1.5h at 100V, (BioRad Western Blot apparatus) onto nitrocellulose membran (Immobilon) in transfer buffer at 4°C. After blocking the membranes for 60min in TBST containing 2.5% (w/v) powdered milk, the membranes were incubated with the appropriate antibodies, diluted in TBST for 2h at room temperature. Then the membranes were washed 3 times for 10min in TBST and incubated with the corresponding secondary antibodies, diluted in TBST, for 1h at room temperature. This was followed by again washing 3 times for 10min in TBST. The antibodies bound to the membranes were detected by Uptilight HRP blot Reagent A (Uptima) or SuperSignal West Dura Extendent Duration Substrate (Pierce).

4.5. Biochemical characterization of two putative DNA ligases in the radioresistant bacterium *Deinococcus radiodurans*

My contribution in this study was the characterization of the divalent cation requirements, as well as the ligation activities. Furthermore, I helped in preparing the manuscript, specially in making the scheme of the ligase domains, represented in Figure 1B. For details see 5.1.1: Original research article "Enzymes involved in the DNA ligation and end-healing in the radioresistant bacterium *Deinococcus radiodurans*" (Blasius et al., BMC Molecular Biology (2007) **8**, 69).

4.6. O6-methylguanine-DNA methyltransferase (MGMT) of *Deinococcus radiodurans*

4.6.1. Cloning of MGMT

Cloning was done using *D. radiodurans* genomic DNA as a template and 400nM of each forward and reverse primer (Forward: 5'-CTAG*CGGATCC*GTTGAGGGCCAGGCCG-3'; Reverse: 5'-CGCCCG*GAATTC*CTACAGAAGACGTTGAGC-3'; restriction sites are

depicted in italic), as well as 50% DMSO, 200μM dNTPs, 1x HF-buffer and 2 units of Phusion™ High-Fidelity DNA pol (both from Finnzymes). PCR was done in a final reaction volume of 50μl; the cycle program was as follows: 95°C for 1min, 95°C for 30sec, 55°C for 30sec and 73°C for 1min. The final elongation was again at 73°C for 5min. The three middle segments were repeated 35 times. After digestion of the PCR-fragment with BamHI and EcoRI (New England Biolabs) for 1h at 37°C, it was ligated into a pRSETb vector (Invitrogen) overnight at 16°C by the T4 DNA Ligase (Fermentas). Then, *E. coli* DH5α cells (Invitrogen) were transformed with the ligation-mix and plated on LB-agarplates, containing ampicillin to select for transformed bacteria. Colonies were picked the next day and an overnight liquid LB culture was inoculated, whereof the following day, the plasmid was purified according to the manufacturers protocol (NucleoBond plasmid purification, high copy plasmid purification by Macherey-Nagel). The plasmid was subsequently sent for sequencing (Microsynth).

4.6.2. Purification of MGMT

2 liters of BL21(DE3) *E. coli* cells (Novagen), carrying the pRSETb-vector with the integrated MGMT-sequence, were grown to an OD_{600} of 0.5 – 0.7 and expression of the MGMT protein was induced by adding IPTG to a final concentration of 1mM. Cells were kept at 20°C for 2h before centrifuging for 30min at 4000 rpm in a pre-cooled Sorvall H6000A rotor. All further purification steps were done at 4°C. The cells were resuspended in 20ml buffer A (10mM Tris/HCl pH 7.5, 30mM KH_2PO_4, 500mM NaCl, 10mM Imidazole and 1mM PMSF), containing lysoszyme (1mg/ml). Cells were kept for lysis for 2h at 4°C. After this, the cells were sonicated (on ice, 10sec, 40% duty cells, Branson Sonifier Cell disruptor B15) and centrifuged for 30min at 20000rpm in a pre-cooled sorvall SS-34 rotor. The supernatant was then loaded onto a 1ml HisTrap™HP column using an ÄKTApurifier™ (both GE Healthcare). After washing with 5 column volumes, the buffer was exchanged to buffer B (10mM Tris/HCl pH 7.5, 30mM KH_2PO_4, 50mM NaCl, 10mM imidazole and 1mM PMSF). After an equilibration step, the protein was eluted from the His-column with buffer C (10mM Tris/HCl pH 7.5, 30mM KH_2PO_4,

50mM NaCl, 1M imidazole and 1mM PMSF). The eluted fractions were pooled according to a Coomassie Blue R250 stained SDS-PAGE, loaded onto a HiTrap^{TM}Q HP column (from GE Healthcare), which was equilibrated in buffer D (50mM Tris/HCl pH7.5, 50mM NaCl, 0.1mM EDTA and 10% (v/v) glycerol). Under these conditions MGMT does not bind. Protein concentrations were determined by Bradford, and the purity of MGMT was estimated on an SDS-PAGE gel stained with Coomassie Blue R250.

4.6.3. Band shift assay

(i) An in DH5α *E. coli* cells amplified and subsequently purified (NucleoBond plasmid purification, high copy plasmid purification by Macherey-Nagel) pRSETb plasmid vector was digested with BamHI and EcoRI to linearize the DNA. Next, 90ng of plasmid DNA was incubated with the putative MGMT in a mix supplemented with 50mM Tris/HCl, pH 7.5. After 15min incubation at 37°C, 50% sucrose was added and the mix loaded onto a 0.75% agarose gel without ethidium bromide. Separation was achieved by running it for 5h with 35-40V. Then, the gel was stained with ethidium bromide for 1h, followed by 3 times 5min destaining.

(ii) An alternative band shift assay was provided by F. Fischer and J. Jiricny from the IMCR: The reaction was done in a final volume of 20μl, containing 10% (v/v) gylcerole, 100mM KCl, 25mM Hepes/KOH pH 7.0, 1mM DTT, 0.5mM $MgCl_2$, 0.1mM ADP, 0.1mg/ml BSA, 60ng polydC, 50fmol template-DNA, and either 0.2U hMGMT from Sigma, or the indicated amounts of the putative MGMT from *D. radiodurans*. The reaction was incubated for 10min at 37°C. Then proteinase K was added to a final concentration of 0.06mg/ml. The reaction was incubated for 15min at 37°C, followed by a heat-inactivation for 15min at 70°C. Then, MutSα was added to a final concentration of 0.0275mg/ml. The reaction was again incubated for 15min at 37°C. Then, 10μl were loaded onto a 5% polyacrylamide gel and the bands were separated.

4.6.4. MGMT DNA-substrate preparation for a trichloroacetic acid assay

500µl calf thymus DNA (2mg/ml) were mixed with 20µl of [^{3}H]MNU (0.2mCi) and put at 37°C for 4h. Then, the DNA was precipitated by adding 0.1 volume of 3M sodium acetate (CH_3COONa) and 2 volumes of cold ethanol and subsequently put at –20°C for at least 1h. The mix was then centrifuged for 30min at 14000rpm at 4°C. The pellet was washed three times with cold 95% (v/v) ethanol; in between it was again centrifuged for 20min. Finally, the pellet was dried and re-dissolved overnight at 4°C in 0.15M sodium chloride (NaCl) containing 0.015M sodium citrate ($Na_3C_6H_5O_7$) (in a total volume of 0.5ml). The next day, the DNA was precipitated and dried as described above. Finall, it was re-dissolved in 0.5ml of 50mM Tris/HCl, pH 8.0 and stored at -20°C until use.

4.6.5. O6-methylguanine-DNA methyltransferase assay

The reaction mix contained 70mM Hepes/KOH pH 7.8, 1mM DTT, 5mM EDTA, 10µg BSA, 78000 dpm DNA and the indicated amounts of MGMT in a final volume of 100µl. Human MGMT from Alexis was used as a positive control. The mix was put at 37°C for 15min, followed by the addition of 500µl 5% (v/v) Trichloroacetic acid (TCA) to terminate the reaction. Then, the reaction was put at 90°C for 15min to hydrolyze the DNA in TCA, followed by cooling down on ice for additional 15min. Then 100µl BSA (1mg/ml) were added and the mix was transferred onto filter under suction (Whatman GF/C filter, 2.5cm in diameter). The filters were washed three times with TCA, followed by one wash with ethanol. Finally, the radioactivity was measured in a liquid scintillation counter.

4.7. Interaction studies of the human apurinic/apyrimidinic endonuclease 1 (Ape1) and its fragments with the Rad9/Rad1/Hus1 (9-1-1) complex

4.7.1. Cloning of wild-type Ape1 and its untagged fragments

Six different truncated Ape1 fragments were generated; all forward primers contained a restriction site for NheI (in italic), all reverse primers one for BamHI (in italic, too).

Forward primer full-lenght fragment: 5`-ATG *GCT AGC* CCC AAG CGT GGG AAA AAG GGA GC-3`;

Reverse primer full-length fragment: 5'-TAG *GGA TCC* TCA CAG TGC TAG GTA TAG GG-3';

Reverse primer fragment A: 5`-TTA *GGA TCC* CTC TGA ACA TTT GGT CTC TTG AAG GC-3';

Forward primer fragment B: 5`-CAT *GCT AGC* GAG AAC AAA CTA CCA GCT GAA CTT CAG G-3';

Reverse primer fragment B 5`-ATA *GGA TCC* GTT CCC CTT GG GTT GCG AAG G-3';

Forward primer fragment C: 5`-TCA *GCT AGC* GGG AAC AAA AAG AAT GCT GGC-3`.

PCR was done in a total volume of 50µl, containing 5ng DNA, 1x HF-buffer, 200µl of each dNTP, 400nM of each forward and reverse primer and 2U Phusion^{TM} High-Fidelity DNA pol. PCR cycles were 30sec at 98°C, 10sec at 98°C, 20sec at 68°C, 20sec at 72°C and final elongation for 5min at 72°C. The middle part was repeated 35 times. PCR products were digested with NheI and BamHI and ligated into a pET11a vector using T4 DNA ligase. The sequences were verified by Microsynth.

4.7.2. Purification of wild-type Ape1 and its untagged fragments

Cultures of *E. coli* BL21(DE3) or *E. coli* BH110 (knock-out strain for *xth* and *nfo*; kindly provided by M. Saparbaev) cells transformed with the respective expression plasmid were grown in LB medium supplemented with the required antibiotics at 37°C to an OD_{600} of 0.4–0.8, then IPTG was added to a

final concentration of 1mM and cells were further incubated for 2–4h at 37°C. Cells were washed with 20ml of washing buffer (20mM Tris/HCl pH 7.5 and 100mM NaCl), resuspended in Buffer A (20mM Hepes/KOH pH 7.5) and lysed with a French press. Cell lysate was centrifuged in a Sorvall SS-34 rotor and the supernatant was diluted to 1/6 final volume of Buffer B (20mM Hepes/KOH pH 7.5, 1M NaCl) and loaded onto a 1ml HiTrap^{TM}Q Sepharose column which was equilibrated with 20% Buffer B. The flow-through was directly loaded onto a 1ml HiTrap^{TM}Heparin column equilibrated with 10% Buffer B. Gradient elution was performed with 10% to 70% Buffer B. The eluted protein was pooled according to a SDS-PAGE gel stained with Coomassie Blue.

4.7.3. Cloning of HA-tagged full-length Ape1 and its fragments

Six different truncated Ape1 fragments were generated; all forward primers contained a restriction site for NheI (in italic), all reverse primers one for BamHI (in italic, too). In addition, the reverse primers harbor the sequence for the HA tag (hemagglutinin epitope of human influenza A virus; underlined).

Forward primer full-lenght fragment: 5`-ATG *GCT AGC* CCC AAG CGT GGG AAA AAG GGA GC-3`;

Reverse primer full-length fragment: 5`-TAG *GGA TC C*TC A<u>TG CGT AGT CAG GCA CGT CGT AAG GAT AAG C</u>CA GTG CTA GGT ATA GGG-3'.

Reverse primer fragment A: 5`-ATA *GGA TCC* <u>TGC GTA GTC AGG CAC GTC GTA AGG ATA AGC</u> GTT CCC CTT GGG GTT GCG AAG G-3'.

Forward primer fragment B: 5`-CAT *GCT AGC* GAG AAC AAA CTA CCA GCT GAA CTT CAG G-3'.

Reverse primer fragment B: 5`-ATT *GGA TCC* TCA <u>TGC GTA GTC AGG CAC GTC GTA AGG ATA AGC</u> CTC TGA ACA TTT GGT CTC TTG AAG GC-3`.

Forward primer fragment C: 5`-TCA *GCT AGC* GGG AAC AAA AAG AAT GCT GGC-3`.

PCR was done as described in 4.7.3. PCR products were digested with NheI and BamHI and ligated into a pET11a vector using T4 DNA ligase. The sequences were verified by Microsynth.

4.7.4. Purification of the HA-tagged full-length Ape1 and its fragments

Purification of the Ape1 fragments A, AB, B, BC and C, as well as the tagged full-length Ape1 was performed by using an adapted protocol as was used for the Ape1 untagged wild-type protein. Since the fragments carry a negative net charge due to changed isoelectric point (pI) values ranging from 5.2 to 6.6, the proteins bind to an anion exchange column such as Q sepharose but not to a cation exchange column with the previously described buffer conditions. The fragments were eluted from Q sepharose and further purified according to the original protocol. Since the purification was not efficient, the pH conditions were then adjusted to pH 5.5 with a Hepes/KOH-based buffer in order to achieve a positive net charge of the fragments, but also with this adjustment, purification was not efficient to achieve reasonable amounts of pure protein.

4.7.5. Preparation of radiolabeled primer/templates for the endonulcease assay with Ape1 fragments on anti-HA beads

To prepare the 100mer oligonucleotide (for sequence see [92]) for the AP endonuclease assay, the 100mer was labeled at its 5` end by T4 polynucleotide kinase (2U) in a final reaction volume of 20µl, containing 1x PNK buffer, 4µM 100mer oligonucleotide with an abasic site (AP site) at position 43 and 20µCi [γ-32P] dATP (Primers were from Mycrosynth, γATP was purchased from Amersham Biosciences, T4 polynucleotide kinase as well as its buffer was from New England Biolabs). The mix was then incubated for 40min at 37°C, the kinase inactivated for 10min at 80°C and the mix centrifuged through a G-25 (Microspin^{TM}) column at 720x g for 2min to remove the free ATP. The reaction was added to the annealing mix containing following reagents in a final volume of 36µl: 4µM 100mer oligonucleotide without AP site and 1x annealing buffer. This mix was heated at 95°C for 10min and slowly cooled down to room temperature overnight to allow the primer to anneal to the template.

4.7.6. Endonuclease assay with HA-tagged Ape1 fragments on anti-HA beads

The reactions were carried out in a reaction mixture (10μl) containing 45mM Hepes/KOH pH 7.8, 70mM KCl, 7.5mM $MgCl_2$, 2mM DDT, 0.5mM EDTA, 0.1mg/ml BSA, 2mM ATP, 50fmol of oligonucleotide substrate and the indicated amounts of Ape1 and its fragments, respectively, as determined by western blot analysis. Reactions were incubated at 37°C for 20min and stopped by adding an equal volume of gel loading buffer. Following incubation at 100°C for 5min, the reaction products were separated by electrophoresis on a 10% denaturing polyacrylamide gel and visualized by autoradiography.

4.7.7. Pull-down assay of HA-tagged Ape1 fragmenst with the 9-1-1 complex

For the HA pull-downs, 120μl of HA-slurry were equilibrated with pull-down buffer (40mM Tris/HCl pH 8.0, 150mM NaCl, 5mM $MgCl_2$, 10% (v/v) glycerol, 0.05% (v/v) NP-40) and then added to the *E. coli* cell lysates, containing the overexpressed Ape1 fragments, followed by incubation for 2h at 4°C. As a negative control, *E. coli* cell lysate containing the empty vector was incubated with the beads. After three times washing for 10min, 5μg of purified 9-1-1 complex was added and incubated for another 2h at 4°C in pull-down buffer. Next, the mix was centrifuged (4000rpm for 1min at 4°C) and the supernatant was removed. Beads were again washed three times in pull-down buffer and then heated to 95°C in Laemmli buffer. The co-precipitated proteins were analyzed by western blot using the corresponding antibodies according to established methods.

4.7.8. Far western

4μg of DNA pol β was loaded onto a SDS-PAGE gel as a positive control, along with 2.5 and 5μg of DNA pol λ and 5 and 10μg BSA as negative controls. After separation, the proteins were transferred onto a nitrocellulose membrane as described under point 4.4 in this thesis. Then, the proteins were renatured on the membrane, using decreasing amounts of guanidine-HCl,

starting with 6M and always dividing the amount by two in the next step. Seven steps were carried out, each for 10min at 4°C, until reaching a concentration of guanidine-HCl of 93.75mM. The membrane was then blocked with TBST (0.3% (v/v) Tween20), containing 10% (w/v) milk powder for 30min at 4°C. Then, the membrane was incubated with the purified bait protein (9-1-1 complex, 5μg in 5ml in protein-binding buffer) and kept at 4°C for 1h. After this, four washing steps, each for 10min and with TBST supplemented with 0.25% (w/v) milk powder were done, whereby in the second wash additionally 0.0001% glutaraldehyd is added. Then, the blot was further processed according to the protocol for western blotting, using as a first antibody one that is directed against the bait protein.

4.8. Interaction studies of human DNA polymerase λ with the 9-1-1 complex

4.8.1 Co-immunoprecicpitation (co-IP) experiments

(i) For co-IPs, 60mg Protein A sepharose beads were coated overnight with 1mg BSA in 1ml IP buffer (50mM Tri/HCl pH8.0, 100mM NaCl, 0.05% (v/v) NP40, 2μg/ml leupeptin, 1μg/ml bestatin, 1μg/ml pepstatin) at 4°C.The next day the beads were washed 3 times with 1ml of IP buffer and resuspended in 0.5ml IP buffer. Subsequently, the beads (40μl per assay point) were incubated for 2h at 4°C with 2.5μl of polyclonal anti-Rad9 antibody in IP buffer. For the negative control antibody was omitted. Beads were then washed three times with IP buffer (0.5ml, 10min at 4°C, then centrifugation with 3000rpm for 1min at 4°C). Meanwhile, 6μg of DNA pol λ was incubated with 3.6μg of the 9-1-1 complex, or with the same volume of dilution buffer, and the mix was incubated at 4°C for 2h. Subsequently, 40μl of beads were added to the pre-incubated proteins and the mix again incubated at 4°C for 1h. Beads were then washed again three times and finally Laemmli buffer was added and samples were analyzed on western blot.

(ii) 1mg of total HeLa cell extract was immunoprecipitated with the indicated antibodies and protein G-sepharose or protein A-sepharose for 1 hour at 4°C. After incubation, the supernatant was removed and the beads were washed

three times in IP buffer and subsequently heated to 95°C in Laemmli buffer. The co-immunoprecipitated proteins were then analyzed by western blot, using the corresponding antibodies according to established methods.
(iii) The other protocol used was established before [120]. In short, protein A-sepharose or protein G-sepharose beads were coated with 10mg/ml BSA in 100μl IP buffer (40mM Tris/HCl pH 7.5, 2.5mM MgCl, 0.5% (v/v) NP40, 2μg/ml leupeptin, 1μg/ml pepstatin and 1μg/ml bestatin) overnight at 4°C. The next day, the beads were washed three times with IP buffer (5min each, at 4°C, spin for 30sec at 5000rpm in cooling centrifuge). Then, they were resuspended in 60μl buffer per sample. The antibodies were incubated with 1mg/ml of the extract in a total volume of 500μl for 2h at 4°C. Then, 60μl of coated beads were added per sample and further incubated for 1h at 4°C. The beads were then washed three times in washing buffer (50mM Tris/HCl pH 8.0, 0.1% (v/v) NP40, 50mM NaCl, 75mM KCl, 2μg/ml leupeptin, 1μg/ml pepstatin and 1μg/ml bestatin) and finally the pellet was eluted in 40μl of Laemmli buffer by boiling for 10min at 95°C and the supernatant analyzed by western blot.

4.9. Paper submitted "Residue 505 of human DNA polymerase λ acts as a molecular gate for O-6-methylguanine lesion bypass"

4.9.1. Site-directed mutagenesis of DNA polymerase λ

Site-directed mutations were preformed according to the protocol of the QuikChange™ Site-Directed Mutagenesis Kit (Stratagene). The mutations were introduced into a human DNA pol λ overexpression plasmid (pRSETb-hpolλ-wt; 5ng per reaction) by a PCR-based method with the following oligonucleotides (0.2 μM final concentration in 50μl total volume):
Y505M_Forward: 5`-GCC TGT GCC CTG CTC ATG TTC ACC GGC TCT GCA C-3`
Y505M_Reverse: 5`-GTG CAG AGC CGG TGA ACA TGA GCA GGG CAC AGG C-3`
R517L_Forward: 5`-CAA CCG CTC CAT GCT AGC CCT GGC CAA AAC

CAA GGG-3`

R517L_Reverse: 5`-CCC TTG GTT TTG GCC AGG GCT AGC ATG GAG CGG TTG-3`

The first segment of the PCR was done for 30sec at 98°C. The second segment was started at 98°C for 30sec, followed by 65°C for 60sec followed by 1min 40sec at 72°C; the final elongation step was done at 72°C for 5min. The PCR products were digested with Dpn1 for 60min at 37°C to remove the template. Phusion buffer and the DNA pol used for PCR were from Finnzyme. Purification of all the mutant plasmids was performed according to the manufactors instructions (NucleoBond plasmid purification, high copy plasmid purification by Macherey-Nagel).

The double mutant was done based on the Y505M mutant, using the primers used before for the single mutant R517L. All plasmids were sent to Microsynth for sequencing before further experiments were performed.

5. Results

5.1. Study of DNA repair enzymes in the radioresistant bacterium *Deinococcus radiodurans*

5.1.1. Original research article; "Enzymes involved in DNA ligation and end-healing in the radioresistant bacterium *Deinococcus radiodurans*" BMC Molecular Biology (2007) 8;69.

I contributed to the designed schematic outline of the predicted domain structures of the *Deinococcus radiodurans* (*D. radiodurans*) putative NAD^+-dependent DNA ligase and ATP-dependent DNA ligase represented in Figure 1B. Furthermore, I was involved in the biochemical characterization of the NAD^+-dependent DNA ligase, mainly in the analysis of the metal ions requirements represented in Figure 3A.

BMC Molecular Biology

BioMed Central

Research article

Open Access

Enzymes involved in DNA ligation and end-healing in the radioresistant bacterium *Deinococcus radiodurans*

Melanie Blasius[1], Rebecca Buob[1], Igor V Shevelev[1,2] and Ulrich Hubscher*[1]

Address: [1]Institute of Veterinary Biochemistry and Molecular Biology, University of Zürich-Irchel, Winterthurerstrasse 190, 8057 Zürich, Switzerland and [2]Donnelly Centre for Cellular and Biomolecular Research (CCBR), Department of Biochemistry & Department of Medical Genetics and Microbiology University of Toronto, 160 College Street, Toronto, Canada

Email: Melanie Blasius - blasius@vetbio.uzh.ch; Rebecca Buob - buob@vetbio.uzh.ch; Igor V Shevelev - igor.chevelev@utoronto.ca; Ulrich Hubscher* - hubscher@vetbio.uzh.ch

* Corresponding author

Published: 16 August 2007

BMC Molecular Biology 2007, **8**:69 doi:10.1186/1471-2199-8-69

Received: 24 April 2007
Accepted: 16 August 2007

This article is available from: http://www.biomedcentral.com/1471-2199/8/69

Abstract

Background: Enzymes involved in DNA metabolic events of the highly radioresistant bacterium *Deinococcus radiodurans* are currently examined to understand the mechanisms that protect and repair the *Deinococcus radiodurans* genome after extremely high doses of γ-irradiation. Although several *Deinococcus radiodurans* DNA repair enzymes have been characterised, no biochemical data is available for DNA ligation and DNA endhealing enzymes of *Deinococcus radiodurans* so far. DNA ligases are necessary to seal broken DNA backbones during replication, repair and recombination. In addition, ionizing radiation frequently leaves DNA strand-breaks that are not feasible for ligation and thus require end-healing by a 5'-polynucleotide kinase or a 3'-phosphatase. We expect that DNA ligases and end-processing enzymes play an important role in *Deinococcus radiodurans* DNA strand-break repair.

Results: In this report, we describe the cloning and expression of a *Deinococcus radiodurans* DNA ligase in *Escherichia coli*. This enzyme efficiently catalyses DNA ligation in the presence of Mn(II) and NAD^+ as cofactors and lysine 128 was found to be essential for its activity. We have also analysed a predicted second DNA ligase from *Deinococcus radiodurans* that is part of a putative DNA repair operon and shows sequence similarity to known ATP-dependent DNA ligases. We show that this enzyme possesses an adenylyltransferase activity using ATP, but is not functional as a DNA ligase by itself. Furthermore, we identified a 5'-polynucleotide kinase similar to human polynucleotide kinase that probably prepares DNA termini for subsequent ligation.

Conclusion: *Deinococcus radiodurans* contains a standard bacterial DNA ligase that uses NAD^+ as a cofactor. Its enzymatic properties are similar to *E. coli* DNA ligase except for its preference for Mn(II) as a metal cofactor. The function of a putative second DNA ligase remains unclear, but its adenylyltransferase activity classifies it as a member of the nucleotidyltransferase family. Characterization of another protein from the same operon revealed a 5'-polynucleotide kinase with a possible role in DNA strand-break repair.

Background

Deinococcus radiodurans

Deinococcus radiodurans (D. radiodurans) exhibits an extraordinary resistance to ionizing radiation. Ionizing radiation generates a variety of DNA damages, including many types of base damages as well as single-strand and double-strand breaks, the latter being the most lethal damage for a living cell. *D. radiodurans* can survive irradiation up to 5,000 Gy without measurable loss of viability, and it seems likely that this resistance is based on mechanisms that ensure limited DNA and protein degradation and provide an efficient and accurate DNA strand-break repair [1]. High intracellular levels of Mn(II) protect proteins and allow fast repair of damaged DNA after irradiation [2,3]. Prokaryotes can repair double-strand breaks by homologous recombination, but proteins implicated in non-homologous end-joining have also been identified recently, such as Ku homologs and additional DNA ligases [4,5]. However, no Ku homolog has been discovered in the genome of *D. radiodurans*. Zahradka *et al*. found that a mechanism called extended synthesis-dependent strand-annealing accounts for most of the strand-break repair [6], although additional DNA repair pathways might contribute to the efficient DNA repair. In any case, a DNA ligase is essential for DNA repair and a 5'-polynucleotide kinase/3'-phosphatase would ensure that DNA strand-breaks could be invariably ligated.

DNA ligases

DNA ligases play essential roles in replication, recombination and repair since they join broken DNA strands by catalysing the formation of a phosphodiester bond between the 3' hydroxyl end of one strand and the 5' phosphate end of another. Ligation occurs via three nucleotidyltransfer steps: (i) a covalent enzyme-adenylate intermediate is formed, (ii) the adenylate group (AMP) is transferred to the 5'-phosphate terminus of the DNA molecule and (iii) the gap in the DNA molecule is sealed when the DNA ligase catalyses displacement of the AMP residue through the attack by the adjacent 3' hydroxyl group of the DNA [7]. For all DNA ligases, the AMP is linked to a highly conserved lysine residue in the catalytic motif of the enzyme. DNA ligases can use either ATP or NAD^+ as an AMP-donor. NAD^+-dependent DNA ligases are found exclusively in bacteria, certain archaea, and viruses whereas ATP-dependent DNA ligases can be found in eukaryotes, archaea and several viruses including bacteriophages. Recently, it was shown that some bacterial genomes also encode an additional ATP-dependent DNA ligase, some of which were further characterised [7].

The *D. radiodurans* genome contains the gene DR2069 encoding an NAD^+-dependent DNA ligase, here designated as LigA. The gene DRB0100 encodes another possible diverged homolog of ATP-dependent ligases. As the function of this protein remains unclear it will be called DRB0100 throughout this paper. This predicted ATP-dependent DNA ligase contains all catalytic residues, and its expression is strongly upregulated upon γ-irradiation [8]. In addition, DRB0100 belongs to a putative DNA repair operon together with the genes DRB0098 and DRB0099. DRB0098 has been predicted to encode a kinase/phosphatase with an unusual domain architecture [9] whereas DRB0099 is classified as a domain of unknown function with weak similarity to the macro domain family [10].

Polynucleotide kinases and 3' phosphatases

Not all DNA strand breaks possess ligatable ends, i.e. a 5' phosphate and a 3' OH terminus. The 5' phosphate can be missing and γ-irradiation and reactive oxygen can lead to the formation of 3' phosphate or phosphoglycolate ends [11,12]. Enzymatic activity is required to remove the 3' phosphate moiety and to phosphorylate the 5' end at the DNA nick to allow for DNA ligation. Both reactions are catalysed by bifunctional PNKPs. The best characterised PNKP is T4 PNK that is involved in the repair of host tRNA [13]. Additional PNKPs were identified in other viruses and all these viral enzymes can use either DNA or RNA as a substrate. PNKPs were also found in some eukaryotes, e.g. human, *Caenorhabditis elegans* and *Schizosaccharomyces pombe*, where they seem to play an important role in the repair of single-strand and double-strand breaks [14-16]. However, the eukaryotic enzymes can only use DNA as a substrate. Pnk1 from *Schizosaccharomyces pombe* possesses both 3'-phosphatase and 5'-polynucleotide kinase activities, whereas TPP1 from *Saccharomyces cerevisiae* shows only 3'-phosphatase activity. In other organisms, the kinase and phosphatase activities seem to be uncoupled as well, e.g. in *Arabidopsis thaliana*. Only one bacterial PNKP from *Clostridium thermocellum* has been characterised so far [17], showing similarity to viral PNKPs. *D. radiodurans* also seems to possess a PNKP encoded by the gene DRB0098, although the PNKP possesses a special domain architecture [9]. The order of the phosphatase and kinase domains is the similar to eukaryotic PNKPs; in contrast, viral PNKPs have a reversed order of the two domains. The predicted phosphatase domain of the *D. radiodurans* PNKP belongs to the HD hydrolase superfamily [18], and, so far, only one viral PNKP containing this domain has been shown to possess 3'-phosphatase activity [19]. The *D. radiodurans* PNKP is part of the putative DNA repair operon together with the predicted ATP-dependent DNA ligase DRB0100 and the expression of this operon is strongly upregulated upon irradiation. Thus, a role for the encoded proteins in DNA repair has been suggested [8].

In this work we analyse two putative DNA ligases and one predicted 5'-polynucleotide kinase/3'-phosphatase from *Deinococcus radiodurans*.

Results

Prediction of two DNA ligases for D. radiodurans

Sequence comparison of the two predicted *D. radiodurans* DNA ligases with other bacterial DNA ligases showed that LigA displays a strong similarity to other NAD^+-dependent DNA ligases (Figure 1A) and comprises the expected adenylation, OB fold and BRCT domains. Like other NAD^+-dependent DNA ligases LigA also contains a zinc finger and a helix-hairpin-helix motif presumably involved in DNA binding (Figure 1B). By contrast, the predicted ATP-dependent DNA ligase DRB0100 shows poor sequence similarity to other bacterial ATP-dependent ligases, but contains all catalytic residues (Figure 1A and [8]). The DRB0100 protein consists of the adenylation domain only and lacks all other domains present in LigA (Figure 1B); especially no DNA binding motif could be detected.

Purification of two recombinant DNA ligases from D. radiodurans

Both genes encoding putative DNA ligases, DRB0100 and DR2069, were amplified from genomic *D. radiodurans* DNA using specific primers (see Table 1) and cloned into a pRSETb vector for recombinant protein expression in *E. coli* cells with a hexahistidine tag at the N terminus. For both proteins, adenylation mutants were created by replacing the conserved lysine residue with an alanine, resulting in a DRB0100 K40A mutant and a LigA K128A mutant, respectively. All wild-type and mutant proteins were expressed in *E. coli* BL21(DE3) cells and purified to near homogeneity over a HisTrap™ HP column and two additional ion exchange columns (Figure 1C).

A DNA ligase from D. radiodurans *performs efficient strand joining in the presence of NAD^+ and Mn(II) and possesses adenylyltransferase activity*

We tested the ability of the LigA wt and the K128A mutant to ligate a duplex DNA substrate containing a single nick. Ligase activity was measured as conversion of a 5'-[^{32}P]-labelled deoxyribose oligomer of 19 nucleotides into an internally labelled oligomer of 44 nucleotides. LigA showed maximum ligation activity with 1 mM $MnCl_2$, 5 μM NAD^+ and a pH of 6.8 at a temperature of 30°C. Higher concentrations of $MnCl_2$ or NAD^+ had an inhibitory effect on the enzymatic activity. The enzyme was 10 times less active in the presence of $MgCl_2$, and even inactive when tested with 1 mM ATP (data not shown). To exclude the possibility that the observed activity is caused by a copurified *E. coli* ligase, we created a K128A mutant that lacks the proposed site of adenylation (Figure 1A). The LigA K128A mutant showed almost no ligation activity confirming that the observed ligation activity results from the *D. radiodurans* NAD^+-dependent DNA ligase (Figure 2A). The residual DNA ligation does probably not result from a contamination with *E. coli* DNA ligase, as the activity was strongly decreased in presence of 4 mM $MgCl_2$, which is optimal for *E. coli* DNA ligase (data not shown). In an adenylyltransferase activity assay LigA wt formed an AMP-ligase complex, whereas complex formation was not detected with the K128A mutant (Figure 2A, right). Thus, lysine 128 is essential for the first step of DNA ligation. The kinetic analysis of the wt reaction using different concentrations of nicked DNA displayed typical Michaelis-Menten kinetics with an apparent K_M of 105 ± 16 nM (Table 2).

Table 1: PCR primer sequences used in this study

Primer name	Used for	Sequence (5'-3')
DRB0100F	cloning of DRB0100wt into pRSETb	CGC*GGATCC*GATGCGAGTCAAATACCCTTC
DRB0100R	cloning of DRB0100wt into pRSETb	CGC*GGATCC*GTCATGACTGCTCCTGGCG
DRB0100_mutF	introduction of K40A mutation into DRB0100	CGTCGTGACCGAG**GC**GCTCGACGGCG
DRB0100_mutR	introduction of K40A mutation into DRB0100	CGCCGTCGAGC**GC**CTCGGTCACGACG
DR2069F	cloning of DR2069 wt into pRSETb	CGC*GGATCC*GATGCGTTACCCTGGGCGC
DR2069R	cloning of DR2069 wt into pRSETb	CGC*GGATCC*GTCAGCTTTCAGCGGGGGC
mut_DR2069F	introduction of K128A mutation into DR2069	CCGGCGAGCTG**GC**AATCGACGGCCT
mut_DR2069R	introduction of K128A mutation into DR2069	CAGGCCGTCGATT**GC**CAGCTCGCCGG
DRB0098F	cloning of DRB0098 into pRSETb	CGC*GGATCC*GATGAACCGCAAAAACCGTAC
DRB0098R	cloning of DRB0098 into pRSETb	CGC*GGATCC*GTCAGGAGGTAGATGAGGGCAG
98_R371LF	introduction of R371K mutation into DRB0098	GGTCAGCTCGGAGCA**AAA**ATCAGCGGGAGAGAGC
98_R371LR	introduction of R371K mutation into DRB0098	GCTCTCTCCCGCTGAT**TTT**TGCTCCGAGCTGACC

All oligonucleotides were desalted and used in a final concentration of 0.4 μM. T7 sequencing primers can be found at the Microsynth webpage. Bold bases represent those exchanged in the site-directed mutagenesis. Restriction sites are shown in italics.

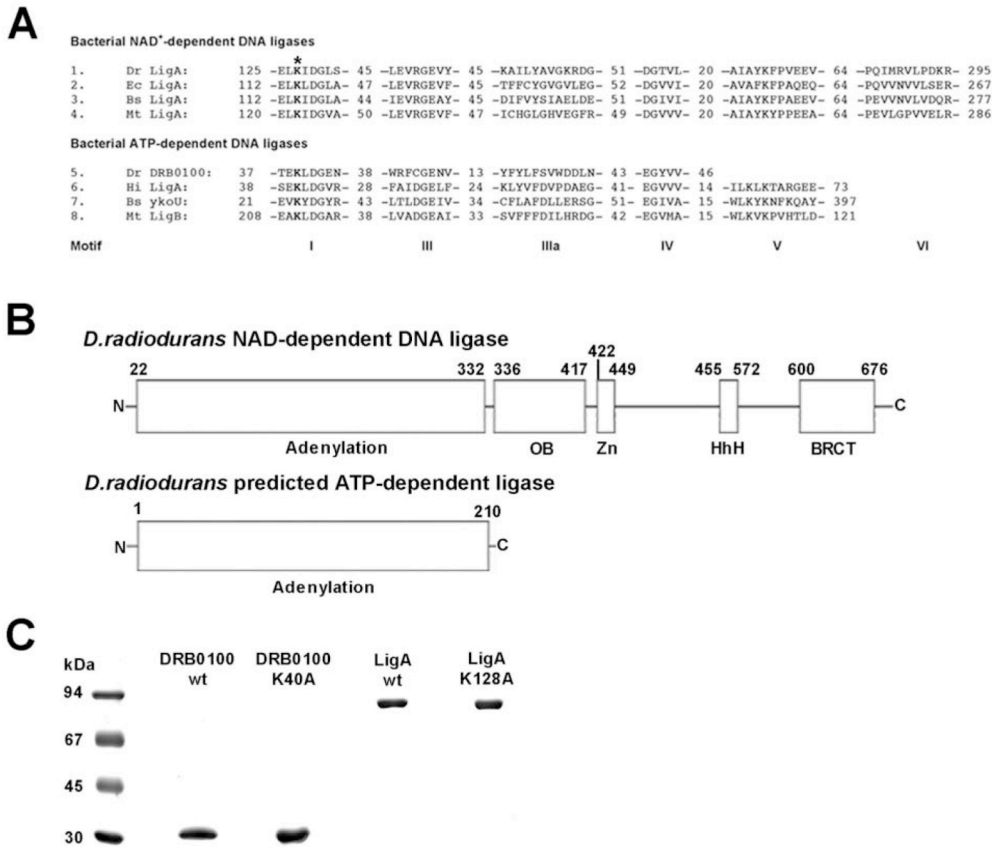

Figure 1

Alignment and purification of two predicted *D. radiodurans* DNA ligases. A. Alignment of eight colinear sequence elements in bacterial DNA ligases based on previous studies of DNA ligase motifs [7, 34] using CLUSTALW alignment [35]. The numbers of amino acids between the motifs are indicated. The alignment of motif VI is not shown for the ATP-dependent DNA ligases since the homology is very poor. Note that the putative ATP-dependent DNA ligase from *D. radiodurans* seems to lack also motif V. The conserved adenylated lysine residue is depicted in bold and labelled with an asterisk. Dr, *Deinococcus radiodurans*, Ec, *Escherichia coli*, Bs, *Bacillus subtilis*, Mt, *Mycobacterium tuberculosis*, Hi, *Haemophilus influenzae*. B. Predicted domain structures of *D. radiodurans* NAD^+-dependent DNA ligase (LigA) and ATP-dependent DNA ligase (DRB0100). The LigA protein scheme is based on homology searches using the NCBI conserved domain database and the SMART conserved domain database. OB, oligonucleotide-binding fold, Zn, zinc finger, HhH, helixhairpin-helix motif 1, BRCT, BRCA1 C-terminal domain. C. LigA and DRB0100 and their corresponding adenylation mutants LigA K128A and DRB0100 K40A were purified over one metal affinity column and two ion exchange columns to near homogeneity as described in Methods. 3 μg of each protein were loaded onto a 10% SDS-PAGE and the gel was stained with Coomassie Blue R250.

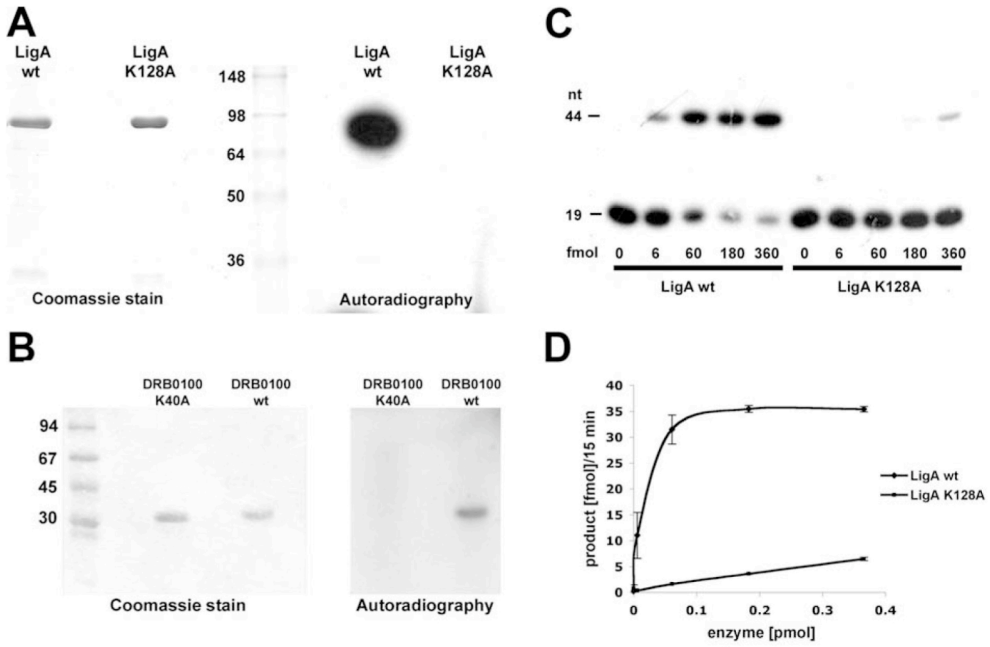

Figure 2
DNA ligation and adenylyltransferase activities of the putative recombinant DNA ligases. A. LigA wt and LigA K128A were incubated with [^{32}P]-NAD$^+$ and adenylyltransferase activity was detected by SDS-PAGE. Protein bands were visualized with Coomassie Blue R250 (left) and by autoradiography (right). B. DRB0100 wt and K40A were incubated with α-[^{32}P]-ATP. Protein-AMP complexes and free α-[^{32}P]-ATP were separated by SDS-PAGE. Proteins were stained with Coomassie Blue R250 (left) and detected by autoradiography (right). C. Titration of LigA wt and LigA K128A on a nicked DNA substrate. Indicated amounts of LigA wt and LigA K128A were incubated with the DNA substrate as described in the Methods section. [^{32}P]-labelled DNA oligonucleotides were visualized by autoradiography. D. Quantification of three independent experiments as shown in C. Error bars are given as the standard error of the mean.

Table 2: K_M values of prokaryotic NAD$^+$-dependent DNA ligases

Organism	T [°C]	K_M [nM]	Reference
D. radiodurans	30	105 ± 16	This work
E. coli	18	179	Georlette *et al*., 2000
E. coli	30	702	Georlette *et al*., 2000
E. coli	45	2040	Georlette *et al*., 2000
P. haloplanktis	4	165	Georlette *et al*., 2000
P. haloplanktis	18	296	Georlette *et al*., 2000
P. haloplanktis	25	631	Georlette *et al*., 2000
T. scotoductus	45	236	Georlette *et al*., 2000
T. scotoductus	60	465	Georlette *et al*., 2000

K_M values for nicked DNA substrates. Details for K_M determination of *D. radiodurans* NAD$^+$-dependent DNA ligase are described in Methods. K_M is the mean of 3 independent experiments and the error is given as standard error of the mean.

Divalent cation dependence and specificity of the DNA strand-joining by LigA

Ligation of a nicked DNA by LigA required a divalent cation cofactor and was best in the presence of 1 mM $MnCl_2$ (Figure 3A). $MnCl_2$ could be replaced by $MgCl_2$ or $CaCl_2$ leading however to a 10-fold decrease of activity (Figure 3A). The optimal concentration of divalent cation was 1 mM for $MgCl_2$ and 2 mM for $CaCl_2$. Only low levels of DNA ligation were observed with $NiCl_2$ and $ZnCl_2$, the optimal concentrations being 2 and 3 mM, respectively (Figure 3B). $CoCl_2$ could not serve as a divalent cation cofactor (Figure 3B).

DRB0100, a predicted ATP-dependent DNA ligase from D. radiodurans*, forms a complex with AMP, but does not ligate DNA or RNA* in vitro

DRB0100 has been predicted to be an ATP-dependent DNA ligase consisting only of the adenylation domain. We first tested whether the DRB0100 protein possesses an adenylation activity using ATP as an AMP-donor and whether lysine residue 40 is indeed essential for AMP binding. The adenylyltransferase activity was tested by incubating 1 μg of recombinant protein with α-[^{32}P]-ATP. A complex was formed between the wild-type protein and [^{32}P]-AMP, which was completely absent for the K40A mutant, confirming that DRB0100 possesses adenylyltransferase activity and therefore belongs to the family of nucleotidyltransferases (Figure 2B). We further tested whether DRB0100 is able to ligate DNA or RNA substrates using NAD^+ or ATP as a cofactor. However, we did not detect a ligation product with any conditions used [see Additional file 1 and Additional file 2].

Purification of a putative 5'-polynucleotide kinase/3'-phosphatase from D. radiodurans *with an unusual domain architecture*

The PNKP encoded by *D. radiodurans* has a phosphatase-kinase domain architecture similar to the eukaryotic PNKPs. In contrast, the viral T4 PNK has a reverse domain order with the kinase domain at the N-terminus and the phosphatase domain at the C-terminus. Comparison of *D. radiodurans* and human PNKP shows that the bacterial protein is smaller than the human homolog and contains a phosphatase domain belonging to the superfamily of HD phosphohydrolases. The human enzyme contains a distinct phosphatase domain with some similarity to histidinol phosphatase and related phosphatases (Figure 4A).

The gene DRB0098 encoding a putative PNKP was amplified via PCR from genomic *D. radiodurans* DNA. The gene was cloned into a pRSETb vector and arginine 371 was mutated to lysine using mutagenic primers for PCR. Arginine 371 was chosen based on sequence comparisons with the well-characterised T4 PNK. We estimated that it should correspond to arginine 126 in T4 PNK, which is required for polynucleotide kinase activity [20].

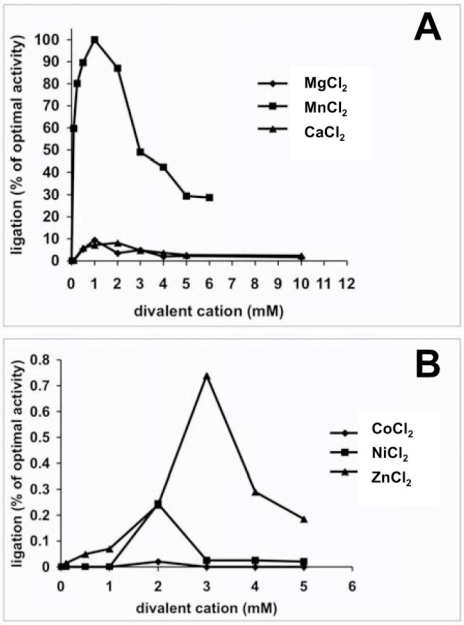

Figure 3
Divalent cation requirements for LigA activity. A. Titration of $MgCl_2$, $MnCl_2$ and $CaCl_2$. Ligation assays were performed with 60 fmol of LigA wt and increasing amounts of divalent cations, and quantified as described in Methods. Ligation activity obtained with 1 mM $MnCl_2$ was set as 100% and relative DNA ligation activity is shown as the average of 2 experiments. B. Titration of $CoCl_2$, $NiCl_2$ and $ZnCl_2$. Ligation assays were performed as in A. Note that the ordinate has a scale of about 2 orders of magnitude lower than in A for better illustration of the divalent cation optima.

Both proteins, DRB0098 wt and DRB0098 R371K were expressed in *E. coli* BL21(DE3) cells with an N-terminal hexa-histidine tag. The proteins were purified over a HisTrap HP™ column, a HiTrap Heparin HP™ column and finally a HiTrap SP HP™ column to apparent homogeneity (Figure 4B).

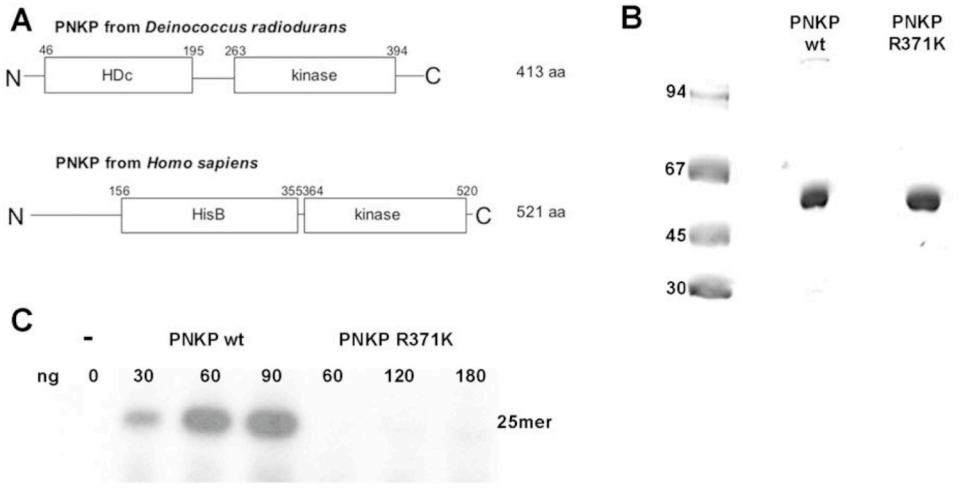

Figure 4
Purification of a putative PNKP from *D. radiodurans* and analysis of its 5' kinase and 3' phosphatase activities. A. Scheme of PNKP from *D. radiodurans* and *H. sapiens*. Protein domains are depicted according to predictions based on sequence similarities [36]. Schemes are not drawn to scale. HD, HD domain, kinase, polynucleotide kinase domain, HisB, histidinol phosphatase and related phosphatases domain. B. 3 μg of either *D. radiodurans* PNKP wt or PNKP R371K mutant were loaded onto a 10% SDS-PAGE and subsequently stained with Coomassie Blue R250. Both proteins were purified over 3 columns. Details are described in Methods. C. Titration of the *D. radiodurans* PNKP wt and PNKP R371K mutant to compare their polynucleotide kinase activity on a 5'OH 25 mer deoxyribose oligonucleotide. Different amounts of enzyme were incubated with the DNA substrate and γ-[^{32}P]-ATP as described in Methods. [^{32}P]-labelled 25 mer was detected by autoradiography.

Analysis of the D. radiodurans *PNKP polynucleotide kinase/3'-phosphatase activity*

Polynucleotide activity for the *D. radiodurans* PNKP was shown as transfer of $^{32}P_i$ from γ-[^{32}P]-ATP to the 5'OH end of a 25 mer oligodeoxyribonucleotide. The resulting 5'[^{32}P]-labelled product was separated from the free γ-[^{32}P]-ATP by polyacrylamide gel electrophoresis and detected by autoradiography. The wild-type protein showed clear 5'-polynucleotide kinase activity with an optimal $MnCl_2$ concentration of only 0.25 mM. Mutation of arginine 371 to a lysine strongly reduced the enzymatic activity (Figure 4C), confirming that the kinase activity is intrinsic to the C-terminal domain. Furthermore, as *E. coli* does not possess a polynucleotide kinase, a contamination can be excluded.

The 3'-phosphatase activity was analysed as conversion of a non-ligatable DNA nick, which is "blocked" by a 3' PO_4 moiety, to a normal 3'OH-5'PO_4 nick that can be subsequently joined by a DNA ligase. Both, D. *radiodurans* LigA and T4 DNA ligase, were able to ligate the blocked substrate if PNKP was present (data not shown). Even though 3'-phosphatase activity has been detected, we cannot conclude whether this activity is intrinsic to the PNKP or not. Samples purified from *E. coli* cells containing only the empty expression vector contained unspecific 3'-phosphatase activity as well and H81A or D82E mutants of DRB0098 did not show any reduced 3'-phosphatase activity, although these two residues represent the conserved HD motif (data not shown). An enzymatic mutant of DRB0098 is required to definitely decide this open question.

Discussion

DNA ligases are important enzymes acting in DNA replication, recombination and repair. They can be classified by cofactor requirement: those requiring NAD^+ and those requiring ATP [21]. For many years it was believed that bacteria possess only NAD^+-dependent DNA ligases. However, several years ago, it became clear that some bac-

teria contain an ATP-dependent DNA ligase in addition to their NAD^+-dependent DNA ligase [22]. The presence of these ligases suggested that prokaryotes, similar to eukaryotes, could have specific DNA ligases that act in DNA repair and recombination.

In this work, we report the identification of LigA, an NAD^+-dependent DNA ligase, and a second putative ATP-dependent DNA ligase in the radioresistant bacterium *D. radiodurans*. NAD^+-dependent DNA ligases are highly conserved and it is likely that they are essential for all bacteria [7]. *D. radiodurans* LigA showed strong ligation activity on a nicked DNA substrate in the presence of NAD^+ and $MnCl_2$, but only a weak activity in the presence of $MgCl_2$. This Mn^{2+} preference is not surprising since it was shown that these ions are present in extremely high levels at the *D. radiodurans* DNA [23] and are essential for γ-radiation resistance [3]. Moreover, several DNA repair enzymes from *D. radiodurans*, such as UV endonuclease β [24] or a family X DNA polymerase with a structure-modulated nuclease activity [25,26], are strongly stimulated by $MnCl_2$. The first step in the ligation process is the formation of an adenylated ligase. According to sequence alignment with other NAD^+-dependent DNA ligases, adenylation of the LigA protein is predicted to occur on lysine 128. Indeed, a mutation of this lysine residue to alanine abolished the ligation as well the adenylation activity.

The product of the *D. radiodurans* gene DRB0100, a diverged homolog of ATP-dependent DNA ligases, contains most of the conserved amino acid residues characteristic of DNA ligases and was shown to be strongly upregulated upon γ-irradation [8]. We could show that this protein possesses adenylyltransferase activity using α-[^{32}P]-ATP as a substrate and that the adenylation occurs specifically at the conserved lysine 40. This transfer of radioactivity to the wild-type enzyme, but not to the K40A mutant, indicates a covalent modification of the respective lysine residue as observed for other ligases. This places DRB0100 in the family of nucleotidyltransferases that includes DNA and RNA ligases as well as RNA capping enzymes. As RNA capping is not characterised for prokaryotes, we focussed our work on the possible ligation activity. However, to our knowledge the presence of RNA capping has not been investigated in *D. radiodurans* and can therefore not completely be excluded. Although different cofactors and various buffer conditions as well as different substrates were used, and the hexa-histidine tag was transferred from the N- to the C-terminus of the protein, we were not able to show that DRB0100 is active as a DNA or RNA ligase. Nicked DNA substrates, nicked DNA-RNA hybrids prepared by annealing of a 5' PO_4 and a 3' OH RNA strand to a template DNA strand, single-stranded RNA and double-stranded DNA with blunt-ends or overhangs were tested (data not shown). In addition, we analysed total *D. radiodurans* extract with or without previous γ-irradiation for DNA ligation activity; however no ATP-dependent ligation activity was detectable, even though NAD^+-dependent DNA ligation could be easily detected (data not shown). DRB0100 does not contain any conventional DNA binding motif, suggesting that an additional protein is required for recruitment to nicked DNA.

As DRB0100 is part of a putative repair operon DRB0098-DRB0100, we purified the other two proteins to analyse whether the three operon proteins would form a complex capable of DNA ligation. DRB0098 contains a HD-hydrolase family phosphatase domain and a polynucleotide kinase domain and resembles the human repair protein PNKP [27]; DRB0099 is an open reading frame with unknown function and weak similarity to macro domains [8,10]. No DNA ligation was detected with any of these three operon proteins or in combinations thereof; thus, we propose the existence of a yet unidentified additional protein involved in the ligation process of DRB0100. Moreover, it cannot be excluded that DRB0100 ligates only special substrates such as specific DNA sequences or RNA intermediates. Interestingly, in several bacteria genes coding for an ATP-dependent DNA ligase have been identified in operons with Ku-homologs. The Ku proteins might recruit the DNA ligase to DNA strand-breaks as is it the case in mammalian cells [28]. In *D. radiodurans*, however, no Ku-homolog has been identified so far. Another interesting protein that might function in a Ku-like manner is the repair protein PprA from *D. radiodurans*, which has been shown to tether DNA ends and to stimulate ATP- and NAD^+-dependent DNA ligases [29,30]. The ATP-dependent DNA ligase might function as a backup system to provide additional ligation activity under conditions of high genotoxic stress.

In this work, we furthermore characterised a novel PNKP from *D. radiodurans*, which phosphorylates 5' OH termini. It remains unclear whether it is also able to remove 3' phosphate groups, thus converting "blocked" DNA nicks to ligatable ones.

PNKPs can be divided into two subgroups according to their domain architecture: the T4-like kinase-phosphatase proteins found in viruses with a function in RNA repair, and the eukaryal-type phosphatase-kinase group involved in DNA repair. The PNKP from *D. radiodurans* possesses a domain architecture that corresponds to the eukaryal type. So far, only one bacterial PNKP from *Chlostridium thermocellum* has been described, which in contrast to the *D. radiodurans* PNKP contains a calcineurin-type phosphatase domain. This enzyme has been shown to possess 5'-polynucleotide kinase, 2'3'-phosphatase and adenylyl-

transferase activity and has been implicated in RNA repair [17]. It remains to be elucidated if *D. radiodurans* PNKP is involved in DNA or RNA repair.

The *D. radiodurans* PNKP possesses an N-terminal phosphatase domain belonging to the HD superfamily. Members of this family are known or predicted phosphohydrolases [18], and a novel subfamily of PNKPs consisting of a 5'-kinase and a 3'-HD phosphohydrolase domain has been proposed based on sequence similarities [8,9,19]. These enzymes have a conserved doublet of HD residues that is likely to be required for enzymatic activity. So far, only one PNKP has been shown to possess a 3'-phosphatase activity residing in the HD domain, but no mutational analysis is available for this enzyme from the bacteriophage RM378 [19]. However, it was shown, that site-directed mutagenesis of the conserved histidine in a cGMP-phosphodiesterase clearly reduced its catalytic activity [31]. We could show that *D. radiodurans* PNKP possesses 5'-polynucleotide kinase activity. However, the 3'-phosphatase activity detected in our assay might result from an unspecific *E. coli* 3'-phosphatase. H81A or D82E mutants of *D. radiodurans* PNKP did not show a reduced activity in our 3'-phosphatase assays (data not shown). Regarding the polynucleotide kinase activity, the absence of a 5'-polynucleotide kinase in *E. coli* and the reduced activity of the DRB0098 R371K mutant exclude the possibility of a contamination. In the case of the third protein of the putative repair operon, DRB0099, binding to ADP-ribose was detected and further work has to be done to elucidate whether ADP-ribosylation might play a role in bacterial DNA repair (Blasius, M., and Hübscher, U., unpublished observation).

Conclusion

D. radiodurans possesses a classical NAD^+-dependent DNA ligase (LigA) that shows a strong preference for Mn(II) as a cofactor. A second predicted ATP-dependent DNA ligase (DRB0100) shows adenylyltransferase activity, but no DNA or RNA ligation could be detected *in vitro*. A predicted 5'-polynucleotide kinase/3'-phosphatase belonging to the same operon was able to convert 5' OH termini to 5' PO_4 termini, thus preparing DNA ends for ligation. In conclusion, *D. radiodurans* PNKP and LigA are able to heal and ligate DNA nicks. It remains to be assessed whether they play any role in DNA repair or RNA repair *in vivo*. Also the function of DRB0100 remains to be elucidated and further proteomic and genomic approaches might give more insight into these unsolved questions.

Methods

Bacterial strains and media

E. coli DH5α cells were used for cloning and plasmid preparation (Invitrogen). Recombinant proteins were produced in *E. coli* BL21(DE3) (Novagen). *E. coli* cells were grown in LB medium supplemented with 100 μg/ml ampicillin where required.

Enzymes and reagents

Oligonucleotides synthesis and DNA sequencing were performed by Microsynth. DNA fragments and plasmids were purified with kits from Qiagen. All chemicals used were purchased from Sigma-Aldrich. Immunoblots during protein purifications were done using Tetra-His antibody (Qiagen).

Molecular cloning

Genomic DNA was isolated from *D. radiodurans* R1 type strain as described previously [32] and used as a template for PCR amplification of the different genes. PCR reaction mixtures (50 μl) contained 1X HF buffer (Finnzymes), 200 μM of each dNTP, 400 nM of each forward and reverse primer, 3% DMSO and 2 units of Phusion™ High-Fidelity DNA Polymerase (Finnzymes). Cycling protocols were designed according to the supplier's recommendations and annealing temperatures were determined using the Tm calculator provided by Finnzymes. PCR products were digested with BamHI and ligated into the pRSETb vector (Invitrogen) using T4 DNA ligase (Fermentas). For site-directed mutageneses the plasmid containing the corresponding wild-type gene was used as a template, the annealing temperature was set to 55°C, cycle number was reduced to 12–16, and the PCR product was digested with DpnI to remove the template plasmid. The mutated PCR product was then transformed into DH5α cells, plasmids were isolated and all constructs were verified by sequencing. PCR primer sequences can be found in Table 1.

Expression and purification of recombinant proteins

Cultures of *E. coli* BL21(DE3) cells transformed with the respective expression plasmid were grown in LB medium supplemented with ampicillin at 37°C to an $OD_{600\ nm}$ of 0.4–0.8, then IPTG was added to 1 mM final concentration and cells were further incubated for 2–4 h at 37°C. Cells were pelleted by centrifugation (4°C, 4,700 g, 30 minutes) in a Sorvall H6000A rotor. All protein purification steps were performed at 4°C or on ice. Cell pellets were resuspended in 30 ml of buffer N (500 mM NaCl, 30 mM phosphate buffer, pH 7.5, 10 mM Tris-HCl, pH 7.5, 10 mM imidazole, and 1 mM PMSF) and lysed with a French press. To ensure complete lysis, cells were in addition sonicated (2 minutes, 40% duty cycle, Branson Sonifier® Cell disruptor B15). The lysate was centrifuged (4°C, 43,000 g, 30 minutes) in a Sorvall SS-34 rotor and the supernatant was loaded onto a 1 ml HisTrap HP™ column (GE Healthcare) using an ÄKTApurifier™ (GE Healthcare). The column was washed with buffer N containing 50 mM NaCl and 50 mM imidazole and protein was eluted with 50 mM NaCl and 300 mM imidazole. Protein was pooled according to a Coomassie Blue R250 stained SDS-PAGE

and loaded onto the next column equilibrated in buffer A (40 mM Tris-HCl, pH 7.5, 50 mM NaCl, 15% (v/v) glycerol, 1 mM EDTA, and 1 mM 2-mercaptoethanol). For LigA wt and K128A mutant the protein was loaded onto a 1 ml Heparin HP™ column and eluted with a gradient from 50 to 1000 mM NaCl in buffer A. LigA eluted at 350 mM NaCl. Protein was pooled, diluted to 50 mM NaCl with buffer A without NaCl and loaded onto a HiTrap Q HP™ column. Elution was done with a gradient from 50–1000 mM NaCl. Protein eluted at 400 mM NaCl. Fractions that contained nearly homogenous LigA protein as judged by SDS-PAGE were pooled, dialysed to buffer S (20 mM Tris-HCl, pH 7.5, 25% (v/v) glycerol, 50 mM NaCl, 1 mM 2-mercaptoethanol, and 0.5 mM EDTA), and stored at -80°C.

For DRB0100 wt and K40A mutant the pool obtained from the HisTrap HP™ column was loaded onto a 1 ml HiTrap SP HP™ column equilibrated with buffer A. DRB0100 was retrieved in the flow-through, which was diluted to 25 mM NaCl and loaded onto a HiTrap Q HP™ column. Elution was done using a gradient from 25–1000 mM NaCl and DRB0100 protein eluted at 50 mM NaCl. The protein pool was dialysed to buffer S and stored at -80°C.

The HisTrap HP™ pools of DRB0098 wt and R371K mutant were loaded onto a 1 ml Heparin column and eluted as described for LigA. Protein was pooled, diluted to 25 mM NaCl and loaded onto a 1 ml SP HP™ column. Protein was eluted at 50 mM NaCl, tested for purity as described above, pooled and dialysed to buffer S for storage at -80°C. Protein concentrations were determined using bovine serum albumin standards and a BioRad protein assay.

Adenylyltransferase activity assays

For DRB0100, reaction mixture (20 μl) containing 50 mM Tris-HCl, pH 7.5, 5 mM dithiothreitol, 5 mM $MgCl_2$, 1.25 μM α-[^{32}P]-ATP and the indicated amounts of protein were incubated for 15 minutes at 30°C. 20 μl of 2X Laemmli buffer were added, samples were heated for 5 minutes at 95°C and products were separated on a 12% standard SDS-PAGE. The intermediates were detected by autoradiography and the gel was stained by Coomassie Blue R250 to visualize the molecular weight markers. For LigA, the reaction mixture (10 μl) contained 50 mM Tris-HCl, pH 6.8, 5 mM dithiothreitol, 1 mM $MnCl_2$, 1 μg of protein and 0.1 μM [^{32}P]-NAD$^+$. The reaction was incubated for 15 minutes at 30°C, stopped with 10 μl of 2X Laemmli buffer, heated for 5 minutes at 95°C and loaded onto a 10% SDS-PAGE. Prestained markers were loaded to compare protein sizes. Free [^{32}P]-NAD$^+$ and ligase-AMP complexes were visualized by autoradiography.

Preparation of DNA substrates

The DNA substrate used to measure the ligation activity on a double-stranded substrate carrying a single-strand nick was prepared as described [33], the 19 nucleotide DNA strand was phosphorylated using γ-[^{32}P]-ATP and T4 polynucleotide kinase (New England Biolabs). Free γ-[^{32}P]-ATP was removed on a MicroSpin™ G-25 column (GE Healthcare). The sequences are presented in Table 3.

Ligation assays

The 5'-[^{32}P]-labelled DNA substrate was incubated for 30 minutes with the indicated amounts of recombinant protein at 30°C. Reactions were performed in a final volume of 10 μl containing 50 fmol of 5'-[^{32}P]-labelled DNA, 50 mM Tris-HCl, pH 6.8, 1 mM $MnCl_2$, 5 mM dithiothreitol and 1 mM ATP or 5 μM NAD$^+$ unless otherwise mentioned. The reactions were stopped by adding 10 μl of loading buffer (95% formamide, 20 mM EDTA, 0.05% bromphenol blue, 0.05% xylene cyanol), heated for 5 minutes at 95°C and products were separated on a 15% denaturing polyacrylamide gel containing 8 M urea and 15% formamide. After autoradiography, the signals were quantified on a PhosphorImager using the ImageQuant software (Molecular Dynamics). Ligation was quantified by calculating the product/(product+substrate) ratio thus allowing a correction for loading errors. To determine the $K_{\text{Mnicked DNA}}$ value of the *D. radiodurans* NAD$^+$-dependent DNA ligase, the reactions contained 50 mM Tris-HCl, pH 6.8, 5 mM dithiothreitol, 1 mM $MnCl_2$, 5 μM NAD$^+$, 10–

Table 3: Oligonucleotide sequences used to prepare DNA substrates for the enzyme assays performed in this study

Oligonucleotide	Length (nt)	Sequence (5'-3')
RNA-5' nick	19	CAGCAGCAAAUGAAAAAUC
DNA-5' nick	19	CAGCAGCAAATGAAAAATC
RNA-3' nick	25	CCUGCAACAGUGCCACGCUGAGAGC
DNA-3' nick	25	CCTGCAACAGTGCCACGCTGAGAGC
DNA-3'P nick	25	CCTGCAACAGTGCCACGCTGAGAGC-P
DNA-opposite	46	AGATTTTTCATTTGCTGCTGGCTCTCAG CGTGGCACTGTTGCAGGC
Kinase-DNA	25	GCTTTCCGAGTACCGGGGTCTTCCG

All oligonucleotides were PAGE purified and labelled as described in the Methods section. P stands for a 3' phosphate group.

150 fmol of [^{32}P]-labelled nicked DNA substrate and 2 ng of enzyme. The reactions were incubated for 15 minutes at 30°C. The ligated products were quantified by PhosphorImager and $K_{\text{Mnicked DNA}}$ was calculated by Lineweaver-Burk plotting as a mean of 3 independent experiments.

Polynucleotide kinase assays

The indicated amounts of recombinant protein were incubated with 1 pmol of DNA substrate (kinase-DNA in Table 3) in a volume of 10 μl containing 50 mM Tris-HCl, pH 7.5, 0.25 mM $MnCl_2$, 5 mM dithiothreitol and 0.25 μCi of γ-[^{32}P]-ATP (GE Healthcare) for 30 minutes at 30°C. Reactions were stopped with 10 μl of loading buffer, heated for 5 minutes at 95°C and separated on a 15% denaturing polyacrylamide gel containing 8 M urea and 15% formamide. Signals of ^{32}P-DNA were visualized by autoradiography.

Authors' contributions

MB performed most of the experiments, did most of the cloning and protein purifications, analysed the data and wrote the manuscript. RB helped characterising the NAD$^+$-dependent DNA ligase. IS performed part of the cloning and protein purification. MB, IS and UH conceived of the study. UH helped analysing the data and preparing the manuscript. All authors read and approved the final version of the manuscript.

Additional material

Additional file 1

Factors tested to detect DNA ligation activity of the DRB0100 gene product. This table lists the various buffer conditions and proteins tested in DNA ligation assays for the DRB0100 gene product.

Click here for file

[http://www.biomedcentral.com/content/supplementary/1471-2199-8-69-S1.pdf]

Additional file 2

Ligation substrates tested to detect DNA ligation activity of the DRB0100 gene product. This table shows the sequences of the different oligonucleotides that were used to prepare ligation substrates for the DRB0100 gene product.

Click here for file

[http://www.biomedcentral.com/content/supplementary/1471-2199-8-69-S2.pdf]

Acknowledgements

We thank M. Toueille, K. Makarova and E. Gaidamakova for helpful suggestions and discussions. We also thank R. Mak and U. Wimmer for critical reading of the manuscript. MB, RB and UH are supported by the Swiss National Science Foundation (Grant 3100A0-109312) and RB, IS and UH by the University of Zurich.

References

1. Cox MM, Battista JR: **Deinococcus radiodurans – the consummate survivor.** *Nat Rev Microbiol* 2005, **3(11):**882-892.
2. Daly MJ, Gaidamakova EK, Matrosova VY, Vasilenko A, Zhai M, Leapman RD, Lai B, Ravel B, Li SM, Kemner KM, Fredrickson JK: **Protein oxidation implicated as the primary determinant of bacterial radioresistance.** *PLoS Biol* 2007, **5(4):**e92.
3. Daly MJ, Gaidamakova EK, Matrosova VY, Vasilenko A, Zhai M, Venkateswaran A, Hess M, Omelchenko MV, Kostandarithes HM, Makarova KS, Wackett LP, Fredrickson JK, Ghosal D: **Accumulation of Mn(II) in Deinococcus radiodurans facilitates gamma-radiation resistance.** *Science* 2004, **306(5698):**1025-1028.
4. Bowater R, Doherty AJ: **Making ends meet: repairing breaks in bacterial DNA by non-homologous end-joining.** *PLoS Genet* 2006, **2(2):**e8.
5. Weller GR, Kysela B, Roy R, Tonkin LM, Scanlan E, Della M, Devine SK, Day JP, Wilkinson A, d'Adda di Fagagna F, Devine KM, Bowater RP, Jeggo PA, Jackson SP, Doherty AJ: **Identification of a DNA nonhomologous end-joining complex in bacteria.** *Science* 2002, **297(5587):**1686-1689.
6. Zahradka K, Slade D, Bailone A, Sommer S, Averbeck D, Petranovic M, Lindner AB, Radman M: **Reassembly of shattered chromosomes in Deinococcus radiodurans.** *Nature* 2006, **443(7111):**569-573.
7. Wilkinson A, Day J, Bowater R: **Bacterial DNA ligases.** *Mol Microbiol* 2001, **40(6):**1241-1248.
8. Liu Y, Zhou J, Omelchenko MV, Beliaev AS, Venkateswaran A, Stair J, Wu L, Thompson DK, Xu D, Rogozin IB, Gaidamakova EK, Zhai M, Makarova KS, Koonin EV, Daly MJ: **Transcriptome dynamics of Deinococcus radiodurans recovering from ionizing radiation.** *Proc Natl Acad Sci USA* 2003, **100(7):**4191-4196.
9. Makarova KS, Aravind L, Wolf YI, Tatusov RL, Minton KW, Koonin EV, Daly MJ: **Genome of the extremely radiation-resistant bacterium Deinococcus radiodurans viewed from the perspective of comparative genomics.** *Microbiol Mol Biol Rev* 2001, **65(1):**44-79.
10. Omelchenko MV, Wolf YI, Gaidamakova EK, Matrosova VY, Vasilenko A, Zhai M, Daly MJ, Koonin EV, Makarova KS: **Comparative genomics of Thermus thermophilus and Deinococcus radiodurans: divergent routes of adaptation to thermophily and radiation resistance.** *BMC Evol Biol* 2005, **5:**57.
11. Henner WD, Grunberg SM, Haseltine WA: **Sites and structure of gamma radiation-induced DNA strand breaks.** *J Biol Chem* 1982, **257(19):**11750-11754.
12. Henner WD, Rodriguez LO, Hecht SM, Haseltine WA: **gamma Ray induced deoxyribonucleic acid strand breaks. 3' Glycolate termini.** *J Biol Chem* 1983, **258(2):**711-713.
13. Amitsur M, Levitz R, Kaufmann G: **Bacteriophage T4 anticodon nuclease, polynucleotide kinase and RNA ligase reprocess the host lysine tRNA.** *Embo J* 1987, **6(8):**2499-2503.
14. Audebert M, Salles B, Weinfeld M, Calsou P: **Involvement of polynucleotide kinase in a poly(ADP-ribose) polymerase-1-dependent DNA double-strand breaks rejoining pathway.** *J Mol Biol* 2006, **356(2):**257-265.
15. Chappell C, Hanakahi LA, Karimi-Busheri F, Weinfeld M, West SC: **Involvement of human polynucleotide kinase in double-strand break repair by non-homologous end joining.** *Embo J* 2002, **21(11):**2827-2832.
16. Whitehouse CJ, Taylor RM, Thistlethwaite A, Zhang H, Karimi-Busheri F, Lasko DD, Weinfeld M, Caldecott KW: **XRCC1 stimulates human polynucleotide kinase activity at damaged DNA termini and accelerates DNA single-strand break repair.** *Cell* 2001, **104(1):**107-117.
17. Martins A, Shuman S: **An end-healing enzyme from Clostridium thermocellum with 5' kinase, 2',3' phosphatase, and adenylyltransferase activities.** *Rna* 2005, **11(8):**1271-1280.
18. Aravind L, Koonin EV: **The HD domain defines a new superfamily of metal-dependent phosphohydrolases.** *Trends Biochem Sci* 1998, **23(12):**469-472.
19. Blondal T, Hjorleifsdottir S, Aevarsson A, Fridjonsson OH, Skirnisdottir S, Wheat JO, Hermannsdottir AG, Hreggvidsson GO, Smith AV, Kristjansson JK: **Characterization of a 5'-polynucleotide kinase/3'-phosphatase from bacteriophage RM378.** *J Biol Chem* 2005, **280(7):**5188-5194.

20. Wang LK, Shuman S: **Mutational analysis defines the 5'-kinase and 3'-phosphatase active sites of T4 polynucleotide kinase.** *Nucleic Acids Res* 2002, **30(4):**1073-1080.
21. Doherty AJ, Suh SW: **Structural and mechanistic conservation in DNA ligases.** *Nucleic Acids Res* 2000, **28(21):**4051-4058.
22. Weller GR, Doherty AJ: **A family of DNA repair ligases in bacteria?** *FEBS Lett* 2001, **505(2):**340-342.
23. Leibowitz PJ, Schwartzberg LS, Bruce AK: **The in vivo association of manganese with the chromosome of Micrococcus radiodurans.** *Photochem Photobiol* 1976, **23(1):**45-50.
24. Evans DM, Moseley BE: **Identification and initial characterisation of a pyrimidine dimer UV endonuclease (UV endonuclease beta) from Deinococcus radiodurans; a DNA-repair enzyme that requires manganese ions.** *Mutat Res* 1985, **145(3):**119-128.
25. Lecointe F, Shevelev IV, Bailone A, Sommer S, Hubscher U: **Involvement of an X family DNA polymerase in double-stranded break repair in the radioresistant organism Deinococcus radiodurans.** *Mol Microbiol* 2004, **53(6):**1721-1730.
26. Blasius M, Shevelev I, Jolivet E, Sommer S, Hubscher U: **DNA polymerase X from Deinococcus radiodurans possesses a structure-modulated 3'-->5' exonuclease activity involved in radioresistance.** *Mol Microbiol* 2006, **60(1):**165-176.
27. Jilani A, Ramotar D, Slack C, Ong C, Yang XM, Scherer SW, Lasko DD: **Molecular cloning of the human gene, PNKP, encoding a polynucleotide kinase 3'-phosphatase and evidence for its role in repair of DNA strand breaks caused by oxidative damage.** *J Biol Chem* 1999, **274(34):**24176-24186.
28. Nick McElhinny SA, Snowden CM, McCarville J, Ramsden DA: **Ku recruits the XRCC4-ligase IV complex to DNA ends.** *Mol Cell Biol* 2000, **20(9):**2996-3003.
29. Narumi I, Satoh K, Cui S, Funayama T, Kitayama S, Watanabe H: **PprA: a novel protein from Deinococcus radiodurans that stimulates DNA ligation.** *Mol Microbiol* 2004, **54(1):**278-285.
30. Murakami M, Narumi I, Satoh K, Furukawa A, Hayata I: **Analysis of interaction between DNA and Deinococcus radiodurans PprA protein by Atomic force microscopy.** *Biochim Biophys Acta* 2006, **1764(1):**20-23.
31. Turko IV, Francis SH, Corbin JD: **Potential roles of conserved amino acids in the catalytic domain of the cGMP-binding cGMP-specific phosphodiesterase.** *J Biol Chem* 1998, **273(11):**6460-6466.
32. Eggington JM, Haruta N, Wood EA, Cox MM: **The single-stranded DNA-binding protein of Deinococcus radiodurans.** *BMC Microbiol* 2004, **4:**2.
33. Smirnova E, Toueille M, Markkanen E, Hubscher U: **The human checkpoint sensor and alternative DNA clamp Rad9-Rad1-Hus1 modulates the activity of DNA ligase I, a component of the long-patch base excision repair machinery.** *Biochem J* 2005, **389(Pt 1):**13-17.
34. Shuman S, Schwer B: **RNA capping enzyme and DNA ligase: a superfamily of covalent nucleotidyl transferases.** *Mol Microbiol* 1995, **17(3):**405-410.
35. Thompson JD, Higgins DG, Gibson TJ: **CLUSTAL W: improving the sensitivity of progressive multiple sequence alignment through sequence weighting, position-specific gap penalties and weight matrix choice.** *Nucleic Acids Res* 1994, **22(22):**4673-4680.
36. Marchler-Bauer A, Bryant SH: **CD-Search: protein domain annotations on the fly.** *Nucleic Acids Res* 2004:W327-331.

5.1.2. The putative O6-methylguanine-DNA methyltransferase (MGMT) of *Deinococcus radiodurans*

5.1.2.1. Cloning, expression and purification of MGMT

The putative O6-methylguanine-DNA methyltransferase (MGMT) of *D. radiodurans* was identified by Makarova et al. by using sequence homology comparisons [20, 121]. In order to analyze its potential role in DNA damage repair, the putative MGMT of *D. radiodurans* was cloned from genomic DNA. Several conditions were tested to achieve optimal protein expression. A soluble protein corresponding to the predicted size of 15.3 kDa was expressed sufficiently when bacteria where grown at 20°C for 2 hours after induction. Based on this result from the small-scale pre-experiments, one liter of *Escherichia coli* (*E. coli*) culture was used for large-scale expression. For purification of the expressed MGMT protein, an affinity chromatography was performed using a Nickel column that binds the expressed MGMT due to its N-terminal His-tag. The eluate from the Nickel column was further purified via a MonoQ column, an anion exchange column. The MGMT protein itself does not bind to this column. After purification through these two columns the MGMT was more than 99% pure as judged on a 15% SDS-PAGE gel (Figure 8).

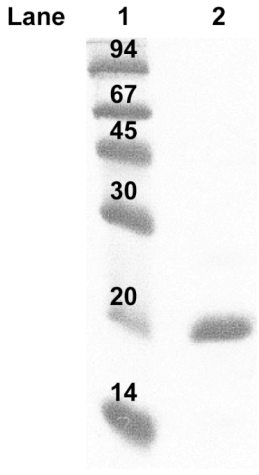

Figure 8. SDS-PAGE gel after purification of the putative MGMT of *D. radiodurans*. The *D. radiodurans* putative MGMT was purified over a Nickel affinity column and a MonoQ anion exchange column to near homogeneity as described in Materials and Methods and in the text. The protein was loaded onto a 15% SDS-PAGE and the gel was stained with Coomassie Blue R250. Lane 1: stained low

molecular weight (LMW) marker proteins and their respective sizes in kDa. Lane 2: purified MGMT protein (2.5μg).

5.1.2.2. Characterization of the putative MGMT

Bandshift assay. First, a band shift assay was used to test whether the putative MGMT of *D. radiodurans* can bind to DNA. For this purpose, the pRSETb vector was linearized and incubated with the purified putative *D. radiodurans* MGMT for 15min at 37°C. Then, the reaction mix was loaded on a 0.75% agarose gel that was stained with ethidium bromide after running. As shown in Figure 9, the main band was gradually disappearing with increasing amounts of the purified protein and two new bands were appearing accordingly (see asterisks in lane 7). One of these bands was running slower than the initial band, the other was running faster. This result suggested that the putative MGMT bound to DNA, resulting in a band that runs slower than the initial linearized DNA. The second band could be due to cutting of the vector DNA at a specific site by the putative MGMT, leading to a smaller fragment that is running faster than the longer, original linearized plasmid. However the purified MGMT might still be contaminated with an endonuclease that was co-purified in trace amounts.

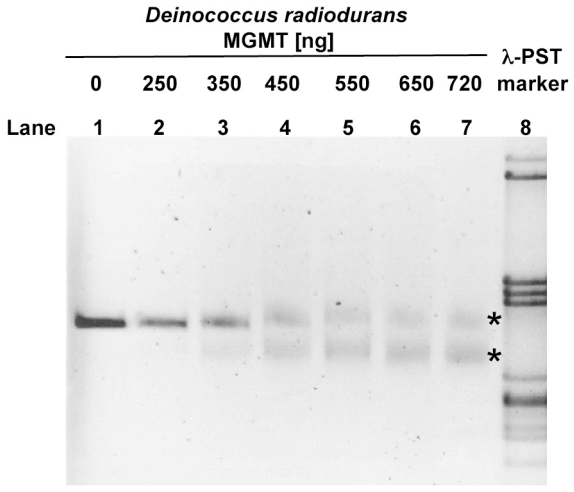

Figure 9. Bandshift assay using a linearized vector as a DNA template. The bandshift assay was performed as described in Materials and Methods. Lane 1: negative control (MGMT dilution buffer only). Lanes 2 to 7: increasing amounts of *D. radiodurans* MGMT protein were tested. Lane 8: λ-PST marker. Asterisks indicate the newly appearing bands, running slower and faster as the original one, respectively.

Indirect bandshift assay. To further investigate the DNA binding capacity of the putative MGMT of *D. radiodurans*, a collaboration with Franziska Fischer from Prof. Dr. J. Jiricny's laboratory at the Institute for Molecular Cancer Research (IMCR, Zürich) was initiated. MutSα binds to G/T mismatches if the respective guanine base is unmodified. In the approach used here, such an unmodified guanine base is achieved by demethylation by MGMT. For the assay, a linear oligonucleotide with a methylated guanine paired to a thymine is incubated with the MGMT proteins (hMGMT from Sigma as a positive control and the putative *D. radiodurans* MGMT under investigation). An active MGMT can transfer the methyl group form the guanine residue to its internal cysteine acceptor site, hence creating an unmodified guanine base. After incubation, proteinase K is added to the reaction mix to ensure removal of all MGMT proteins from the template. After heat inactivation of proteinase K, MutSα is added and can bind to the available G/T mismatches. The resulting DNA-protein complex can be detected by separation on an gel, as the respective DNA band is shifted in comparison to a template-only fragment. The positive control using an unmodified template showed a bandshift upon incubation with MutSα, in agreement with binding of MutSα to the template, resulting in a DNA-protein complex migrating slower than the template-only (Figure 10, lane 1). Upon incubation of the methylated template with MutSα no shift was detected, as MutSα cannot bind to a methylated guanine base (lane 2). Incubation of the methylated template with hMGMT prior to the addition of MutSα resulted in a shifted band, indicating removal of the methyl group from the DNA (lane 3). Upon incubation of the methylated template with the putative MGMT of *D. radiodurans*, a bandshift was observed. However, this shifted band was running at an intermediate position compared to the template-only band and the observed shifted band for the template bound by MutSα (see lanes 7-9, asterisks). This might be due to the fact that the *D. radiodurans* MGMT bound to the DNA but was afterwards not digested by proteinase K, thus remaining on the DNA. This could then impede the binding of MutSα, hence, the observed shift would rather be a result of MGMT binding to the DNA than MutSα. Although the reaction conditions were varied (without

KCl or substituting KCl by NaCl), no bandshift indicating MutSα binding to the template was observed.

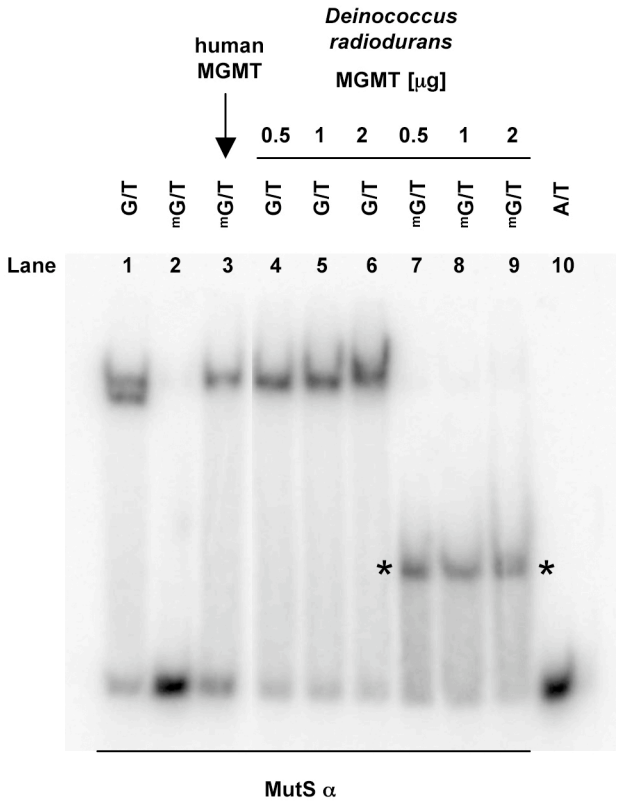

Figure 10. Bandshift assay using a template with a G/T-mismatch. The bandshift assay was performed as described in Materials and Methods. Two templates were used; in one, the guanine was not modified, in the other it was methylated. Lanes 1 and 2: unmodified and modified template, respectively, incubated with MutSα only. Lane 3: methylated template, preincubated with the human MGMT before the addition of MutSα. Lanes 4 to 9: titration of the *D. radiodurans* MGMT using the indicated amounts. Lane 10: control template with a A/T match. Asterisks indicate intermediate shifts.

O6-methylguanine-DNA methyltransferase activity of MGMT

Trichloroacetic acid (TCA)-Assay. The purified putative MGMT from *D. radiodurans* was next tested for its ability to transfer a radiolabeled methyl group from a previously prepared calf-thymus DNA substrate onto its internally located cystein acceptor residue. In a trichloroacetic acid (TCA) assay titrating the putative *D. radiodrurans* MGMT, the highest activity was observed with an amount of 500pmol (Figure 11A). With higher amounts, a higher activity was not evident, in contrary, the relative activity decreased significantly. However, the expression efficiency of the protein was very variable and therefore not always batches of purified proteins that would have

allowed the use of 500pmol could be achieved. Each experiment was performed in triplicate and all experiments were repeated at least three times. However, significant variations were observed between triplicates as well as between experiments, which is reflected in the high standard deviations (see for example Figure 11A). Furthermore, the actually measured counts per minute (cpm) numbers were close to the limit of detection. Accordingly, the observed relative activity of the positive control, namely purchased purified human MGMT (hMGMT; from Alexis), was not significantly above background levels (see Figure 11E). Nevertheless, different reaction conditions were tested in order to optimize the TCA assay. However, neither different amounts of EDTA (Fig. 11B), titration of different cations such as Na^{+} or Mn^{2+} (Figure 11C and D) or variation of pH (Figure 11E) in the reaction conditions, nor the application of *D. radiodurans* whole cell extracts (Figure 11F) in the TCA assay resulted in conclusive results.

In summary, it was impossible to detect any MGMT activity in the putative MGMT protein. The previous data suggested that the protein was correctly folded since it could bind to DNA. However, an explanation for the unapparent methyltransferase activity could lie in the reaction mechanism of MGMTs; in contrast to classical enzymes, an individual MGMT protein cannot catalyze in a classical way; it only enables one single transferase action. Thus, it was generally difficult to detect MGMT protein activity with this assay, which was confirmed by the low activity of the hMGMT (see also Discussion).

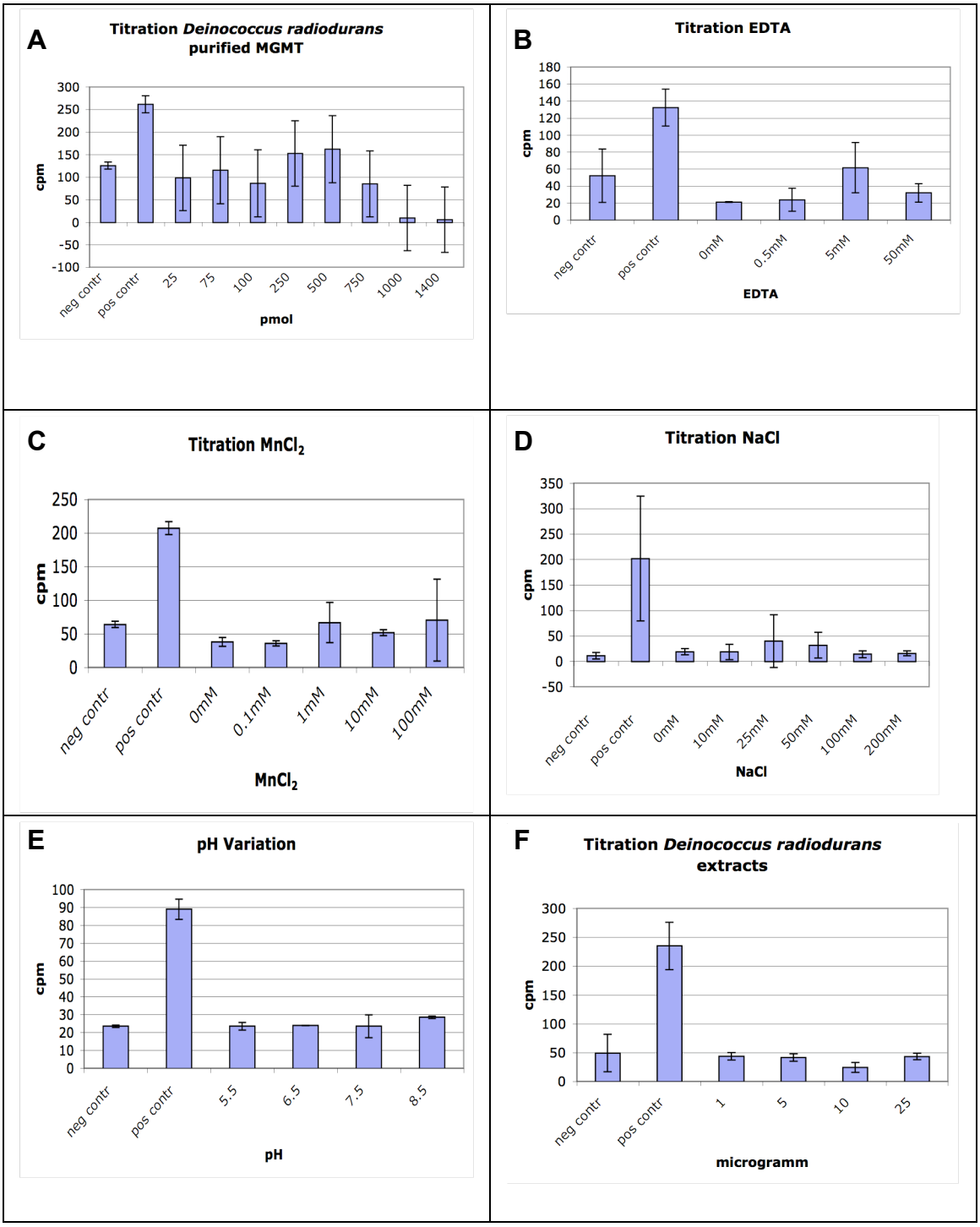

Figure 11. Activity measurements of *D. radiodurans* putative MGMT. The assay was performed as described in Materials and Methods. *D. radiodurans* putative MGMT amount was kept constant (100pmol in all the experiments except for 11A and F). **A)** Titration of the *D. radiodurans* putative MGMT. Note the high standard deviations as well as the negative results with high amounts of the purified protein. **B)** Titration of EDTA. **C)** Titration of $MnCl_2$. **D)** Titration of NaCl. **E)** Test of different pH conditions. **F)** Titration of *D. radiodurans* cell extracts. As a positive control, the human MGMT was used in all the experiments; as a negative control MGMT dilution buffer only was added. All experiments were done at least in triplicates and standard deviations are given. Y-axis: cmp = counts per minute.

However, the results obtained, even though disappointing at the time made, became clearer in the view of a very recent publication, suggesting that MGMTs and alkyltransferase-like (ATL) proteins from prokaryotes as well as from lower eukaryotes are inactive *in vitro*, since they simply flip the alkylated base out of the DNA helix, leaving the lesion to be repaired by proteins of the nucleotide exision repair pathway. Those data support the negative findings with the *D. radiodurans* MGMT protein ([122] and Discussion).

5.2. Studies of human DNA repair enzymes

5.2.1. Interaction of the human apurinic/apyrimidinic endonuclease 1 (Ape1) with the Rad9/Rad1/Hus1 (9-1-1) complex

5.2.1.1. Previous results

Components of the base excision repair (BER) pathway were previously shown to interact with the 9-1-1 complex. The latest findings came from Gembka et al. [92], showing that the 9-1-1 complex not only interacts with Ape1 but also stimulates its endonuclease activity in an *in vitro* reconstituted BER system. Tabelle 1 documents a summary of the so far known BER-participating interaction partners of the 9-1-1 complex.

LP-BER component	Functional consequence	Reference
MutY DNA glycosylase	Stimulation of glycosylase activity	[90, 94]
Ape1	Stimulation of AP endonuclease activity	[92]
DNA pol β	Stimulation of polymerase and strand displacement activities	[96]
Fen 1	Stimulation of endo- and exonuclease activities	[91, 97]
Lig I	Stimulation of ligase activity	[95, 98]

To further study the interaction of the 9-1-1 complex with Ape1, Ape1 fragments were generated to narrow down the interaction site and get more insights about its functional relevance.

5.2.1.2. Cloning, expression and purification of human Ape1 fragments

Ape1 was subdivided into three distinct regions according to their predicted functions [65], namely an N-terminal part, a middle part and a C-terminal part (see Figure 12). The N-terminal part (further referred to as part A) encloses the nuclear localization signal (NLS) and residues, which are required for the redox and endonucleatic functions. The middle part (further referred to as part B) harbors three predicted binding motifs suggested to be involved in the interaction with the 9-1-1 complex [123]. The C-terminal part (further referred to as part C) contains putative phosphorylation sites as well as residues that are supposedly essential for the protein`s conformation and catalysis .

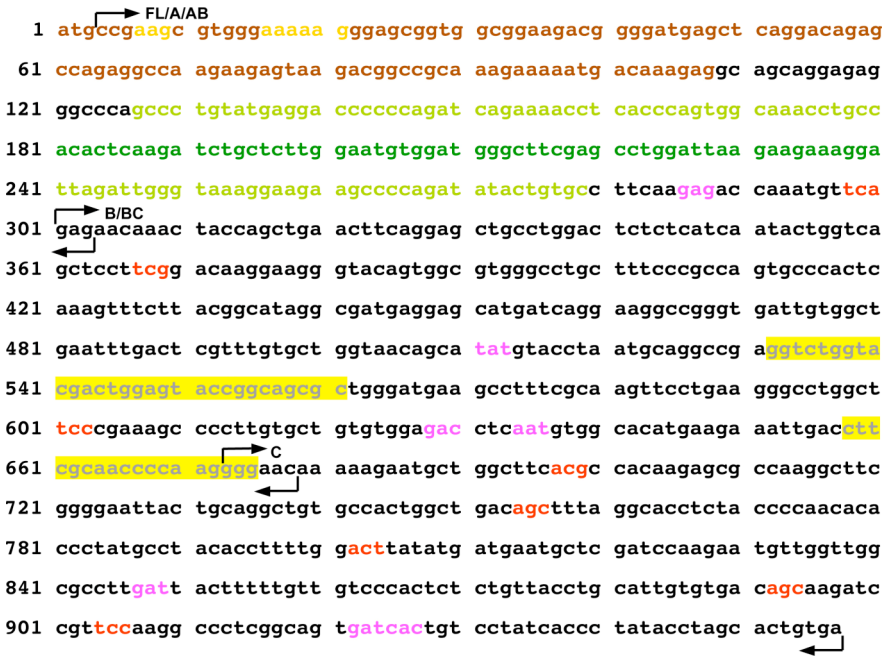

Figure 12. Nucleotide sequence of the human Ape1 gene according to the PubMed database. The nuclear localization signal is depicted in brown and the acetylation sites in yellow. Nucleotides encoding residues required for redox activity and endonuclease activity are in light green and dark green, respectively. Nucleotides encoding potential phosphorylation sites are shown in red, nucleotides encoding residues that are important for conformation and catalysis are in pink. Highlighted with yellow boxes are the putative 9-1-1 interaction motifs 1 & 2, and 3, respectively. Arrows indicate beginning and ends of the fragments.

In a first step, the three fragments and combinations thereof were cloned without an additional tag for detection. However, the subsequent purification failed due to detection problems. The anti-Ape1 antibody used was sufficiently specific to detect the purified wild-type Ape1, but a clear distinction of the expressed Ape1 fragments from unspecific bands in *E. coli* lysates was not possible. The expression of the fragments could not be boosted to sufficiently high levels either, which would have allowed clear discrimination from unspecific bands without an antibody. In any case no further experiments could be performed with the untagged Ape1 fragments. As the Rad9 subunit of the 9-1-1 complex was already carrying a hexa-histidine tag (his-tag) and a GST-tag would have been rather large compared to the small Ape1 fragments, an HA-tag was introduced at the C-terminus of each fragment. The HA-tag consists of nine amino acids and thus interferes usually not with the folding of the tagged protein. After successful cloning and verification of the sequence by Microsynth, the truncated proteins were expressed in BH110 *E. coli* cells (kindly provided by M. Saparbaev), which are double mutants for the *E. coli* Ape1 homologs *xth* and *nfo*. The expression conditions were optimized for each fragment in a small-scale experiment; overnight expression at 16°C turned out to be optimal for fragments A and AB, expression overnight at 20°C was best for fragment B and BC, and tagged full-length Ape1 and fragment C were expressed best after 4 hours at 37°C. Figure 13A shows a schematic representation of the different truncated protein fragments. In Figure 13B a representative western blot is shown for the expression efficiency of the different fragments after optimizing the conditions. Despite various attempts at achieving higher expression levels of the truncated proteins, the observed expression remained low. In combination with the frequently observed impaired cell growth and cell death, respectively, after induction of protein expression, this indicated a toxic effect of the protein fragments on the *E. coli* cells.

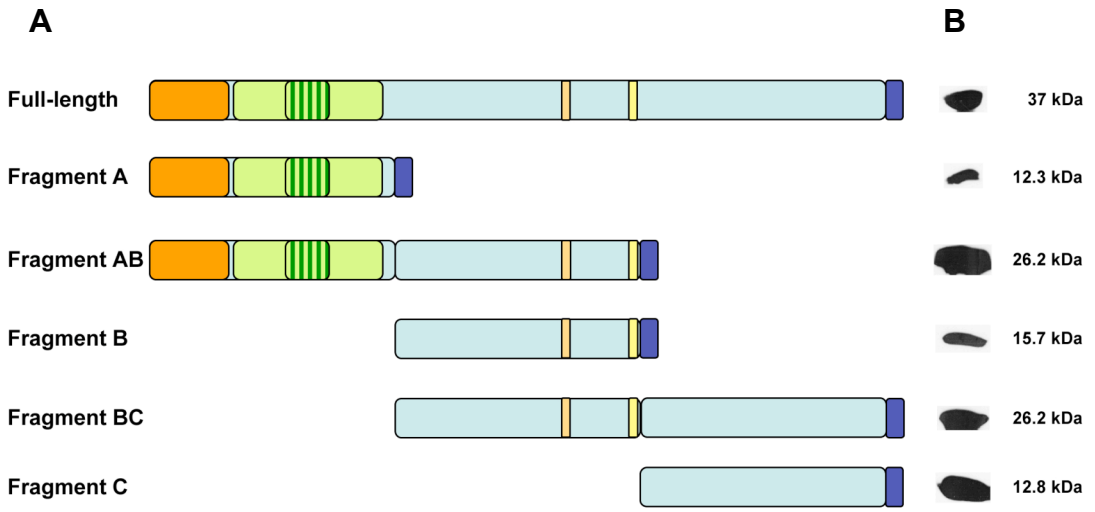

Figure 13. Schematic representation of the Ape1 fragments and their expression. A) Schematic representation of the fragments. Full-length; A; AB, which consists of A and B; B; BC, which consists of the middle and the C-terminal parts, and C. All fragments are C-terminally HA-tagged (dark blue). Dark orange is the NLS, light green represents the residues necessary for the redox activity, in dark green are the amino acids important for the endonuclease activity. Light orange and yellow represent the putative interaction sites with the 9-1-1 complex. **B)** Western blot analysis of expressed fragments with their predicted size, detected on a 15% SDS-Page gel incubated with anti-HA antibody; 20µl of total cell lysate was loaded per fragment.

For protein purification, an one liter culture of *E. coli* BH110 bacteria was grown and expression of the tagged full-length Ape1 and of each of the five fragments was induced by adding 1mM IPTG after reaching an OD_{600} of 0.5-0.6. Purification from the *E. coli* cell extracts was performed by using three chromatography columns, being a HiTrap™ Q-sepharose anion exchange column, a HiTrap™Heparin HP affinity/cation exchanger column and an HiTrap™SP HP cation exchange column. In contrast to the purification of wild-type Ape1, only little binding of the truncated proteins to the columns was observed. This might be due to differences in the isoelectrical point (pI) of the wild-type protein and the five fragments. Whereas the untagged wild-type Ape1 has a pI of 8.7, the respective protein fragments have pIs ranging from 6.6 to 5.2, thus resulting in a difference in their net charges. Therefore, next the pH of the purification buffers was adjusted to pH 5.5 to achieve a net charge of the fragments similar to that of the wild-type Ape1. Despite this pH change, the truncated proteins could not be purified in sufficient amounts for further experiments.

Finally, anti-HA agarose beads were used to improve the purification efficiency of the five fragments. In this case, the protein fragments bound efficiently to the matrix but no significant elution was achieved with the recommended low pH buffer. Therefore, all further experiments were conducted with protein fragments bound to anti-HA beads.

5.2.1.3. Characterization of the Ape1 fragments and their interaction with the 9-1-1 complex

Endonuclease experiments. First, the endonuclease activity of the fragments was tested and compared to the untagged full-length Ape1. For this the fragments were first coupled to the anti-HA beads followed by washing as described in Materials and Methods. Then the beads were incubated with a radioactively labeled 100mer oligonucleotide containing an AP site at position 43. As depicted in Figure 14, 100% cutting at the AP site was detected for both, the purified untagged Ape1 and the full-length HA-tagged Ape1 bound to anti-HA beads. In case of the fragment A about 50% residual endonuclease activity was observed, whereas all other fragments showed no cutting. This was expected, since an N-terminally located endonuclease domain was predicted [65]. However, quantification of the observed results was not possible due to variations in AP endonuclease product formation as well as differences in the coupling efficiency of the different protein fragments to the anti-HA beads. Therefore, further investigations with a different approach will have to be performed to verify the observed results.

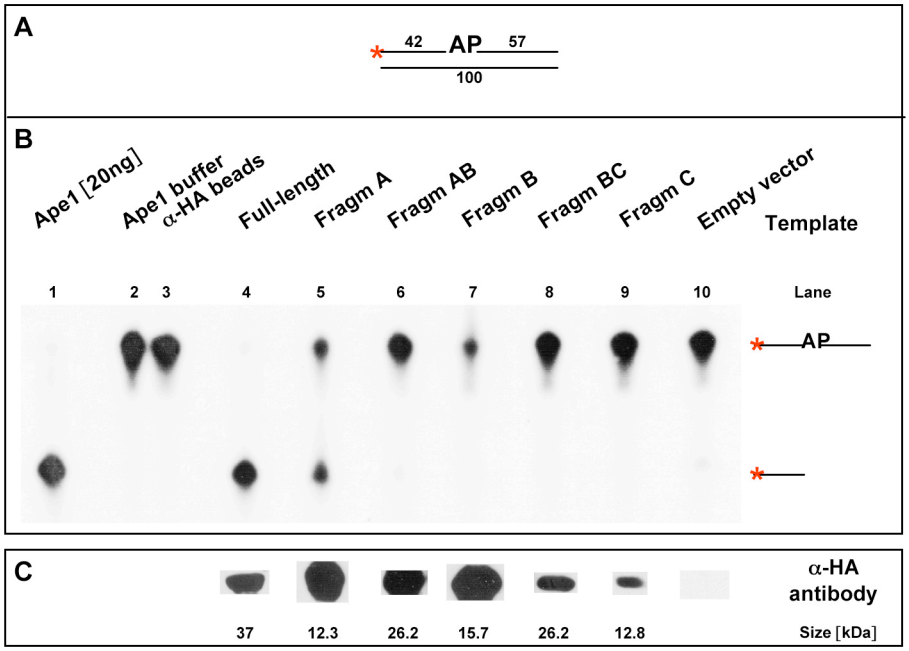

Figure 14. Endonuclease activity of Ape1 and its fragments on beads. The assay was performed as described in Materials and Methods. **A)** Template used in the assay: 100mer containing an abasic site at position 43. **B)** Endonuclease assay with Ape1 protein fragments coupled to HA-beads. Right is the schematic representation of the formed DNA after cutting by Ape1 and its fragments. **C)** Western blot representing the coupling efficiency of the different fragments to the HA-beads.

Pull-down experiments. To further characterize the interaction between the 9-1-1 complex and Ape1 [92], pull-down experiments were performed with the five Ape1-fragments. In contrast to the experiments described by Gembka et al, the fragments carried a HA-tag and were not purified prior to the incubation. Instead, the expressed protein fragments from *E. coli* extracts were bound to anti-HA agarose beads, washed and incubated with purified 9-1-1 complex. As a positive control, HA-tagged full-length Ape1 was tested. The results are shown in Figure 15.

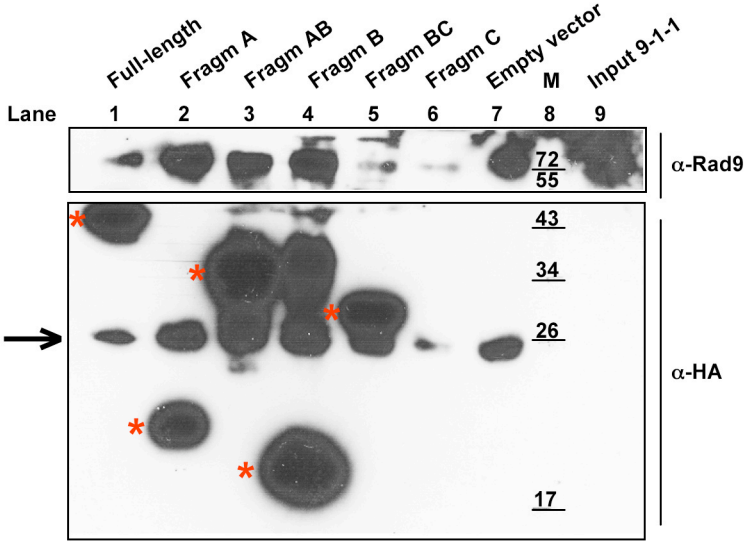

Figure 15. Pull down with Ape1 and its five fragments. The HA-tagged protein fragments from *E. coli* cell extracts were bound to HA-beads and incubated with 5μg of purified 9-1-1 complex as described in Materials and Methods. Lanes 1 to 6: full-length Ape1 and the different protein fragments, respectively, as indicated by asterisk. Lane 7: cell lysate with the empty vector only. Lane 8: low molecular weight marker in kDa. Lane 9: 2% input of the 9-1-1 complex. The blot was incubated with anti-Rad9 antibody for detection of the interaction with the 9-1-1 complex and anti-HA antibody for detection of the bound Ape1 proteins as indicated. The HA-antibody also recognizes the antibody light chain, which has a size of roughly 25kDa and is indicated with an arrow.

A moderate interaction with the 9-1-1 complex was observed for full-length Ape1. In contrast to sequence alignments of Ape1 predicting interaction sites in the middle part of the protein (Figure 12 and schematic representation in Fig 13), all of the generated fragments appeared to interact with the 9-1-1 complex (Figure 15). In addition, a band indicating an interaction was detected for the negative control, although anti-HA agarose beads were in this case incubated with cell extract from BH110 *E. coli* cells transformed with the empty vector. However, it cannot be excluded that the HA-tag might have some effect that is interfering with the interaction between the Ape1 and the 9-1-1 complex. Still it might be possible that the truncated proteins are folded differently as compared to the wild-type protein. However, detection of the Rad9 subunit in the performed pull-down experiments was considered representative for an interaction with the 9-1-1 complex. However, it turned out that the anti-Rad9 antibody also recognizes the antibody heavy chains present on the anti-HA agarose beads (Figure 16); the resulting western blot

band can hardly be separated from the band of the Rad9 subunit. As the available anti-Rad1 and anti-Hus1 antibodies cannot be used for these assays due to their low sensitivity and the specificity of the anti-His antibody is not sufficient, a new antibody would have to be generated for further investigations.

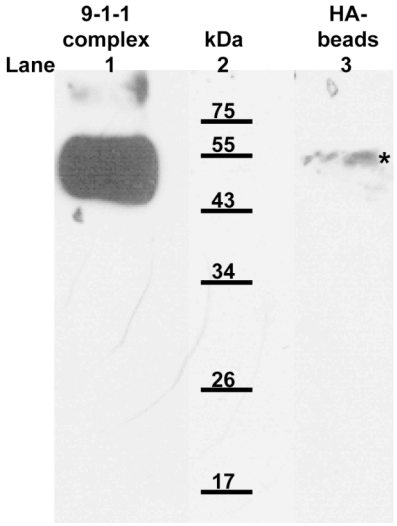

Figure 16. The anti-Rad9 antibody recognizes the antibody heavy chain of the HA-beads. Lane 1: 2μg purified 9-1-1 complex. Lane 2: Pre-stained low molecular weight marker. Lane 3: 20μl slurry HA-beads, after washing with IP-buffer. The unspecific band is indicated by an asterisk. The blot was incubated with anti-Rad9 antibody.

Far western experiments. The interaction the of 9-1-1 complex with the five fragments of Ape1 was further tested by far western. In order to establish optimal reaction conditions, the previously described interaction of DNA pol β with the 9-1-1 complex [96] was verified along with DNA pol λ and BSA as negative controls.

For DNA pol β the expected interaction with the Rad9 subunit was observed. However, a band indicating an interaction was also detected for DNA pol λ and the 9-1-1 complex (Figure 17, lanes 3 and 4). As expected, no interaction was observed with BSA as a negative control.

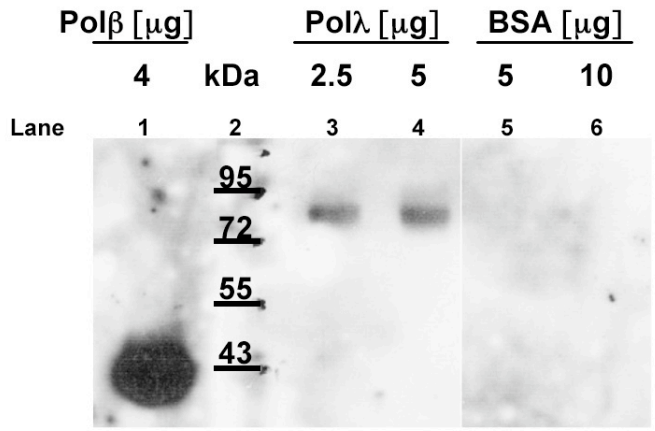

Figure 17. Interaction of DNA pol λ with the 9-1-1 complex. The assay was performed as described in Materials and Methods. Lane 1: Interaction of DNA pol β and Rad9 of the 9-1-1 complex. Lane 2: Pre-stained low molecular weight marker. Lanes 3 and 4: interaction of Rad9 with DNA pol λ in the indicated amounts. Lanes 5 and 6: BSA as a negative control in two different amounts. The blot was incubated with anti-Rad9 antibody.

5.2.4. DNA Polymerase λ interaction with the 9-1-1 complex

Immunoprecipitation (IP) assay. In order to verify the interaction of DNA pol λ with the 9-1-1 complex, immunoprecipitation (IP) experiments were performed using purified 9-1-1 complex and DNA pol λ. Since the anti-Rad9 antibody used binds also to antibody heavy chains in addition to Rad9, and the respective signals cannot be clearly separated on SDS-PAGE gels for western blots. Therefore, immunoprecipitation of DNA pol λ via an anti-DNA pol λ antibody and subsequent detection of co-immunoprecipitated 9-1-1 complex via the anti-Rad9 antibody was not possible. Thus, a vice versa approach was tested with immunoprecipitating the 9-1-1 complex via the anti-Rad9 antibody and subsequent detection of a DNA pol λ interaction by the available DNA pol λ antibody. However, no such interaction was observed with this approach. In addition, all *in vivo* immunoprecipitation experiments utilizing HeLa cell extracts showed no obvious interaction of the 9-1-1 complex and DNA pol λ. Further experiments are required to verify these initial results indicating a putative interaction of the 9-1-1 complex and DNA pol λ.

5.2.5. Manuscript in preparation

My contribution to this work was the cloning of the DNA pol λ mutants used in this study as described in Materials and Methods.

Residue 505 of human DNA polymerase λ acts as a molecular gate for O-6-methylguanine lesion bypass

Prasanna Parasuraman[1], Rebecca Buob[1], Giovanni Maga[2] and Ulrich Hübscher [1,*]

[1] Institute for Veterinary Biochemistry and Molecular Biology, University of Zürich – Irchel, Winterthurerstrasse 190, CH-8057 Zürich (Switzerland).

[2] Institute of Molecular Genetics IGM-CNR, via Abbiategrasso 207, I-27100 Pavia (Italy)

[*] Corresponding author: Ulrich Hübscher, Phone: +41 44 635 54 72, Fax: + 41 44 635 68 40, Mail: hubscher @ vetbio.uzh.ch

Running title: DNA polymerase λ faithful bypass of O-6-mG

Abstract

DNA polymerase λ (pol λ) a member of the DNA polymerase X family has a role in non-homologous end-joining and is believed to play an important role as an accurate translesion pol in base excision repair after DNA replication. We show here that a hydrophobic substitution mutant of the highly conserved residue at the active site of human pol λ (Y505M) allows better incorporation of the correct nucleotide (dCTP) over an O-6-methylguanine (O-6-mG) template relative to the non complementary nucleotide (dTTP). In contrast the wild-type pol λ incorporated as expected preferentially the incorrect dTTP. This is the first report of a pol showing faithful bypass of the O-6-mG lesion and can help to elucidate the molecular basis for the mutagenic potential of this lesion. These studies also highlight the importance to explore the impact of hydrogen bonding network on pol selectivity, which can be extended to other lesions to understand the functional and structural mechanism of lesion bypass by pol λ and by other pols (e.g. Y family pols) as well.

Introduction

DNA is subjected to a variety of chemical modifications that alter its structure. One such modification is non-enzymatic DNA methylation, which can be caused by endogenous chemicals, products of metabolism, environmental exposure or treatment with cancer chemotherapeutics(1). Methylating agents primarily react with exocyclic

nitrogen or oxygen atoms on purines and pyrimidines, with the relative ratio of oxygen to nitrogen modifications depending on the reaction mechanism of the respective agent (S_N1 or S_N2 nucleophilic substitution)(2). S_N1 methylating agents that produce O-6-methylguanine (O-6-mG) adducts include (i) N-methyl-N-nitrosourea (MNU), a mammary gland carcinogen in rat and lymphomagen in the mouse, (ii) N-methyl-N′-nitro-N-nitrosoguanidine, a hepatic carcinogen and (iii) 4-(methylnitrosamino)-1-(3-pyridyl)-1-butanone (NNK), a lung carcinogen that can be found in tobacco smoke(3,4). O-6-mG lesions are recognized under normal circumstances by O-6-mG DNA methyltransferase (MGMT) a specific DNA repair enzyme which transfers the mutagenic alkyl group from the O-6 position of guanine to a cysteine residue within its active site and is then targeted for degradation(5). When MGMT, however, does not remove the methyl group from 6 position of guanine, than O-6-mG persists in DNA and can pair with dTMP during replication, thus creating a promutagenic O-6mG:T mismatch(6). Such mismatches can result in G:C→A:T transition mutations upon the next round of replication or can bring about cell cycle arrest and cell death in a mismatch repair (MMR)-dependent manner(7,8). It has recently been shown that repair-dependent processing of methylation damage gives rise to persistent single-strand gaps in newly replicated DNA. Due to the persistence of O-6-mG in the exposed template strand, repair synthesis cannot take place, leaving a gap behind the replication fork. The consequence is that in the next S phase these gaps cause replication fork collapse with the consequence of recombination and cell cycle arrest(9). DNA lesions often stall the progression of DNA polymerases (pols), and it has been shown that O-6-mG lesion blocked *E.coli* pol I Klenow fragment as well as the eukaryotic pol α and pol β, involved in DNA replication and DNA repair, respectively(10-12). Moreover, it has been shown that translesion pols (Y family e.g. pols η, ι, κ) show similar efficiencies for insertion of dCTP and dTTP opposite the O-6-mG, excluding pol ι, which had strong preference for dTTP(13). Another report suggested that pol κ is a poor translesion pol over O-6-mG, but when it incorporated either T or C efficient elongation is achieved by pol δ(14). Several reports have shown that mutation of one or few key residues in the active sites of pols is sufficient to increase their fidelity(15,16). The recently solved X-ray crystal structures of O-6-mG in complex with the *Bacillus stearothermophilus* pol, showed that substrate specificity can be achieved by selecting for the nucleotide

with shape and hydrogen-bonding patterns that resemble a canonical DNA base pair(17).

We generated a novel pol λ mutant by exchanging the conserved tyrosine residue 505 of the active site with methionine (Y505M). We have previously shown that this residue is intricately connected to its neighbouring residues and likely plays a major role in the fidelity of the enzyme(18-21). The hydrophobic Y505M mutation enabled pol λ to faithfully bypass O-6-mG (correct dCTP incorporation), which is in contrast to the parental pol λ wild-type (wt) that, as expected, incorporated the wrong nucleotide dTTP.

Materials and Methods

Oligonucleotide synthesis

Oligonucleotides were synthesized by the Purimex. All the oligonucleotides were purified by denaturing polyacrylamide gels (PAGE).

Mutation, expression, and purification of human DNA pol λ

The bacterial expression plasmid pRSET-B encoding human pol λ wt with an N-terminal hexahistidyl sequence has been described previously, Ramadan et al (22). Site-directed mutagenesis was performed to obtain a pol λ mutant using Plasmid pSET-B and Phusion™-High-Fidelity DNA Polymerase according to the manufactures instructions (Finnzymes, Finland) using the following pairs of mutagenic oligonucleotides (Microsynth).

Y505M-up: 5'GCCTGTGCCCTGCTCATGTTCACCGGCTCTGCAC-3'

Y505M-down: 5'GTGCAGAGCCGGTGAACATGAGCAGGGCACAGGC-3'

Expression of mutant pol λ was conducted in *E.coli* BL21 (DE3) cells, grown at 37°C to an OD_{600} of 0.6 in LB medium supplemented with 100µg/ml ampicillin. Expression of human His-pol λ wt and mutant protein was induced by incubation with 1 mM IPTG for 3h and cells were pelleted. All futher purification steps were carried out at 4°C. Cells were resuspended in 60ml buffer A (50mM Tris-HCl pH 7.5, 10% (v/v) glycerol, 0.05% (v/v) NP-40, 1mM PMSF, 1µg/ml pepstatin, 1µg/ml bestatin, 1µg/ml leupeptin) supplemented with 500mM NaCl and disrupted with a french press.

Insoluble material was pelleted by centrifugation for 30m at 48,000g and the supernatant was diluted to a final concentration of 100mM NaCl in buffer A. The extracts were loaded onto a 15ml phosphocellulose equilibrated in buffer A with 100mM NaCl and rolled for 2h at 4°C. After intensive washing with buffer A with 100mM NaCl, elution was performed with buffer A with 500mM NaCl (4x15ml). The pooled eluate was diluted with an equal volume of buffer B (50mM Tris-HCl pH 7.5, 150mM NaCl, 10% (v/v) glycerol, 0.05% (v/v) NP-40, 1mM PMSF, 1µg/ml pepstatin, 1µg/ml bestatin, 1µg/ml leupeptin) and adjusted to 10mM imidazole. 0.5 volumes were loaded onto a 1ml His Trap TM HP column (GE Healthcare) equilibrated with buffer B and 10mM imidazol using an AKTA purifier TM (GE Healthcare). After washing the column with 5 ml buffer B with 10mM imidazol, elution was performed using a gradient from 10 to 500mM imidazol in buffer B and fractions containing His-pol λ were pooled. The pool was diluted 1:3 with buffer A, and loaded onto a 1ml HiTrap TM Heparin HP column (GE Healthcare) equilibrated with buffer A with 50mM KCl.The column was washed with 5ml buffer A with 100mM KCl and eluted using a gradient from 100mM to 1M KCl in buffer A as well as a final step with buffer A with 2M KCl. The final fractions containing purified His-pol λ and the Y505M mutant proteins were dialyzed to buffer C (20mM Tris-HCl pH 7.5, 20% (v/v) glycerol, 100mM NaCl, 1mM DTT) and stored in small aliquots in liquid nitrogen.

Primer extension assays

The primer was labelled at its 5′- end with [γ -32P] ATP (Hartmann Analytic) and T4 polynucleotide kinase (Fermentas). The primers were then hybridised to equimolar amounts of the appropriate template oligonucleotides in the presence of 50mM Tris-HCl (pH 7.5) and 0.3M NaCl, heated to 80°C for 10min before slowly cooling down to room temperature overnight. The primer extension assays were carried out in reaction mixture (10µl) containing 50mM Tris-HCl pH 7.0, 0.25mg/ml BSA, 10mM DTT and 10fmol of the 5′^{32}P-labelled primer template, and 1.0mM Mg^{2+}, 10µM dNTP and the indicated concentration of wt and Y505M enzyme in the Figure, and incubated at 37°C for 15 min. After incubation, the reactions were stopped by adding loading buffer (10mM EDTA, 95% formamide and 0.03% bromophenol blue, and

0.3% cyanol blue). The products were analysed by 15% denaturating PAGE by autoradiography.

Single nucleotide insertion assays

The primer/template complexes (whose sequence as indicated in the respective figure) were annealed as described in the primer extension assay. The reactions were initiated by adding 10μM of the indicated dNTP, in a reaction mixture (10μl) containing 50mM Tris-HCl pH 7.0, 0.25mg/ml BSA, 10mM DTT and 10fmol of the $5'^{32}$P-labelled primer template, pol λ wt and Y505M at 40nm and 1.0mM Mg^{2+}, and incubated at 37°C for 15min. After incubation, reactions were stopped by adding loading buffer (95% formamide, 10mM EDTA, Xylene cyanol and Bromophenol blue) heated at 95°C for 3min, loaded and separated on a 7M Urea 15% polyacrylamide gel and the products mixture analysed by autoradiography.

Sequence dependent incorporation assay

The primer/template complexes were annealed as described in primer extension assays (sequence as depicted in the respective Figure). In order to determine the rates of dCTP and dTTP incorporation with respect to nucleotide substitution after the lesion, dCTP and dTTP were titrated from 1 to 100μM in reaction conditions as stated above in the primer extension assay. The observed rates of nucleotide incorporation were calculated from the values of integrated gel band intensities.

I^*_T/I_T-1

Where T is the target site, the template position of interest; I^*_T is the sum of the integrated intensities at positions T, T + 1,……, T + *n*

All the intensity values were normalized to the total intensity of the corresponding lane to correct for difference in gel loading. The apparent K_m and k_{cat} values were calculated by plotting the initial velocities in dependence of the nucleotide concentration [dCTP] and [dTTP], and fitting the data according to the Michaelis – Menten equation:

$K_{cat}\,[E]_o/(I+k_m/[dNTP])$

Where $[E]_0$, was the input enzyme concentrations. Nucleotide concentrations used were 1μM, 10μM and 100μM. Nucleotide incorporation efficiencies were defined as

the k_{cat}/K_m ratio. Under single nucleotide incorporation conditions $k_{cat}=k_{pol}k_{off}/(k_{pol}+k_{off})$ and $K_m=K_sk_{off}/(k_{pol}+k_{off})$, where k_{pol} is the true polymerization rate, koff is the constant for nucleotide binding. Thus, k_{cat}/K_m values are equal to k_{pol}/K_s.

Results

Cloning, expression, purification and initial characterization of pol λ Y505M

The human pol λ wt and the active site mutant Y505M carrying a His tag were cloned in *E.coli,* over-expressed and purified to apparent homogeneity (Fig 1a). Pol λ, either the wt or the Y505M mutant were tested in a pol assay with a 5′- end -labelled 39:72 primer/template DNA oligonucleotide substrate. Y505M pol λ apparently displayed an increased distributivity when compared to the wt on the control template (Fig 1b), resulting in the generation of shorter products.

Mutant pol λ Y505M but neither pol λ wt nor pol β can incorporate the correct dCTP opposite a O-6-mG in a single nucleotide insertion assay

Both wt and Y505M pol λ were next analysed on 39:72 template, but containing a single O-6-mG lesion, in the presence of the indicated dNTP. Y505M incorporated the "correct" nucleotide (dCTP) opposite O-6-mG almost 9 fold better when compared to the dCTP insertion by wt (Table 1 and Fig 2a), whereas no difference was noticed against undamaged dG (Fig 2b). On the opposite the mutant Y505M catalysed "incorrect" dTTP insertion opposite O-6-mG at a highly reduced rate compared to the wt. In comparison, the family X pol β showed, as expected incorporation of the incorrect dTTP at a much higher rate, than the correct dCTP. Neither wt nor Y505M showed any difference in misincorporation of dTTP opposite dG (Fig 2c), suggesting that Y505M does not induce any increase in discrimination against a normal T:G mismatch. When both the wt and Y505M pols were tested in the presence of 8-oxo-G lesion, they both incorporated dCTP better than dATP opposite the lesion, without differences between them, suggesting that the observed effect for the mutant Y505M was specific for dCTP incorporation against O-6-mG (Fig 2d). Similarly, when tested on an 8-oxo-A template, both enzymes showed preferential incorporation of dGTP without difference between wt and Y505M (Fig 2e). These

two control experiments suggested that the Y505M mutant did not have an intrinsic preference for the incorporation of dCTP.

Pol Y505M favours dCTP incorporation opposite O-6-mG independently from the sequence context.

To test for the effect of flanking nucleotides on O-6-mG, we next titrated dCTP and dTTP on primer/template where the first nucleotides in the template strand was O-6-mG, followed by either G, A, T or C respectively. No significant difference was observed, with respect to dCTP or dTTP incorporation, on O-6-mG/C and O-6-mG/T templates (Figure S1A). With the O-6-mG/G template, it was seen that the Y505M mutant was more efficient than wt in incorporating dCTP (Fig 3a) and less efficient in incorporating dTTP (Fig 3c). Similarly, with the template O-6-mG/A the wt was more efficient than Y505M in incorporating dTTP (Fig 3b) but less efficient in incorporating dCTP (Fig 3d). As expected most product accumulated at position +2 (Fig 3a and b). However significant accumulation of +3/4 products could be seen with the O-6-mG/G template and dCTP as substrate (Fig 3a), whereas only very few +3 products were generated with the O-6-mG/A template in combination with dTTP (Fig 3b). This indicated that in the presence of dCTP, pol λ makes template slippage at the C, at +3 position, thus the +3/4 products are generated by using the GG at position 4 and 5 as the templating bases. This explains the fact that only a minimal amount of +3 products are detected with 6-mG/A template in combination with dTTP, since in such case no slippage can occur.

Extension beyond the O-6-mG lesion paired to dCTP or dTTP by DNA pol λ wt and Y505M shows no significant difference.

To further characterize the efficiency of extension of a primer paired to O-6-mG by pol λ wt and Y505M, dCTP was titrated at varying concentration in the presence of template/primers terminating with either a 3′-OH O-6-mG/dC or a O-6-mG/dT base pair, respectively. Pol λ wt and Y505M showed no significant difference in elongation, starting from a respect “correct” O-6-mG:dC base pair, with respect to an “incorrect” O-6-mG:dT (Fig 4). No significant difference under these conditions was noticed for the extension at the undamaged template dG:dC.

Discussion

The results presented in this study, show that mutation of the active site residue Y505 of pol λ, which is believed to be involved in dNTP binding, completely changed nucleotide incorporation selectivity opposite O-6-mG lesion. Although methylation of the O6 position of guanine constitutes only a fraction of the total alkylation damages, this lesion is among the most carcinogenic(23). The fact that all known pols to date show a preferential incorporation of T opposite O-6-mG, led us to investigate the molecular mechanisms for nucleotide selection by pols opposite this particular lesion. We choose as a model enzyme the X family pol λ. Recent data from our laboratories suggested that pol λ was most accurate in dealing with 8-oxo-G, in combination with the auxiliary proteins PCNA and RP-A(24). In this study we show that mutant pol λ carrying a hydrophobic amino-acid methionine instead of a tyrosine at position 505 was able to bypass an O-6-mG lesion, by preferentially incorporating the correct nucleotide dCTP. PCNA and RP-A showed no effect (data not shown). Preliminary molecular modelling studies suggested the intriguing hypothesis that the 505 Methionine side chain, could disrupt one H-bond between dTTP and O-6-mG but not between dCTP and O-6-mG (data not shown), which might explain the reduced incorporation of dTTP. This hypothesis however has to be confirmed. We also showed that the preferential incorporation of dCTP opposite O-6-mG by Y505, is specific for this lesion, since no differences in incorporation opposite 8-oxo-G or 8-oxo-A between the Y505M mutant and the wt enzyme could be seen. Our results showing that the pol λ wt and Y505M misincorporation frequency of deoxynucleotide triphosphate opposite O-6-mG are not influenced by each possible nearest-neighbour context, contrasts with *in vitro* primer extension studies showing that misincorporation by other pols is dependent on the surrounding sequence(25). With reference to the extension step, when starting from an O-6-mG primer basepair, most eukaryotic pols combine relative high discrimination and low efficiency. In contrast to published data, pol λ with respect to O-6-mG showed no differences between extension of matched (O-6mG:dC) and mismatched (O-6-mG:dT), primers under the chosen conditions(26). Besides giving new insights into hydrophobic substitution and pol fidelity mechanism, the knowledge gleaned form the present investigation can enhance our understanding of the carcinogenic mechanism of O-6-mG.

Supplementary Data

Supplementary Data are available at NAR Online

Acknowledgements

We thank U.Wimmer for her guidance and E. Ferrari for instructions in protein purification.We also thank A. Marx for the 8-oxo-A template. PP is supported by the "UBS in Auftrag eines Kunden" and by "Oncosuisse", RB by the Swiss National Science Foundation and UH by the University of Zurich.

Conflict of interest statement. None declared.

References

1. Sedgwick, B. (2004) Repairing DNA-methylation damage. *Nat Rev Mol Cell Biol*, **5**, 148-157.
2. Bodell, W.J. and Singer, B. (1979) Influence of hydrogen bonding in DNA and polynucleotides on reaction of nitrogens and oxygens toward ethylnitrosourea. *Biochemistry*, **18**, 2860-2863.
3. Boiteux, S. and Laval, J. (1982) Mutagenesis by alkylating agents: coding properties for DNA polymerase of poly (dC) template containing 3-methylcytosine. *Biochimie*, **64**, 637-641.
4. Larson, K., Sahm, J., Shenkar, R. and Strauss, B. (1985) Methylation-induced blocks to in vitro DNA replication. *Mutat Res*, **150**, 77-84.
5. Margison, G.P. and Santibanez-Koref, M.F. (2002) O6-alkylguanine-DNA alkyltransferase: role in carcinogenesis and chemotherapy. *Bioessays*, **24**, 255-266.
6. Kat, A., Thilly, W.G., Fang, W.H., Longley, M.J., Li, G.M. and Modrich, P. (1993) An alkylation-tolerant, mutator human cell line is deficient in strand-specific mismatch repair. *Proc Natl Acad Sci U S A*, **90**, 6424-6428.
7. Karran, P. and Bignami, M. (1994) DNA damage tolerance, mismatch repair and genome instability. *Bioessays*, **16**, 833-839.

8. Snow, E.T., Foote, R.S. and Mitra, S. (1984) Base-pairing properties of O6-methylguanine in template DNA during in vitro DNA replication. *J Biol Chem*, **259**, 8095-8100.
9. Mojas, N., Lopes, M. and Jiricny, J. (2007) Mismatch repair-dependent processing of methylation damage gives rise to persistent single-stranded gaps in newly replicated DNA. *Genes Dev*, **21**, 3342-3355.
10. Dosanjh, M.K., Galeros, G., Goodman, M.F. and Singer, B. (1991) Kinetics of extension of O6-methylguanine paired with cytosine or thymine in defined oligonucleotide sequences. *Biochemistry*, **30**, 11595-11599.
11. Singh, J., Su, L. and Snow, E.T. (1996) Replication across O6-methylguanine by human DNA polymerase beta in vitro. Insights into the futile cytotoxic repair and mutagenesis of O6-methylguanine. *J Biol Chem*, **271**, 28391-28398.
12. Voigt, J.M. and Topal, M.D. (1995) O6-methylguanine-induced replication blocks. *Carcinogenesis*, **16**, 1775-1782.
13. Haracska, L., Prakash, S. and Prakash, L. (2000) Replication past O(6)-methylguanine by yeast and human DNA polymerase eta. *Mol Cell Biol*, **20**, 8001-8007.
14. Haracska, L., Prakash, L. and Prakash, S. (2002) Role of human DNA polymerase kappa as an extender in translesion synthesis. *Proc Natl Acad Sci U S A*, **99**, 16000-16005.
15. Rudinger, N.Z., Kranaster, R. and Marx, A. (2007) Hydrophobic amino acid and single-atom substitutions increase DNA polymerase selectivity. *Chem Biol*, **14**, 185-194.
16. Marx, A., Summerer, D., Sauter, K.B., Gloeckner, C. and Rudinger, N.Z. (2007) Chemical biology of DNA polymerases: from selectivity to new functions. *Nucleic Acids Symp Ser (Oxf)*, 81-82.
17. Warren, J.J., Forsberg, L.J. and Beese, L.S. (2006) The structural basis for the mutagenicity of O(6)-methyl-guanine lesions. *Proc Natl Acad Sci U S A*, **103**, 19701-19706.
18. Crespan, E., Hubscher, U. and Maga, G. (2007) Error-free bypass of 2-hydroxyadenine by human DNA polymerase lambda with Proliferating Cell Nuclear Antigen and Replication Protein A in different sequence contexts. *Nucleic Acids Res*, **35**, 5173-5181.

19. Crespan, E., Alexandrova, L., Khandazhinskaya, A., Jasko, M., Kukhanova, M., Villani, G., Hubscher, U., Spadari, S. and Maga, G. (2007) Expanding the repertoire of DNA polymerase substrates: template-instructed incorporation of non-nucleoside triphosphate analogues by DNA polymerases beta and lambda. *Nucleic Acids Res*, **35**, 45-57.

20. Crespan, E., Zanoli, S., Khandazhinskaya, A., Shevelev, I., Jasko, M., Alexandrova, L., Kukhanova, M., Blanca, G., Villani, G., Hubscher, U. *et al.* (2005) Incorporation of non-nucleoside triphosphate analogues opposite to an abasic site by human DNA polymerases beta and lambda. *Nucleic Acids Res*, **33**, 4117-4127.

21. Shevelev, I., Blanca, G., Villani, G., Ramadan, K., Spadari, S., Hubscher, U. and Maga, G. (2003) Mutagenesis of human DNA polymerase lambda: essential roles of Tyr505 and Phe506 for both DNA polymerase and terminal transferase activities. *Nucleic Acids Res*, **31**, 6916-6925.

22. Ramadan, K., Maga, G., Shevelev, I., Villani, G., Blanco, L,. Hubscher, U. (2003) Human DNA polymerase lambda possesses terminal deoxyribonucleotidyl transferase activity and can elongate RNA primers: implications for novel functions. *J Mol Biol*, 328(1), 63-72.

23. Gerson, S.L. (2004) MGMT: its role in cancer aetiology and cancer therapeutics. *Nat Rev Cancer*, **4**, 296-307.

24. Maga, G., Villani, G., Crespan, E., Wimmer, U., Ferrari, E., Bertocci, B. and Hubscher, U. (2007) 8-oxo-guanine bypass by human DNA polymerases in the presence of auxiliary proteins. *Nature*, **447**, 606-608.

25. Singer, B., Chavez, F., Goodman, M.F., Essigmann, J.M. and Dosanjh, M.K. (1989) Effect of 3' flanking neighbors on kinetics of pairing of dCTP or dTTP opposite O6-methylguanine in a defined primed oligonucleotide when Escherichia coli DNA polymerase I is used. *Proc Natl Acad Sci U S A*, **86**, 8271-8274.

26. Picher, A.J. and Blanco, L. (2007) Human DNA polymerase lambda is a proficient extender of primer ends paired to 7,8-dihydro-8-oxoguanine. *DNA Repair (Amst)*, **6**, 1749-1756.

Figure legend

Figure 1. Purification of pol λ wt and Y505M and determination of their enzymatic activities. (**A**) Purified recombinant His tagged pol λ wild type (wt) and Y505M proteins were analysed on a 10% SDS-PAGE. (**B**) Primer extension assays were performed as described in Materials and methods in the presence of 5′labelled 39/72-mer template in the presence of increasing amounts (40nM, 80nM, 120nM) of wt (lanes 2,3,4) and Y505M (lanes 5,6,7) and 10μM dNTP. Lane 1 is control reaction in the absence of enzyme. The sequence of the template strand is indicated in the Figure.

Figure 2. Translesion synthesis by human pol λ, wt and Y505M. The template sequence are as indicated on top of each panel. The experiments were carried out as indicated in Materials and methods. (**A**) Single nucleotide incorporation opposite O-6-mG by wt pol λ (lanes 2,3,4,5) and Y505M (lanes 7,8,9,10) or pol β (Lanes 12,13,14,15). Lane 1 is control reaction in the absence of dNTP's. Lane 6,11 and 16 are reactions in the presence of all four dNTP's. (**B**) As in panel A, but in the presence of undamaged dG for all four dNTP's. (**C**) Incorporation of dTTP opposite dG by human pol λ wt (lanes 2,3,4) and Y505M (lanes 6,7,8) at the indicated concentration. Lanes 1 and 5 are control reaction in the absence of dTTP. (**D**) Single nucleotide incorporation opposite 8-oxo-G by pol λ wt (lanes 2,3,4,5), Y505M (lanes 7,8,9,10) or pol β (Lanes 12,13,14 and 15). Lanes 6,11 and 16 are in the presence of all four dNTP's (**E**) 8-oxo-A. Incorporation of respective dNTP by pol λ wt (lanes 2,3,4,5) and Y505M (lanes 7,8,9,10) or pol β (Lanes 12,13,14 and15). Lane 1 is control reaction in the absence of dNTP's. Lanes 6,11and 16 are in the presence of all four dNTP's.

Figure 3. The fidelity of 6-O-mG bypass by pol λ wt and Y505M is not influenced by the sequence context. Experiments were performed as described in Materials and methods. The template sequences are indicated on top of each panel. (**A**) Relative dCTP incorporation opposite the indicated template by pol λ wt and Y505M at 0.1 μM and 1 μM. Product length is indicated on the bottom axis. (B) Relative dTTP incorporation opposite the indicated template by pol λ wt and Y505M

at 1μM and 10μM. Product length is indicated on the bottom axis. (C) Relative dTTP incorporation opposite the template indicated by pol λ wt and Y505M at 0.1 μM and 1 μM (D) Relative dTTP incorporation opposite the indicated template by pol λ wt and Y505M at 1μM and 10μM .

Figure 4. Extension of mismatched primers containing O-6-mG lesion by human pol λ wt and Y505M. (A) Experiments were performed as described in Materials and methods. The template sequences are indicated on top of each panel. (A) G:C control template - dCTP incorporation by pol λ wt (lane 2, 3, 4) and Y505M (lane 6, 7, 8). Lanes 1 and 5 are control reactions in the absence of dCTP. (B) O-6-mG:C template – dCTP incorporation by pol λ wt (lane 10, 11, 12) and Y505M (lane 14,15,16). Lanes 9 and 13 are control reactions in the absence of dCTP. (C) O-6-mG:T–dCTP incorporation by pol λ wt (lane 18,19,20) and Y505M (lane 22,23,24). Lanes 17 and 21 are control reaction in the absence of dCTP.

Figure S1A: **The fidelity of 6-O-mG bypass by pol λ wt and Y505M is not influenced by the sequence context**

Experiments were performed as described in Materials and methods. The template sequence are indicated on top of each panel. **(A)** Relative dCTP (lanes 2,3,4) and dTTP (lanes 6,7,8) incorporation opposite O-6-mG by wt pol λ. dCTP (lanes 10,11, 12) and dTTP (lanes 14,15,16) incorporation opposite O-6-mG by Y505M. Lanes 1,5,9,13 are control reactions in the absence of dNTP's. **(B)** Relative dCTP (lanes 18,19,20) and dTTP (lanes 22,23,24) incorporation opposite O-6-mG by wt pol λ. dCTP (lanes 26,27,28) and dTTP (lanes30,31,32) incorporation opposite O-6-mG by Y505M. Lanes 17,21,25,29 are control reactions in the absence of dNTP's**.**

A

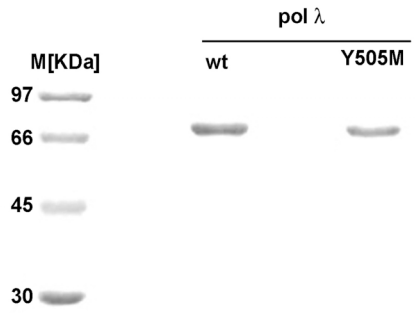
pol λ
M[KDa]
wt
Y505M
97
66
45
30

B

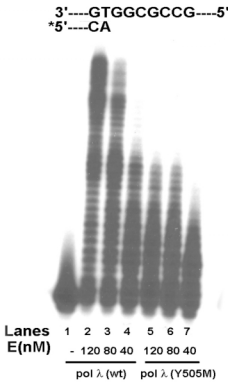
3'----GTGGCGCCG----5'
*5'----CA
Lanes 1 2 3 4 5 6 7
E(nM) - 120 80 40 120 80 40
pol λ (wt)
pol λ (Y505M)

Fig 1

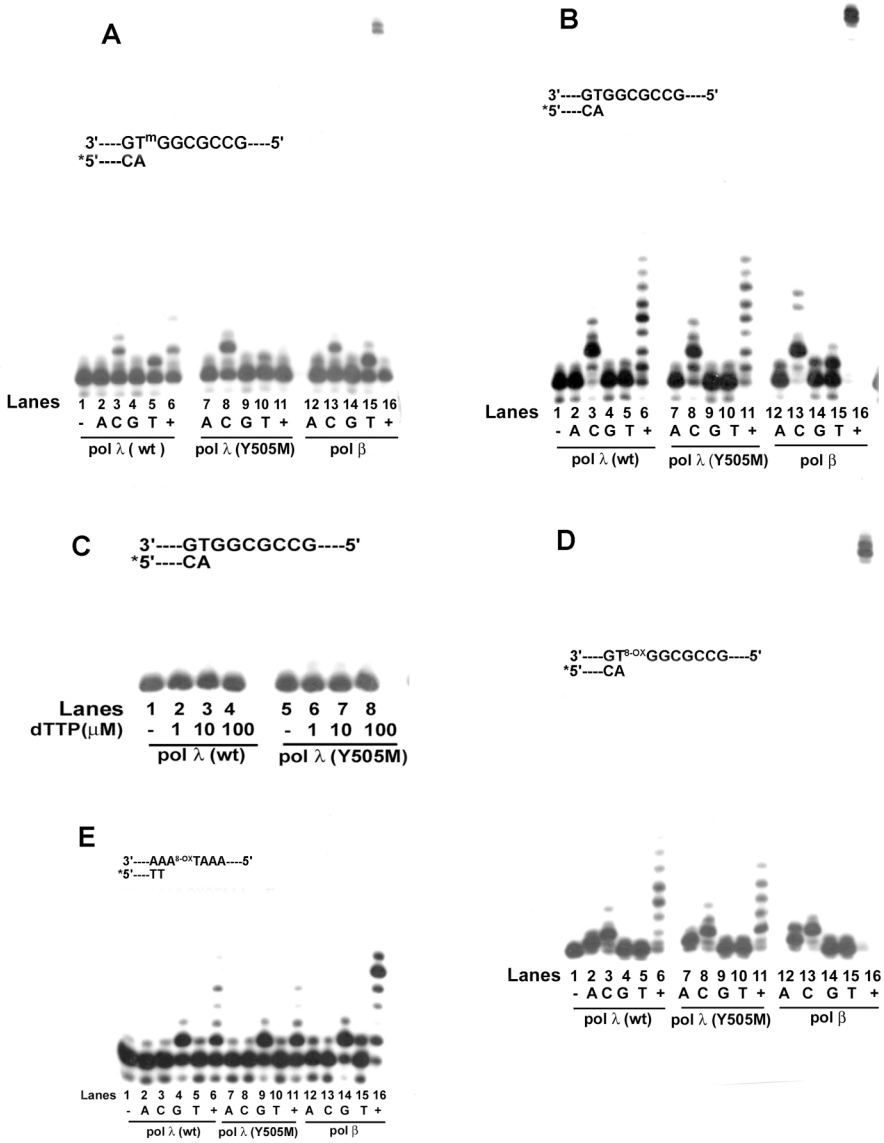
A
3'----GT^mGGCGCCG----5'
*5'----CA
Lanes 1 2 3 4 5 6 7 8 9 10 11 12 13 14 15 16
- A C G T + A C G T + A C G T +
pol λ (wt) pol λ (Y505M) pol β
B
3'----GTGGCGCCG----5'
*5'----CA
Lanes 1 2 3 4 5 6 7 8 9 10 11 12 13 14 15 16
- A C G T + A C G T + A C G T +
pol λ (wt) pol λ (Y505M) pol β
C
3'----GTGGCGCCG----5'
*5'----CA
Lanes 1 2 3 4 5 6 7 8
dTTP(μM) - 1 10 100 - 1 10 100
pol λ (wt) pol λ (Y505M)
D
3'----GT^8-OXGGCGCCG----5'
*5'----CA
Lanes 1 2 3 4 5 6 7 8 9 10 11 12 13 14 15 16
- A C G T + A C G T + A C G T +
pol λ (wt) pol λ (Y505M) pol β
E
3'----AAA^8-OXTAAA----5'
*5'----TT
Lanes 1 2 3 4 5 6 7 8 9 10 11 12 13 14 15 16
- A C G T + A C G T + A C G T +
pol λ (wt) pol λ (Y505M) pol β

Fig 2

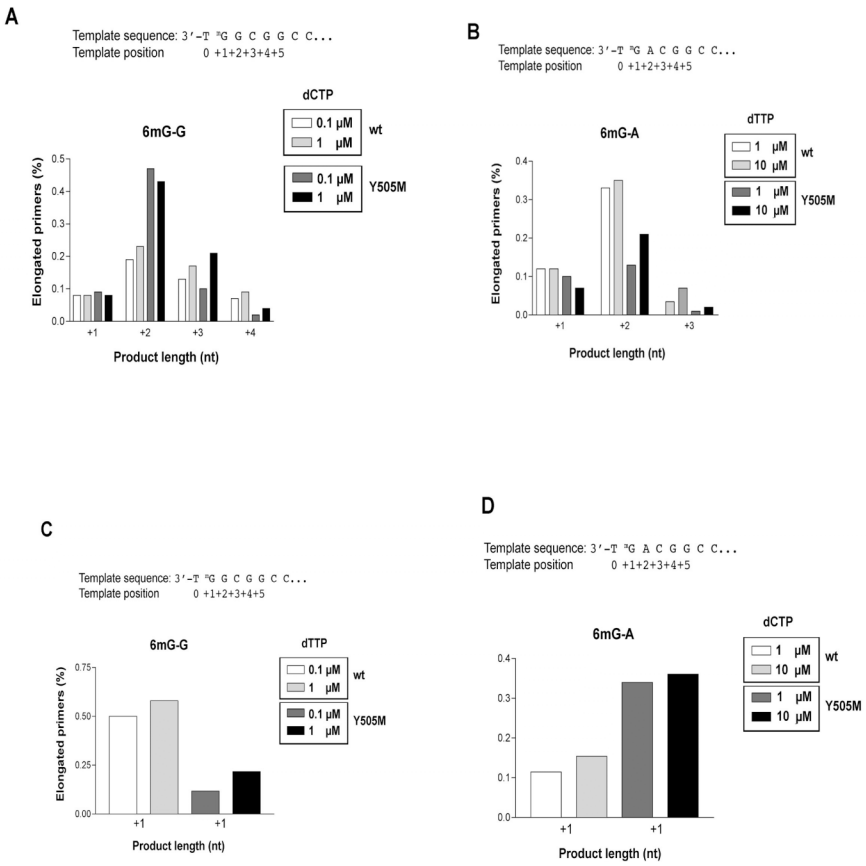
A
Template sequence: 3′-T mG G C G G C C...
Template position 0 +1+2+3+4+5
6mG-G
dCTP
0.1 μM
1 μM
wt
0.1 μM
1 μM
Y505M
Elongated primers (%)
Product length (nt)
B
Template sequence: 3′-T mG A C G G C C...
Template position 0 +1+2+3+4+5
6mG-A
dTTP
1 μM
10 μM
wt
1 μM
10 μM
Y505M
Elongated primers (%)
Product length (nt)
C
Template sequence: 3′-T mG G C G G C C...
Template position 0 +1+2+3+4+5
6mG-G
dTTP
0.1 μM
1 μM
wt
0.1 μM
1 μM
Y505M
Elongated primers (%)
Product length (nt)
D
Template sequence: 3′-T mG A C G G C C...
Template position 0 +1+2+3+4+5
6mG-A
dCTP
1 μM
10 μM
wt
1 μM
10 μM
Y505M
Product length (nt)

Fig 3

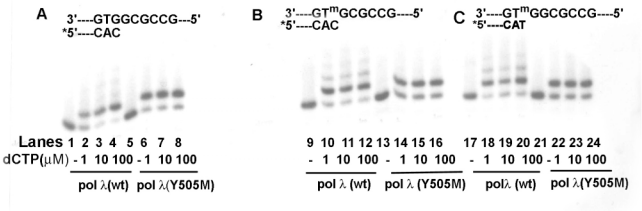
A
3'-----GTGGCGCCG---5'
*5'-----CAC
B
3'-----GT^mGCGCCG----5'
*5'-----CAC
C
3'----GT^mGGCGCCG----5'
*5'----CAT
Lanes 1 2 3 4 5 6 7 8
dCTP(μM) - 1 10 100 - 1 10 100
pol λ(wt) pol λ(Y505M)
9 10 11 12 13 14 15 16
- 1 10 100 - 1 10 100
pol λ (wt) pol λ (Y505M)
17 18 19 20 21 22 23 24
- 1 10 100 - 1 10 100
polλ (wt) pol λ(Y505M)

Fig 4

Table 1: Steady state kinetic parameters for nucleotide incorporation opposite O-6-mG by pol λ wt and the Y505M mutant

Pol λ	dCTP			dTTP		
	Km[1] (μM)	kcat (min-1)	kcat/Km (μM-1min-1)	Km (μM)	kcat (min-1)	kcat/Km (μM-1min-1)
Wt	0.18	0.013	0.07	0.04	0.008	0.2
Y505M	0.024	0.015	0.625	n.d[2]	n.d	n.d

1. Kinetic parameters were as described in Material and Methods
2. n.d., not determined. Incorporation by the Y505M mutant was too low to be measured under the assay conditions used.

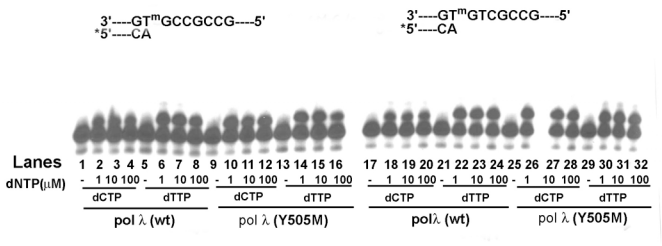
3'----GTmGCCGCCG----5'
*5'----CA
3'----GTmGTCGCCG----5'
*5'----CA
Lanes
dNTP(μM)
1 2 3 4 5 6 7 8 9 10 11 12 13 14 15 16
17 18 19 20 21 22 23 24 25 26 27 28 29 30 31 32
- 1 10 100 - 1 10 100 - 1 10 100 - 1 10 100
dCTP dTTP dCTP dTTP
pol λ (wt)
pol λ (Y505M)
polλ (wt)
pol λ (Y505M)

S Fig 1

6. Discussion

6.1. Studies with the model organism *Deinococcus radiodurans*

6.1.1. Characterization of two putative DNA ligases of *D. radiodurans*

In the first part of this thesis, the identification of a NAD^+-dependent DNA ligase, together with a second putative ATP-dependent DNA ligase of the radioresistant bacterium *D. radiodurans* is reported. For many years it was supposed that bacteria contain only NAD^+-dependent DNA ligases. Several years ago however, the identification of bacterial ATP-dependent DNA ligases was published [124], suggesting that also bacteria might have specific DNA ligases for different tasks. Bacterial NAD^+-dependent DNA ligases are commonly highly conserved, which is also the case for the *D. radiodurans* enzyme. This suggests that the NAD^+-dependent DNA ligases are essential [19].

As described in Blasius et al. [125], the NAD^+-dependent DNA ligase of *D. radiodurans* had strong ligation activity on a nicked substrate in the presence of NAD^+ and $MnCl_2$. This is not surprising, keeping in mind that Mn^{2+} ions are present in high internal levels in *D. radiodurans* and are also essential for γ-radiation resistance [126]. Additionally, other enzymes from *D. radiodurans* such as e.g. the family X DNA pol, have been shown to be stimulated by Mn^{2+} [14]. Furthermore, the above mentioned finding of the generally high conservation amongst bacterial NAD^+-dependent DNA ligases could also be confirmed for the *D. radiodurans* ligase as mutating the conserved lysine 128 to alanin abolished ligation activity as well as adenylation of the ligase, which is the first step in the ligation process. However, the second DNA ligase studied and described in Blasius et al. [125] is a putative ATP-dependent DNA ligase. In contrast to the before described NAD^+-dependent DNA ligase, this second ligase is strongly upregulated upon γ-irradiation [121], further undermining the hypothesis that also bacteria employ different ligases for different functions. Also this DNA ligase contains most of the conserved amino acid residues present in other ATP-dependent DNA ligases. However, as already discussed in Blasius et al. [125], although a specific adenylyltransferase intermediate could be shown, no ligase activity was

detected. However, the adenylyltransferase activity was intrinsic to the putative ATP-dependent DNA ligase, as mutation of the conserved lysine 40 to alanine abolished the reaction. Certainly, it cannot be ruled out that this ligase has particular requirements for specific substrates, although various substrates were tested, like nicked DNA, nicked DNA-RNA hybrids, single-stranded RNA, double-stranded DNA with blunt ends or also with overhangs. However, the putative ATP-dependent DNA ligase of *D. radiodurans* does not display any conventional DNA-binding motif what suggests that an additional protein might be required as it is the case for mammalian DNA-ligase III, which requires the XRCC I protein [18]. Another Deinococcal protein might serve this function: PprA was shown to act in a Ku-like manner, tethering free DNA ends together. Furthermore, PprA was shown to stimulate ATP- and NAD^+-dependent DNA ligases [127, 128]. Surely this will need further experiments, as also other groups were not successful in clarifying the specific requirement that this putative ATP-dependent DNA ligase might have or in elucidating potential auxiliary proteins (Mike Cox, personal communication).

6.1.2. Characterization of a putative O6-methylguanine-DNA methyltransferase (MGMT) of *D. radiodurans*

O6-methylguanine-DNA methyltransferases (MGMT) exist in all three kingdoms of life [30]. However, their primary sequence similarity is rather low, but the overall domain structure is very similar, comprising a very conserved active site cysteine residue, which covalently binds the methyl group of the substrate [30]. This covalent linkage is very stable, the enzyme cannot be recycled, thus repair of O6-methylguanine lesions occurs in a stoichiometric fashion, which quickly leads to saturation if the lesion is too abundantly present. In other words, each O6-methylguanine not only acts as a substrate, but also as an irreversible inhibitor of the MGMT protein. The MGMT is therefore often referred to as “kamikaze” or “suicidal” protein. Thus, it is clear that working with MGMT is not trivial, which was confirmed in the studies presented here. Although the protein was correctly folded, which was shown with different DNA-binding assays, it was not possible to clearly show transferase activity, although different cations such as Mn^{2+} (Figure 11C) and

Mg^{2+} (data not shown) and various buffer conditions were tested. Even when testing whole cell extracts of *D. radiodurans*, it was not possible to detect methyltransferase activity although e.g. NAD^{+}-dependent DNA ligase activity has been observed in extracts. However, *E.coli* cells that are not previously treated with sublethal doses of alkylating agents before exposing them to higher doses of the reagents have been shown to only contain a few dozen MGMT molecules; however, after an adaption phase MGMT protein levels accumulate to several thousand molecules per cell (reviewed in [129]). Thus, it is not surprising that with extract from unadapted cells, no intrinsic MGMT activity could be shown due to the low number of MGMT proteins present. Furthermore, also a commercially available human MGMT showed only minimal transferase activity, which was at the limit of detection. Nevertheless, it is very unlikely that the MGMT needs an additional auxiliary protein, as it might be the case for the putative ATP-dependent ligase mentioned before. MGMTs are known to act without co-factors, which was confirmed in our studies, at least for the DNA-binding ability of the Deinococcal MGMT.

However, another group reported very recently the finding of a new class of proteins, named alkyltransferase-like proteins (ATLs) [122]. These ATLs are characterized by the lack of the reactive cysteine, to which the methyl group is transferred in MGMTs; rather, they have replaced the cysteine residue of the active site PCHRV sequence motif by tryptophane, alanine or another residue. Indeed, a BLAST search for the putative MGMT of *D. radiodurans* revealed the substitution of the active site cysteine by tryptophane, giving rise to a modified sequence motif (PWQRV) and thus suggesting that the Deinococcal MGMT belongs to the ATL family of proteins rather than to the MGMT family [122]. Due to the absence of the reactive cysteine residue, the ATL proteins do not posses any alkyltransferase activity, but are suggested to act through the binding of the O6-methylguanine DNA lesion, thereby bending the DNA by about 45°, which might mark the DNA for recognition by proteins involved in the nucleotide excision repair (NER) pathway finally repairing the damage. This is in agreement with the observed DNA-binding capability of the putative MGMT of *D. radiodurans*, as well as with its apparent lack of alkyltransferase activity. Thus, the findings with the putative MGMT of *D.*

radiodurans presented in this study fit nicely into the described characteristics for an alkyltransferase-like protein.

6.2. Studies with human DNA repair enzymes

6.2.1. Interaction of the Rad9/Rad1/Hus1 (9-1-1) complex with apurinic/apyrimidinic endonuclease 1 (Ape1) and its fragments

Based on the findings in our Institute (Gembka et al. [92]), the interaction of the Rad9/Rad1/Hus1 (9-1-1) complex with the apurinic/apyrimidinic endonuclease 1 (Ape1) was examined closer. The Ape1 protein was subdivided into five fragments. In a first attempt, the fragments were left untagged in order not to interfere with the folding of the proteins, as the fragments are quite small, only being about 12 to 26 kDa in size. However, the low expression efficiency of the fragments, paired with the inefficient recognition by the antibody due to its low sensitivity and specificity, led us to re-clone the fragments, including a HA-tag. Although the anti-HA antibody detected the light chain of the antibody additionally to the HA-tagged fragments, a clear discrimination between the fragments and unspecific proteins could be achieved, yet purification was not successful. As already observed with the untagged fragments, the expression efficiency remained rather low, also with the tagged proteins. Furthermore, an inducible lethality of the bacteria expressing the fragments was noticed, which suggests an unbeneficial effect of the truncated proteins on the bacteria. This was not due to the fact that the bacteria used to express the proteins were knock-outs for the bacterial homologs of Ape1, *xth* and *nfo*, as also with other bacterial strains the same effect was observed (data not shown). However, in addition to the inconveniencies with the expression, purification was handicapped by the fact that elution from the anti HA-beads, which were used for the purification of the tagged proteins, was very inefficient with a pH of 2.5, which was recommended by the manufacturer. Even more so, pH as low as this might lead to an irreversible inactivation of the protein fragments, thus it seemed reasonable to work with the unpurified fragments coupled to the beads, without prior elution. This was feasible as endonuclease activity

assays indicated that the proteins are active even when they reminded coupled to the beads. Moreover, these assays confirmed that the endonuclease activity lies in the N-terminal part of the protein, which is in agreement with published data [69, 71]. However, when it came to pull-down experiments, using the fragments coupled to the anti HA-beads, it emerged that this approach was not suitable, as the Rad9 antibody, which was used to assess the putative interaction between the 9-1-1 complex and the different Ape1 fragments, turned out to recognize the heavy chains of the antibodies, present on the anti-HA beads. Although the heavy chain normally runs at a size of 55 kDa and the Rad9 protein at 72 kDa, it was not possible to separate the two bands conclusively with the 15% SDS-PAGE gels that were used. However, neither anti-Rad1 nor anti-Hus1 antibodies could be used to detect the interacting 9-1-1 complex due to their low specificity and sensitivity. Still, the initially made observation by Gembka et al. [92] could be reproduced using purified proteins. For further pull-down purposes it might be convenient to work with purified proteins to circumvent inconveniences derivng from additional unspecific bands, as it is the case for the antibody light and heavy chains. However, additional experiments are required to pin down the exact interaction site between the 9-1-1 complex and Ape1.

6.2.2. Interaction of the Rad9/Rad1/Hus1 (9-1-1) complex with human DNA polymerase λ

In the last part of the thesis, observations were made suggesting a novel interaction between the 9-1-1 complex and DNA pol λ. This finding makes sense in the light of various findings made by different groups that place DNA pol λ, besides its role in non-homologous end joining (NHEJ), also in the context of base excision repair (BER). For example, Maga et al. showed that DNA pol λ is the DNA pol that most faithfully incorporates a correct dCTP opposite a 7,8-dihydro-8-oxoguanine (8-oxo-G) when proliferating nuclear antigen (PCNA) and replication protein A (RP-A) are present [119]. In their latest findings [118], Maga et al. went a step further, suggesting PCNA and RP-A as molecular switches, which activate the highly efficient and faithful repair of an A:8-oxo-G mismatch by DNA pol λ, simultaneously repressing DNA pol β activities. Very recent observations made by Van Loon and

Hübscher place DNA pol λ, in cooperation with MUTYH, in a novel long patch (LP) BER event that prevents C:G to A:T transversion mutations (Manuscript submitted). Together with the fact that the 9-1-1 complex interacts and stimulates various enzymes involved in BER as sumarazied in Table 1, these findings argue for a repair mechanism that proceeds via the coordinated stimulation of the different BER enzymes, all tethered together, thus building a multienzyme DNA repair complex, as suggested by Balakrishnan et al. [130], whereby DNA pol β can be substituted by DNA pol λ to allow faithful repair of specific DNA damages. Although the putative interaction between the 9-1-1 complex and DNA pol λ found here would perfectly fit into the suggested model, further experiments have to be performed to sustain those preliminary findings.

7. References

1. Blasius, M., S. Sommer, and U. Hubscher, *Deinococcus radiodurans: what belongs to the survival kit?* Crit Rev Biochem Mol Biol, 2008. **43**(3): p. 221-38.
2. Battista, J.R., *Against all odds: the survival strategies of Deinococcus radiodurans.* Annu Rev Microbiol, 1997. **51**: p. 203-24.
3. Anderson AW, N.H., Cain RF, Parrish G, Duggan D, *Studies on a radio-resistant Micrococcus .1. Isolation, Morphology, Cultural Characteristics, and Resistance to Gamma Radiation.* Food Technology, 1956. **10**(12): p. 575-578.
4. White, O., et al., *Genome sequence of the radioresistant bacterium Deinococcus radiodurans R1.* Science, 1999. **286**(5444): p. 1571-7.
5. Hansen, M.T., *Multiplicity of genome equivalents in the radiation-resistant bacterium Micrococcus radiodurans.* J Bacteriol, 1978. **134**(1): p. 71-5.
6. Harsojo, S. Kitayama, and A. Matsuyama, *Genome multiplicity and radiation resistance in Micrococcus radiodurans.* J Biochem (Tokyo), 1981. **90**(3): p. 877-80.
7. Cox, M.M. and J.R. Battista, *Deinococcus radiodurans - the consummate survivor.* Nat Rev Microbiol, 2005. **3**(11): p. 882-92.
8. Moseley, B.E. and A. Mattingly, *Repair of irradiation transforming deoxyribonucleic acid in wild type and a radiation-sensitive mutant of Micrococcus radiodurans.* J Bacteriol, 1971. **105**(3): p. 976-83.
9. Smith, M.D., et al., *Gene expression in Deinococcus radiodurans.* Gene, 1991. **98**(1): p. 45-52.
10. Bonura, T., et al., *The influence of oxygen on the yield of DNA double-strand breaks in x-irradiated Escherichia coli K-12.* Radiat Res, 1975. **63**(3): p. 567-77.
11. Burrell, A.D., P. Feldschreiber, and C.J. Dean, *DNA-membrane association and the repair of double breaks in x-irradiated Micrococcus radiodurans.* Biochim Biophys Acta, 1971. **247**(1): p. 38-53.
12. Zahradka, K., et al., *Reassembly of shattered chromosomes in Deinococcus radiodurans.* Nature, 2006. **443**(7111): p. 569-73.
13. Slade, D., et al., *Recombination and replication in DNA repair of heavily irradiated Deinococcus radiodurans.* Cell, 2009. **136**(6): p. 1044-55.
14. Lecointe, F., et al., *Involvement of an X family DNA polymerase in double-stranded break repair in the radioresistant organism Deinococcus radiodurans.* Mol Microbiol, 2004. **53**(6): p. 1721-30.
15. Daly, M.J., *A new perspective on radiation resistance based on Deinococcus radiodurans.* Nat Rev Microbiol, 2009. **7**(3): p. 237-45.
16. Timson, D.J., M.R. Singleton, and D.B. Wigley, *DNA ligases in the repair and replication of DNA.* Mutat Res, 2000. **460**(3-4): p. 301-18.
17. Doherty, A.J. and S.W. Suh, *Structural and mechanistic conservation in DNA ligases.* Nucleic Acids Res, 2000. **28**(21): p. 4051-8.
18. Martin, I.V. and S.A. MacNeill, *ATP-dependent DNA ligases.* Genome Biol, 2002. **3**(4): p. reviews3005.1-3005.7.
19. Wilkinson, A., J. Day, and R. Bowater, *Bacterial DNA ligases.* Mol Microbiol, 2001. **40**(6): p. 1241-8.

20. Makarova, K.S., et al., *Genome of the extremely radiation-resistant bacterium Deinococcus radiodurans viewed from the perspective of comparative genomics.* Microbiol Mol Biol Rev, 2001. **65**(1): p. 44-79.
21. Shuman, S. and C.D. Lima, *The polynucleotide ligase and RNA capping enzyme superfamily of covalent nucleotidyltransferases.* Curr Opin Struct Biol, 2004. **14**(6): p. 757-64.
22. Johnson, A. and M. O'Donnell, *DNA ligase: getting a grip to seal the deal.* Curr Biol, 2005. **15**(3): p. R90-2.
23. Rydberg, B. and T. Lindahl, *Nonenzymatic methylation of DNA by the intracellular methyl group donor S-adenosyl-L-methionine is a potentially mutagenic reaction.* EMBO J, 1982. **1**(2): p. 211-6.
24. Taverna, P. and B. Sedgwick, *Generation of an endogenous DNA-methylating agent by nitrosation in Escherichia coli.* J Bacteriol, 1996. **178**(17): p. 5105-11.
25. Hecht, S.S., *DNA adduct formation from tobacco-specific N-nitrosamines.* Mutat Res, 1999. **424**(1-2): p. 127-42.
26. Hurley, L.H., *DNA and its associated processes as targets for cancer therapy.* Nat Rev Cancer, 2002. **2**(3): p. 188-200.
27. Margison, G.P., et al., *Alkyltransferase-like proteins.* DNA Repair (Amst), 2007. **6**(8): p. 1222-8.
28. Margison, G.P. and M.F. Santibanez-Koref, *O6-alkylguanine-DNA alkyltransferase: role in carcinogenesis and chemotherapy.* Bioessays, 2002. **24**(3): p. 255-66.
29. Kleibl, K., *Molecular mechanisms of adaptive response to alkylating agents in Escherichia coli and some remarks on O(6)-methylguanine DNA-methyltransferase in other organisms.* Mutat Res, 2002. **512**(1): p. 67-84.
30. Drablos, F., et al., *Alkylation damage in DNA and RNA--repair mechanisms and medical significance.* DNA Repair (Amst), 2004. **3**(11): p. 1389-407.
31. Sedgwick, B., et al., *Repair of alkylated DNA: recent advances.* DNA Repair (Amst), 2007. **6**(4): p. 429-42.
32. Liu, L. and S.L. Gerson, *Targeted modulation of MGMT: clinical implications.* Clin Cancer Res, 2006. **12**(2): p. 328-31.
33. Hegi, M.E., et al., *Correlation of O6-methylguanine methyltransferase (MGMT) promoter methylation with clinical outcomes in glioblastoma and clinical strategies to modulate MGMT activity.* J Clin Oncol, 2008. **26**(25): p. 4189-99.
34. Engelward, B.P., et al., *Base excision repair deficient mice lacking the Aag alkyladenine DNA glycosylase.* Proc Natl Acad Sci U S A, 1997. **94**(24): p. 13087-92.
35. Elder, R.H., et al., *Alkylpurine-DNA-N-glycosylase knockout mice show increased susceptibility to induction of mutations by methyl methanesulfonate.* Mol Cell Biol, 1998. **18**(10): p. 5828-37.
36. Engelward, B.P., et al., *Repair-deficient 3-methyladenine DNA glycosylase homozygous mutant mouse cells have increased sensitivity to alkylation-induced chromosome damage and cell killing.* EMBO J, 1996. **15**(4): p. 945-52.
37. Tsuzuki, T., et al., *Targeted disruption of the DNA repair methyltransferase gene renders mice hypersensitive to alkylating agent.* Carcinogenesis, 1996. **17**(6): p. 1215-20.

38. Paik, J., et al., *Sensitization of human carcinoma cells to alkylating agents by small interfering RNA suppression of 3-alkyladenine-DNA glycosylase.* Cancer Res, 2005. **65**(22): p. 10472-7.
39. Branch, P., et al., *Defective mismatch binding and a mutator phenotype in cells tolerant to DNA damage.* Nature, 1993. **362**(6421): p. 652-4.
40. Ceccotti, S., et al., *Processing of O6-methylguanine by mismatch correction in human cell extracts.* Curr Biol, 1996. **6**(11): p. 1528-31.
41. Humbert, O., et al., *Mismatch repair and differential sensitivity of mouse and human cells to methylating agents.* Carcinogenesis, 1999. **20**(2): p. 205-14.
42. Kawate, H., et al., *Separation of killing and tumorigenic effects of an alkylating agent in mice defective in two of the DNA repair genes.* Proc Natl Acad Sci U S A, 1998. **95**(9): p. 5116-20.
43. Hoeijmakers, J.H., *Genome maintenance mechanisms for preventing cancer.* Nature, 2001. **411**(6835): p. 366-74.
44. Sancar, A., et al., *Molecular mechanisms of mammalian DNA repair and the DNA damage checkpoints.* Annu Rev Biochem, 2004. **73**: p. 39-85.
45. Friedberg, E.C., *A brief history of the DNA repair field.* Cell Res, 2008. **18**(1): p. 3-7.
46. Hakem, R., *DNA-damage repair; the good, the bad, and the ugly.* EMBO J, 2008. **27**(4): p. 589-605.
47. Hansen, W.K. and M.R. Kelley, *Review of mammalian DNA repair and translational implications.* J Pharmacol Exp Ther, 2000. **295**(1): p. 1-9.
48. Almeida, K.H. and R.W. Sobol, *A unified view of base excision repair: lesion-dependent protein complexes regulated by post-translational modification.* DNA Repair (Amst), 2007. **6**(6): p. 695-711.
49. Wood, R.D., M. Mitchell, and T. Lindahl, *Human DNA repair genes, 2005.* Mutat Res, 2005. **577**(1-2): p. 275-83.
50. Wallace, S.S., *Enzymatic processing of radiation-induced free radical damage in DNA.* Radiat Res, 1998. **150**(5 Suppl): p. S60-79.
51. Hegde, M.L., T.K. Hazra, and S. Mitra, *Early steps in the DNA base excision/single-strand interruption repair pathway in mammalian cells.* Cell Res, 2008. **18**(1): p. 27-47.
52. Fortini, P., et al., *Different DNA polymerases are involved in the short- and long-patch base excision repair in mammalian cells.* Biochemistry, 1998. **37**(11): p. 3575-80.
53. Stucki, M., et al., *Mammalian base excision repair by DNA polymerases delta and epsilon.* Oncogene, 1998. **17**(7): p. 835-43.
54. Wilson, D.M., 3rd and V.A. Bohr, *The mechanics of base excision repair, and its relationship to aging and disease.* DNA Repair (Amst), 2007. **6**(4): p. 544-59.
55. Tudek, B., *Base excision repair modulation as a risk factor for human cancers.* Mol Aspects Med, 2007. **28**(3-4): p. 258-75.
56. Ema, M., et al., *Molecular mechanisms of transcription activation by HLF and HIF1alpha in response to hypoxia: their stabilization and redox signal-induced interaction with CBP/p300.* EMBO J, 1999. **18**(7): p. 1905-14.
57. Huang, L.E., et al., *Activation of hypoxia-inducible transcription factor depends primarily upon redox-sensitive stabilization of its alpha subunit.* J Biol Chem, 1996. **271**(50): p. 32253-9.

58. Lando, D., et al., *A redox mechanism controls differential DNA binding activities of hypoxia-inducible factor (HIF) 1alpha and the HIF-like factor.* J Biol Chem, 2000. **275**(7): p. 4618-27.
59. Xanthoudakis, S., et al., *Redox activation of Fos-Jun DNA binding activity is mediated by a DNA repair enzyme.* EMBO J, 1992. **11**(9): p. 3323-35.
60. Jayaraman, L., et al., *Identification of redox/repair protein Ref-1 as a potent activator of p53.* Genes Dev, 1997. **11**(5): p. 558-70.
61. Gaiddon, C., N.C. Moorthy, and C. Prives, *Ref-1 regulates the transactivation and pro-apoptotic functions of p53 in vivo.* EMBO J, 1999. **18**(20): p. 5609-21.
62. Xanthoudakis, S., et al., *The redox/DNA repair protein, Ref-1, is essential for early embryonic development in mice.* Proc Natl Acad Sci U S A, 1996. **93**(17): p. 8919-23.
63. Ludwig, D.L., et al., *A murine AP-endonuclease gene-targeted deficiency with post-implantation embryonic progression and ionizing radiation sensitivity.* Mutat Res, 1998. **409**(1): p. 17-29.
64. Meira, L.B., et al., *Heterozygosity for the mouse Apex gene results in phenotypes associated with oxidative stress.* Cancer Res, 2001. **61**(14): p. 5552-7.
65. Evans, A.R., M. Limp-Foster, and M.R. Kelley, *Going APE over ref-1.* Mutat Res, 2000. **461**(2): p. 83-108.
66. Tell, G., et al., *The intracellular localization of APE1/Ref-1: more than a passive phenomenon?* Antioxid Redox Signal, 2005. **7**(3-4): p. 367-84.
67. Mitra, S., et al., *Intracellular trafficking and regulation of mammalian AP-endonuclease 1 (APE1), an essential DNA repair protein.* DNA Repair (Amst), 2007. **6**(4): p. 461-9.
68. Akiyama, K., et al., *Structure, promoter analysis and chromosomal assignment of the human APEX gene.* Biochim Biophys Acta, 1994. **1219**(1): p. 15-25.
69. Gorman, M.A., et al., *The crystal structure of the human DNA repair endonuclease HAP1 suggests the recognition of extra-helical deoxyribose at DNA abasic sites.* EMBO J, 1997. **16**(21): p. 6548-58.
70. Wilson, S.H. and T.A. Kunkel, *Passing the baton in base excision repair.* Nat Struct Biol, 2000. **7**(3): p. 176-8.
71. Barzilay, G., et al., *Identification of critical active-site residues in the multifunctional human DNA repair enzyme HAP1.* Nat Struct Biol, 1995. **2**(7): p. 561-8.
72. Kakolyris, S., et al., *Expression and subcellular localization of human AP endonuclease 1 (HAP1/Ref-1) protein: a basis for its role in human disease.* Histopathology, 1998. **33**(6): p. 561-9.
73. Kakolyris, S., et al., *Human apurinic endonuclease 1 expression in a colorectal adenoma-carcinoma sequence.* Cancer Res, 1997. **57**(9): p. 1794-7.
74. Kakolyris, S., et al., *Human AP endonuclease 1 (HAP1) protein expression in breast cancer correlates with lymph node status and angiogenesis.* Br J Cancer, 1998. **77**(7): p. 1169-73.
75. Zhou, B.B. and S.J. Elledge, *The DNA damage response: putting checkpoints in perspective.* Nature, 2000. **408**(6811): p. 433-9.
76. Niida, H. and M. Nakanishi, *DNA damage checkpoints in mammals.* Mutagenesis, 2006. **21**(1): p. 3-9.

77. Parrilla-Castellar, E.R., S.J. Arlander, and L. Karnitz, *Dial 9-1-1 for DNA damage: the Rad9-Hus1-Rad1 (9-1-1) clamp complex.* DNA Repair (Amst), 2004. **3**(8-9): p. 1009-14.
78. Burtelow, M.A., S.H. Kaufmann, and L.M. Karnitz, *Retention of the human Rad9 checkpoint complex in extraction-resistant nuclear complexes after DNA damage.* J Biol Chem, 2000. **275**(34): p. 26343-8.
79. Burtelow, M.A., et al., *Reconstitution and molecular analysis of the hRad9-hHus1-hRad1 (9-1-1) DNA damage responsive checkpoint complex.* J Biol Chem, 2001. **276**(28): p. 25903-9.
80. Caspari, T., et al., *Characterization of Schizosaccharomyces pombe Hus1: a PCNA-related protein that associates with Rad1 and Rad9.* Mol Cell Biol, 2000. **20**(4): p. 1254-62.
81. Griffith, J.D., L.A. Lindsey-Boltz, and A. Sancar, *Structures of the human Rad17-replication factor C and checkpoint Rad 9-1-1 complexes visualized by glycerol spray/low voltage microscopy.* J Biol Chem, 2002. **277**(18): p. 15233-6.
82. Kaur, R., C.F. Kostrub, and T. Enoch, *Structure-function analysis of fission yeast Hus1-Rad1-Rad9 checkpoint complex.* Mol Biol Cell, 2001. **12**(12): p. 3744-58.
83. Lindsey-Boltz, L.A., et al., *Purification and characterization of human DNA damage checkpoint Rad complexes.* Proc Natl Acad Sci U S A, 2001. **98**(20): p. 11236-41.
84. Shiomi, Y., et al., *Clamp and clamp loader structures of the human checkpoint protein complexes, Rad9-1-1 and Rad17-RFC.* Genes Cells, 2002. **7**(8): p. 861-8.
85. Venclovas, C. and M.P. Thelen, *Structure-based predictions of Rad1, Rad9, Hus1 and Rad17 participation in sliding clamp and clamp-loading complexes.* Nucleic Acids Res, 2000. **28**(13): p. 2481-93.
86. Volkmer, E. and L.M. Karnitz, *Human homologs of Schizosaccharomyces pombe rad1, hus1, and rad9 form a DNA damage-responsive protein complex.* J Biol Chem, 1999. **274**(2): p. 567-70.
87. St Onge, R.P., et al., *The human G2 checkpoint control protein hRAD9 is a nuclear phosphoprotein that forms complexes with hRAD1 and hHUS1.* Mol Biol Cell, 1999. **10**(6): p. 1985-95.
88. Chen, M.J., et al., *ATM-dependent phosphorylation of human Rad9 is required for ionizing radiation-induced checkpoint activation.* J Biol Chem, 2001. **276**(19): p. 16580-6.
89. Bao, S., et al., *ATR/ATM-mediated phosphorylation of human Rad17 is required for genotoxic stress responses.* Nature, 2001. **411**(6840): p. 969-74.
90. Chang, D.Y. and A.L. Lu, *Interaction of checkpoint proteins Hus1/Rad1/Rad9 with DNA base excision repair enzyme MutY homolog in fission yeast, Schizosaccharomyces pombe.* J Biol Chem, 2005. **280**(1): p. 408-17.
91. Friedrich-Heineken, E., et al., *The two DNA clamps Rad9/Rad1/Hus1 complex and proliferating cell nuclear antigen differentially regulate flap endonuclease 1 activity.* J Mol Biol, 2005. **353**(5): p. 980-9.
92. Gembka, A., et al., *The checkpoint clamp, Rad9-Rad1-Hus1 complex, preferentially stimulates the activity of apurinic/apyrimidinic endonuclease 1 and DNA polymerase beta in long patch base excision repair.* Nucleic Acids Res, 2007. **35**(8): p. 2596-608.

93. Guan, X., et al., *The human checkpoint sensor Rad9-Rad1-Hus1 interacts with and stimulates DNA repair enzyme TDG glycosylase.* Nucleic Acids Res, 2007. **35**(18): p. 6207-18.
94. Shi, G., et al., *Physical and functional interactions between MutY glycosylase homologue (MYH) and checkpoint proteins Rad9-Rad1-Hus1.* Biochem J, 2006. **400**(1): p. 53-62.
95. Smirnova, E., et al., *The human checkpoint sensor and alternative DNA clamp Rad9-Rad1-Hus1 modulates the activity of DNA ligase I, a component of the long-patch base excision repair machinery.* Biochem J, 2005. **389**(Pt 1): p. 13-7.
96. Toueille, M., et al., *The human Rad9/Rad1/Hus1 damage sensor clamp interacts with DNA polymerase beta and increases its DNA substrate utilisation efficiency: implications for DNA repair.* Nucleic Acids Res, 2004. **32**(11): p. 3316-24.
97. Wang, W., et al., *The human Rad9-Rad1-Hus1 checkpoint complex stimulates flap endonuclease 1.* Proc Natl Acad Sci U S A, 2004. **101**(48): p. 16762-7.
98. Wang, W., et al., *Mechanism of stimulation of human DNA ligase I by the Rad9-rad1-Hus1 checkpoint complex.* J Biol Chem, 2006. **281**(30): p. 20865-72.
99. Venclovas, C., M.E. Colvin, and M.P. Thelen, *Molecular modeling-based analysis of interactions in the RFC-dependent clamp-loading process.* Protein Sci, 2002. **11**(10): p. 2403-16.
100. Hirai, I., T. Sasaki, and H.G. Wang, *Human hRad1 but not hRad9 protects hHus1 from ubiquitin-proteasomal degradation.* Oncogene, 2004. **23**(30): p. 5124-30.
101. Zou, L., D. Cortez, and S.J. Elledge, *Regulation of ATR substrate selection by Rad17-dependent loading of Rad9 complexes onto chromatin.* Genes Dev, 2002. **16**(2): p. 198-208.
102. Lieberman, H.B., et al., *A human homolog of the Schizosaccharomyces pombe rad9+ checkpoint control gene.* Proc Natl Acad Sci U S A, 1996. **93**(24): p. 13890-5.
103. Dang, T., S. Bao, and X.F. Wang, *Human Rad9 is required for the activation of S-phase checkpoint and the maintenance of chromosomal stability.* Genes Cells, 2005. **10**(4): p. 287-95.
104. Pandita, R.K., et al., *Mammalian Rad9 plays a role in telomere stability, S- and G2-phase-specific cell survival, and homologous recombinational repair.* Mol Cell Biol, 2006. **26**(5): p. 1850-64.
105. Marathi, U.K., et al., *RAD1, a human structural homolog of the Schizosaccharomyces pombe RAD1 cell cycle checkpoint gene.* Genomics, 1998. **54**(2): p. 344-7.
106. Bao, S., et al., *Disruption of the Rad9/Rad1/Hus1 (9-1-1) complex leads to checkpoint signaling and replication defects.* Oncogene, 2004. **23**(33): p. 5586-93.
107. Hopkins, K.M., et al., *Deletion of mouse rad9 causes abnormal cellular responses to DNA damage, genomic instability, and embryonic lethality.* Mol Cell Biol, 2004. **24**(16): p. 7235-48.
108. Weiss, R.S., P. Leder, and C. Vaziri, *Critical role for mouse Hus1 in an S-phase DNA damage cell cycle checkpoint.* Mol Cell Biol, 2003. **23**(3): p. 791-803.

109. Lupardus, P.J. and K.A. Cimprich, *Phosphorylation of Xenopus Rad1 and Hus1 defines a readout for ATR activation that is independent of Claspin and the Rad9 carboxy terminus.* Mol Biol Cell, 2006. **17**(4): p. 1559-69.
110. Hubscher, U., G. Maga, and S. Spadari, *Eukaryotic DNA polymerases.* Annu Rev Biochem, 2002. **71**: p. 133-63.
111. Garcia-Diaz, M., et al., *DNA polymerase lambda (Pol lambda), a novel eukaryotic DNA polymerase with a potential role in meiosis.* J Mol Biol, 2000. **301**(4): p. 851-67.
112. Garcia-Diaz, M., et al., *Structure-function studies of DNA polymerase lambda.* DNA Repair (Amst), 2005. **4**(12): p. 1358-67.
113. Steitz, T.A., *DNA polymerases: structural diversity and common mechanisms.* J Biol Chem, 1999. **274**(25): p. 17395-8.
114. Garcia-Diaz, M., et al., *A structural solution for the DNA polymerase lambda-dependent repair of DNA gaps with minimal homology.* Mol Cell, 2004. **13**(4): p. 561-72.
115. Maga, G., et al., *DNA elongation by the human DNA polymerase lambda polymerase and terminal transferase activities are differentially coordinated by proliferating cell nuclear antigen and replication protein A*. J Biol Chem, 2005. **280**(3): p. 1971-81.
116. Maga, G., et al., *Human replication protein A can suppress the intrinsic in vitro mutator phenotype of human DNA polymerase lambda.* Nucleic Acids Res, 2006. **34**(5): p. 1405-15.
117. Crespan, E., U. Hubscher, and G. Maga, *Error-free bypass of 2-hydroxyadenine by human DNA polymerase lambda with Proliferating Cell Nuclear Antigen and Replication Protein A in different sequence contexts.* Nucleic Acids Res, 2007. **35**(15): p. 5173-81.
118. Maga, G., et al., *Replication protein A and proliferating cell nuclear antigen coordinate DNA polymerase selection in 8-oxo-guanine repair.* Proc Natl Acad Sci U S A, 2008. **105**(52): p. 20689-94.
119. Maga, G., et al., *8-oxo-guanine bypass by human DNA polymerases in the presence of auxiliary proteins.* Nature, 2007. **447**(7144): p. 606-8.
120. Wimmer, U., et al., *Control of DNA polymerase lambda stability by phosphorylation and ubiquitination during the cell cycle.* EMBO Rep, 2008. **9**(10): p. 1027-33.
121. Liu, Y., et al., *Transcriptome dynamics of Deinococcus radiodurans recovering from ionizing radiation.* Proc Natl Acad Sci U S A, 2003. **100**(7): p. 4191-6.
122. Tubbs, J.L., et al., *Flipping of alkylated DNA damage bridges base and nucleotide excision repair.* Nature, 2009. **459**(7248): p. 808-13.
123. Markkanen, E.E., *Studies on the interaction of a checkpoint clamp with components of the base excision repair machinery*, in *Institute of Veterinary biochemistry and Molecular biology*. 2006, University of Zurich: Zurich.
124. Weller, G.R. and A.J. Doherty, *A family of DNA repair ligases in bacteria?* FEBS Lett, 2001. **505**(2): p. 340-2.
125. Blasius, M., et al., *Enzymes involved in DNA ligation and end-healing in the radioresistant bacterium Deinococcus radiodurans.* BMC Mol Biol, 2007. **8**: p. 69.
126. Daly, M.J., et al., *Accumulation of Mn(II) in Deinococcus radiodurans facilitates gamma-radiation resistance.* Science, 2004. **306**(5698): p. 1025-8.

127. Narumi, I., et al., *PprA: a novel protein from Deinococcus radiodurans that stimulates DNA ligation.* Mol Microbiol, 2004. **54**(1): p. 278-85.
128. Murakami, M., et al., *Analysis of interaction between DNA and Deinococcus radiodurans PprA protein by atomic force microscopy.* Biochim Biophys Acta, 2006. **1764**(1): p. 20-3.
129. Mitra, S., *MGMT: a personal perspective.* DNA Repair (Amst), 2007. **6**(8): p. 1064-70.
130. Balakrishnan, L., et al., *Long patch base excision repair proceeds via coordinated stimulation of the multienzyme DNA repair complex.* J Biol Chem, 2009. **284**(22): p. 15158-72.

8. Acknowledgements

I am most grateful to Professor Ulrich Hübscher, who gave me the opportunity to do my PhD thesis in his lab and all the other opportunities I had during this time and last but not least also for being a very caring and warmhearted supervisor during all the years of my PhD thesis. I have learned a lot!

My huge thanks goes to Professor Josef Jiricny and Professor Suzanne Sommer for interesting scientific discussions and for being part of my PhD committee.

Next I would like to thank all the members of Ueli's lab, past and present; special thanks go to Dr. Melanie Blasius for introducing me to the lab and its techniques and members, as well as to Dr. Ursula Wimmer for her constant scientific support and being a great person to discuss with. Furthermore, my thank goes to Elena Ferrari for being the "good angel" (and sometimes also the "dragon") of the Institute.

Also all the other people from the Institute of Veterinary Biochemistry and Molecular Biology should be acknowledged for making it a very pleasant time up there.

My warmest thanks go to my beloved family, my mum, my dad and also my little sister and my grandmother, without their constant help and mental comfort I would never be where I am now. Sometimes it takes a bit more time to realize things like that.

Furthermore I would like to thank Martin without whom I would never have gotten so far. Thank you for giving me all the peace and quietness and love that I needed and for the understanding and mental support during all of these years.

And last but not least I would like to thank Carolin for being a very good friend and standing by my side during all of these four years – and hopefully beyond of that.

And actually all the other friends who are always with me and encourage me in all the things I did and do.

10. Curriculum vitae

Personal Details

Name	BUOB
First name	Rebecca
Date of Birth	22 January 1979
Nationality	Swiss

Education

• **August 2005-August 2009**	PhD-Thesis at the Institute of Veterinary Biochemistry and Molecular Biology in the group of Prof. Ulrich Hübscher
• **March 2005 – June 2005**	Course "Cambridge Institute in Advanced English" in Totness, UK with Certificate
• **October 2004 – March 2005**	Employment as Scientific assistant at the Institute for Molecular Biology in the group of Prof. Konrad Basler
• **October 2002-October 2004**	Diploma in Molecular Biology Second subject Microbiology
• **October 2000**	Begin of the studies at the University of Zürich in Biology/Molecular Biology
• **Spring and Autumn 2000**	Federal Matura (Typus D) in Basel and Bern
• **1997 – 2000**	AKAD, Zürich; Maturatypus D
• **1992 – 1997**	Grammar school „Hohe Promenade", Zürich

Conferences and Retreats

• **August 2006**	Cancer Network Zurich; Retreat Monte Verita Poster-Presentation
• **December 2005**	REBBIOTECH; European Research Network, Brest (F) Talk

Publications

- „Enzymes involved in DNA ligation and end-healing in the radioresistant bacterium *Deinococcus radiodurans*`
  M. Blasius, **R. Buob**, I. Shevelev and U.Hübscher, BMC Molecular Biology (2007), **8**, 69.